NOAA Contract Report NMFS-NWFSC-CR-2023-09

https://doi.org/10.25923/963j-pd86

Evaluating Effects of Climate Change, Restoration Scenarios, and Hatchery Effects on Chinook Salmon in the Stillaguamish River Basin with the HARP Model

October 2023

U.S. DEPARTMENT OF COMMERCE

National Oceanic and Atmospheric Administration
National Marine Fisheries Service
Northwest Fisheries Science Center

NOAA Contract Report Series NMFS-NWFSC-CR

Recommended citation:

(Beechie et al. 2023)[1]

[1] Beechie, T. J., A. Goodman, M. Lowe, O. Stefankiv, B. Timpane-Padgham, and J. Jorgensen. 2023. Evaluating Effects of Climate Change, Restoration Scenarios, and Hatchery Effects on Chinook Salmon in the Stillaguamish River Basin with the HARP Model. U.S. Department of Commerce, NOAA Contract Report NMFS-NWFSC-CR-2023-09.

https://doi.org/10.25923/963j-pd86

NOAA FISHERIES

Evaluating Effects of Climate Change, Restoration Scenarios, and Hatchery Effects on Chinook Salmon in the Stillaguamish River Basin with the HARP Model

Timothy J. Beechie,[1] Arianna Goodman,[2] Michaela Lowe,[3] Oleksandr Stefankiv,[1] Britta Timpane-Padgham,[1] and Jeff Jorgensen[1]

https://doi.org/10.25923/963j-pd86

October 2023

[1]Fish Ecology Division
Northwest Fisheries Science Center
2725 Montlake Boulevard East
Seattle, Washington 98112

[2]Saltwater, Inc.
733 N Street
Anchorage, Alaska 99501

[3]Washington Department of Fish and Wildlife
1111 Washington Street Southeast
Olympia, Washington 98501

U.S. DEPARTMENT OF COMMERCE

National Oceanic and Atmospheric Administration
National Marine Fisheries Service
Northwest Fisheries Science Center

Table of Contents

Acknowledgements

The HARP Model implementation in the Snohomish and Stillaguamish River basins relied on the Life-cycle Model Workgroup, including Frank Leonetti (Snohomish County), and Neala Kendall, Jim Scott, and Gwendolyn Hannam (Washington Department of Fish and Wildlife). We were also assisted by local scientists and stakeholders who provided data or recommendations on model options (Mike Crewson, Jason Griffith, Diego Holmgren, Kurt Nelson, Peter Verhey, Jared Siegel, Aimee Fullerton, and Guillaume Mauger). Jeff Jorgensen, Peter Kiffney, and Aimee Fullerton of NOAA Northwest Fisheries Science Center also assisted with the life-cycle modeling and spatial analyses. Helpful reviews of the draft report were provided by Thomas Buehrens, Neala Kendall, and Kurt Nelson.

Funding for the project was approved by the Pacific Salmon Commission (PSC) U.S. Commissioners for FY2022, with recommendation from the Chinook Technical Committee. The project addresses Research Theme 3 for FY2022 Letter of Agreement (LOA) New Projects in the PSC Chinook Technical Committee Request for Proposals: Improvement of Methods for Abundance-based Management in that we seek to, “Improve existing methods or develop new approaches to model, estimate, manage, predict abundance, or assess productivity bottlenecks of U.S. Chinook salmon stocks harvested in PSC fisheries.” Funding was awarded to the Northwest Fisheries Science Center (NWFSC) from NMFS West Coast Region.

Executive Summary

The goals of this project were to use the Habitat Assessment and Restoration Planning (HARP) Model to evaluate potential effects of climate change on Stillaguamish Chinook salmon, identify restoration actions and strategies that will most increase spawner abundance and resilience to climate change, and evaluate if hatchery practices could help ameliorate climate change effects. This required addition of climate change effects and hatchery components to the model, as well as development of additional restoration scenarios.

A key uncertainty in the Stillaguamish Chinook salmon life-cycle model is whether (or to what degree) adult returns are affected by high stream temperatures during upstream migration and spawning. This led us to run two-alternative models, one with a temperature effect on prespawn mortality (Model 1) and one without (Model 2). The latter assumes that migration timing and holding locations of Stillaguamish Chinook salmon are adapted to avoid temperature-related prespawn mortality, and that adults can avoid high temperatures in the future.

Climate Change and Habitat Restoration

The diagnostic scenario analysis with Model 1 (with temperature-related prespawn mortality) showed that four freshwater habitat restoration actions (floodplain reconnection, wood augmentation, bank armor removal, shade restoration) are most likely to increase Chinook salmon spawner abundance under current climate conditions (Figure ES-1). In addition, estuary restoration may provide a significant benefit, particularly if other management actions can increase fry outmigrant abundance to maximize use of estuary rearing capacity. The alternative model without temperature-related prespawn mortality (Model 2) suggests that wood augmentation and bank armor removal would be priority actions, while shade and floodplain reconnection have low or no benefit because temperature reduction has less influence on the population and the Chinook life history is not heavily dependent on floodplain habitats.

Model 1 suggests that climate change is likely to reduce abundance of Stillaguamish Chinook salmon by 65% by the late century (2080s) in the absence of habitat restoration (Figure ES-2), suggesting that this Chinook population is very vulnerable to climate change. Specific climate change effects included in the HARP Model are increased summer stream temperature, increased flood flows, and decreased low flows, but Chinook vulnerability to climate change is likely most driven by temperature effects on prespawn mortality and flood flow effects on incubation survival. Model 2 (without temperature-related prespawn mortality) predicts a spawner abundance decline of 33% in the no-action scenario, indicating that the degree to which prespawning adults are sensitive to temperature is a key uncertainty in the model.

We also compared modeled outcomes of six habitat restoration strategies comprised of the five most important restoration action types: floodplain reconnection, wood augmentation, shade restoration, bank armor removal, and estuary restoration. Four strategies were

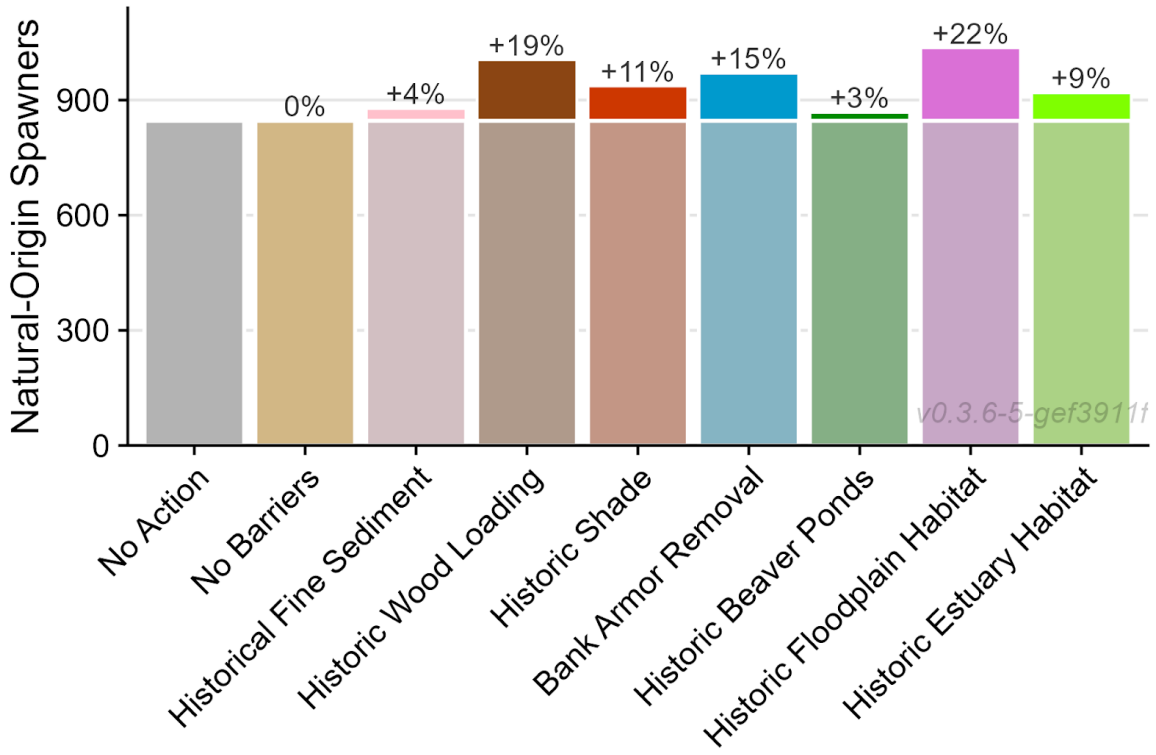

Figure ES-1. Modeled median 2020s spawner abundances under each diagnostic scenario.

developed using fixed criteria for inclusion of an action type and setting its restoration intensity, with each subbasin evaluated separately so that habitat restoration actions and intensities were tailored to each subbasin. Two additional strategies were developed by the Stillaguamish Technical Advisory Group (TAG), which were intended to represent (1) restoration actions and intensity based on current feasibility and (2) a more optimistic scenario that was less constrained by current feasibility.

In the Model 1 results, five of the six restoration scenarios combining multiple actions produce at least 30% increases in modeled spawner abundance under current climate conditions, and most produce larger percent increases under future climate conditions (Figure ES-3). However, total modeled abundance is projected to be lower than current abundance by late century even with habitat restoration. The modeled percent increase in spawner abundance for the TAG 1 scenario ranges from 7%-9% across all three time periods, and the modeled percent increase for the TAG2 scenario ranges from 28%-30% across all three time periods. Chinook 1a and 2a show modest increases in the mid-century (35% and 36%, respectively) and late-century (36% and 37%, respectively). The Chinook 1b and Chinook 2b scenarios (which are based on 2080s diagnostic scenarios) provide the most restoration potential in the late century. Chinook 1b produces the highest spawner response of all custom restoration and single-action diagnostic scenarios with 56% restoration potential in the late-century. This strategy also produces the highest spawner response in the mid-century.

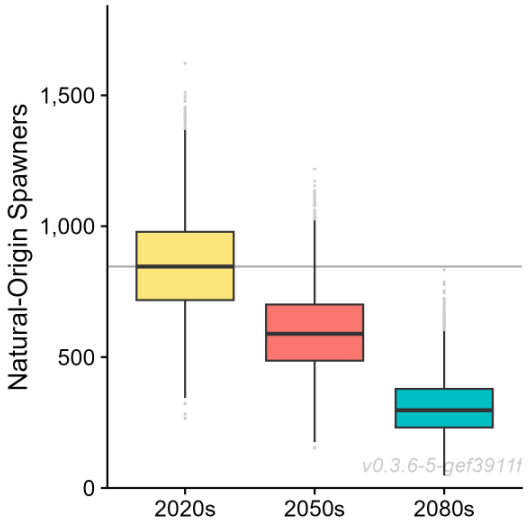

Figure ES-2. Modeled natural-origin spawner abundances under current (2020s), mid-century (2050s), and late-century (2080s) climate conditions without habitat restoration (no-action scenario). Thick black lines show median natural-origin spawner abundance.

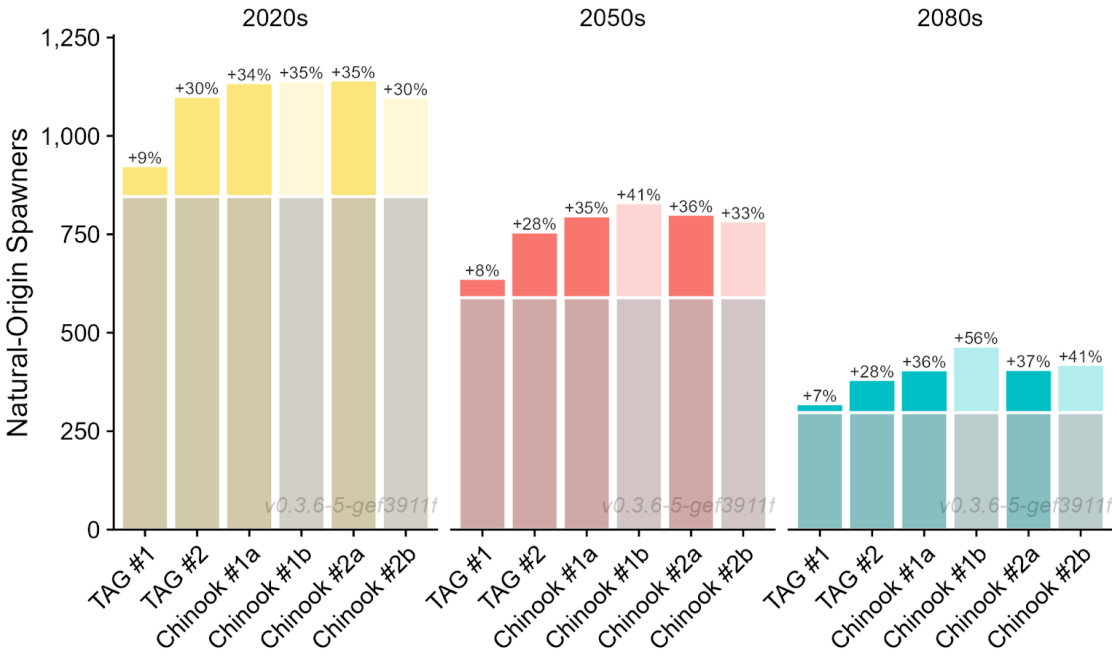

Figure ES-3. Modeled spawner abundances under six custom restoration scenarios under current (2020s), mid-century (2050s), and late-century (2080s) climate conditions. Scenarios Chinook 1b and Chinook 2b, which were designed specifically for late-century conditions, are shown in lighter shades. No-action modeled spawner abundances are indicated by shaded bars for each climate condition.

The Model 2 results are broadly similar, except that predicted increases in natural-origin spawner abundance are slightly lower for each restoration scenario (Appendix F). Under current climate conditions, all scenarios except TAG1 have predicted spawner increases of 27% to 29%. Under late-century climate conditions, all scenarios except TAG1 have predicted increases between 26% and 29%.

Hatchery Influences

Under current Stillaguamish Chinook hatchery management strategies, the HARP Model projects declines in both natural-origin and hatchery-origin spawners under mid- and late-century climate conditions (Figure ES-4). However, the reduction of hatchery-origin spawners in each time period is substantially less than the natural-origin spawners. This pattern reflects the assumption that hatcheries continue to produce the same number of juvenile outmigrants per adult spawner (i.e., they are not exposed to increased temperature or decreasing flows), while smolts per spawner for natural-origin fish will likely decrease due to climate change effects on temperature and flow.

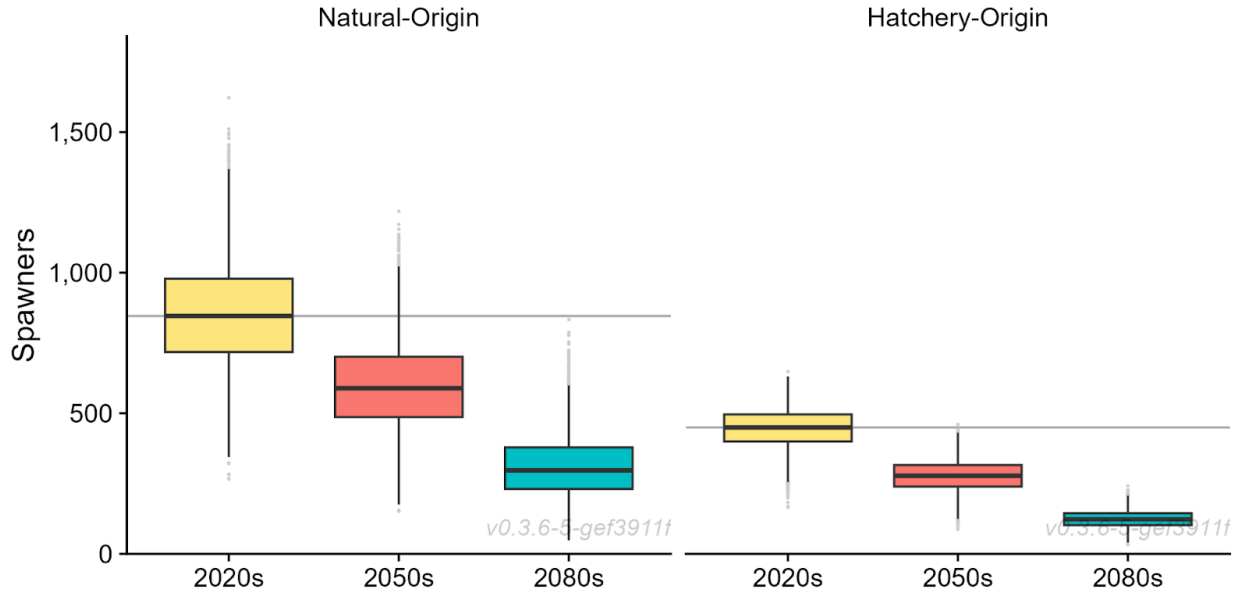

Figure ES-4. Modeled natural-origin (left) and hatchery-origin (right) spawner abundances under current (2020s), mid-century (2050s), and late-century (2080s) climate conditions without habitat restoration. Thick black lines are the median spawner abundance.

The model results also suggest that there is a small negative effect on natural-origin Chinook under current hatchery practices, but the reduction in natural-origin spawners is small relative to a low-production hatchery scenario. That is, reducing broodstock take and juvenile releases to about 25% of current levels could slightly increase abundance of natural-origin spawners. Current hatchery practices do not appear to benefit natural-origin Chinook under future climate scenarios, indicating that hatchery supplementation is unlikely to offset climate change effects. Moreover, continued hatchery production levels would substantially increase percent hatchery-origin spawners (pHOS) as well as the percentage of natural-origin North Fork spawners taken as broodstock under mid- and late-century climate conditions. That is, as the spawner population gets smaller, a higher percentage of natural-origin spawners would be taken as broodstock, further reducing abundance of natural-origin spawners in the future. While reduced hatchery production may produce a small increase in natural-origin Chinook spawner abundance, the increase would not be sufficient to offset decreases due to climate change.

Model 2 predicts a smaller predicted decline in natural-origin fish, and North Fork broodstocking practices become more sustainable as they take a smaller proportion of the total North Fork natural-origin returns. Also, modeled hatchery returns remain constant because hatchery-origin spawners are no longer influenced by warming temperatures in the model.

Marine Survival Influence

Since the 1980s, Puget Sound Chinook subyearling marine survival has dropped from over 2% to less than 0.4% (including harvest), and the current low marine survival rate appears to limit population size and the effectiveness of restoration actions. In particular, effectiveness of estuary restoration is low because there are too few fry migrants to fully utilize available estuary rearing capacity, and low fry migrant abundance may be in part due to low marine survival contributing to very low escapement levels. While there is no single obvious cause of the marine survival decline, potential contributors include: declines in juvenile herring and zooplankton prey, increased predation by marine mammals, and density dependence in the nearshore resulting from high hatchery outplants in years with high pink salmon abundance. Increasing marine survival could substantially increase population size and responses to restoration actions if effective management actions can be identified.

Conclusions

Based on the HARP Model results we arrived at five main summary points.

1. The HARP Model 1 (with temperature-related prespawn mortality) suggests that Stillaguamish Chinook salmon are very vulnerable to climate change, and their vulnerability largely stems from temperature effects on prespawn mortality and flood flow effects on incubation survival. However, Model 2 (without temperature-related prespawn mortality) suggests a much less severe future for these populations. Moreover, the potential for channel adjustment and phenological shifts

may further ameliorate potential effects of climate change on stream flow and temperature.

2. A restoration strategy that emphasizes five key actions (floodplain reconnection, wood augmentation, bank armor removal, shade restoration, and estuary reconnection) is likely to most benefit Chinook salmon under current climate conditions. Strategies with increased emphasis on floodplain reconnection appear to most increase resilience to climate change, as they provide larger increases in modeled spawner abundance in the late-century climate.
3. Lack of fry migrants currently limits modeled effectiveness of estuary restoration. Because fry migrant abundance is very low relative to estuary rearing capacity, expanding estuary rearing capacity through habitat restoration does not generate a significant increase in modeled spawner abundance.
4. Extremely low marine survival since the 1980s limits modeled population size and effect of restoration actions. Since the 1980s, sub-yearling marine survival has dropped from over 2% to 0.36% (for natural-origin spawners, including harvest). Increasing marine survival could substantially increase population size and the population response to restoration actions. For comparison, the marine survival rate for natural-origin spawners without harvest is estimated at 0.59%.
5. Current hatchery practices do not increase abundance of natural-origin Chinook in the current climate, nor in any future climate scenario. The model suggests that reducing hatchery production to about 25% of current production may produce a small increase in natural-origin Chinook spawner abundance in all climate scenarios. However, modeled percent hatchery-origin spawners (pHOS) would increase under mid- and late-century climate conditions. At the same time, maintaining a constant percent natural-origin adult broodstock in the future would substantially increase the percentage of natural-origin adult returns removed for hatchery broodstock, further reducing natural origin spawners in the future.

These conclusions suggest that it may be challenging to increase spawner abundance of Stillaguamish Chinook salmon through habitat restoration in the future, primarily because marine survival is extremely low and climate change is expected to decrease spawner abundance. However, we only modeled the most extreme greenhouse gas emissions scenario (RCP 8.5), which currently appears to be the most accurate projection of mid-century climate change but may overestimate emissions in the late-century. Hence, maintaining an emphasis on floodplain and estuary restoration actions may ultimately be an important component of increasing resilience to climate change. The HARP Model does not suggest that hatchery supplementation can offset effects of climate change. Increased marine survival—whether through management actions or ocean regime shift—may be necessary to substantially offset climate change effects.

1. Introduction

The objectives of this project were outlined in a joint proposal to the Pacific Salmon Commission by the Washington Department of Fish and Wildlife (WDFW) and the Northwest Fisheries Science Center (NWFSC), seeking funding under the FY2022 Letter of Agreement (LOA). The three main objectives of this project are to evaluate how Chinook salmon spawner abundance in the Stillaguamish River basin may be influenced by:

1. Climate change (flood flows, low flows, and stream temperature),
2. Alternative habitat restoration scenarios, and
3. Hatchery management.

The purpose of these objectives is to inform future habitat restoration and hatchery management practices for Chinook salmon in the Stillaguamish River basin.

This project builds on prior HARP Modeling that evaluated restoration potential for individual restoration actions and identified important restoration actions for Chinook salmon in each subbasin (Beechie et al. 2022). (The model spatial structure and Chinook salmon species distribution are shown in Appendix A). That assessment (Phase 1) showed that four freshwater habitat restoration actions were likely most important to Chinook salmon recovery in the Stillaguamish River basin: floodplain reconnection, bank armor removal, wood augmentation, and shade restoration. Estuary restoration did not appear to have significant restoration potential because the abundance of fry migrants is too low to take full advantage of current estuary rearing capacity, let alone increased capacity from restoration. If we assume a substantial increase in fry migrant abundance in the future, then estuary restoration may have a greater influence on Chinook salmon recovery.

These prior results were used to inform alternative restoration scenarios for this project, with restoration scenarios generally focusing on restoration actions that most increased Chinook salmon spawner abundance in each subbasin. Two scenarios were developed by the Stillaguamish Technical Advisory Group (TAG), based on local knowledge and anticipated feasibility. Two additional scenarios were developed based on the most influential restoration actions identified in Phase 1, and the final two scenarios were developed based on projected effectiveness of restoration actions under 2080s climate conditions. The climate-change related stream flow changes were adopted from the University of Washington Climate Impacts Group (Mauger et al. 2021), and adjustments to the functional relationship between stream temperature and Chinook adult prespawn mortality for hatchery origin spawners were based on a study in the Columbia River basin (Bowerman et al. 2021). To examine how climate change might affect restoration effectiveness, all restoration scenarios were run under three different climate periods: current, mid-century (2050s), and late century (2080s). Effects of hatchery practices were modeled based on a number of studies documenting supplementation effects, competition effects, and differential survivals among hatchery and wild fish.

2. The Habitat Assessment and Restoration Planning (HARP) Model

In the HARP Model, the habitat and salmon population assessments are based on a process-based conceptual model that links landscape processes to habitat conditions, and then habitat conditions to salmon populations (Figure 2-1). The modeling process includes four main steps:

1. Collecting and processing geospatial data to quantify current landscape and habitat attributes in the basin,
2. Translating changes in drivers into current and historical habitat conditions for each 200-m reach in the basin,
3. Translating habitat areas and qualities into life-stage parameters for the life-cycle models, and
4. Running the salmon life-cycle models.

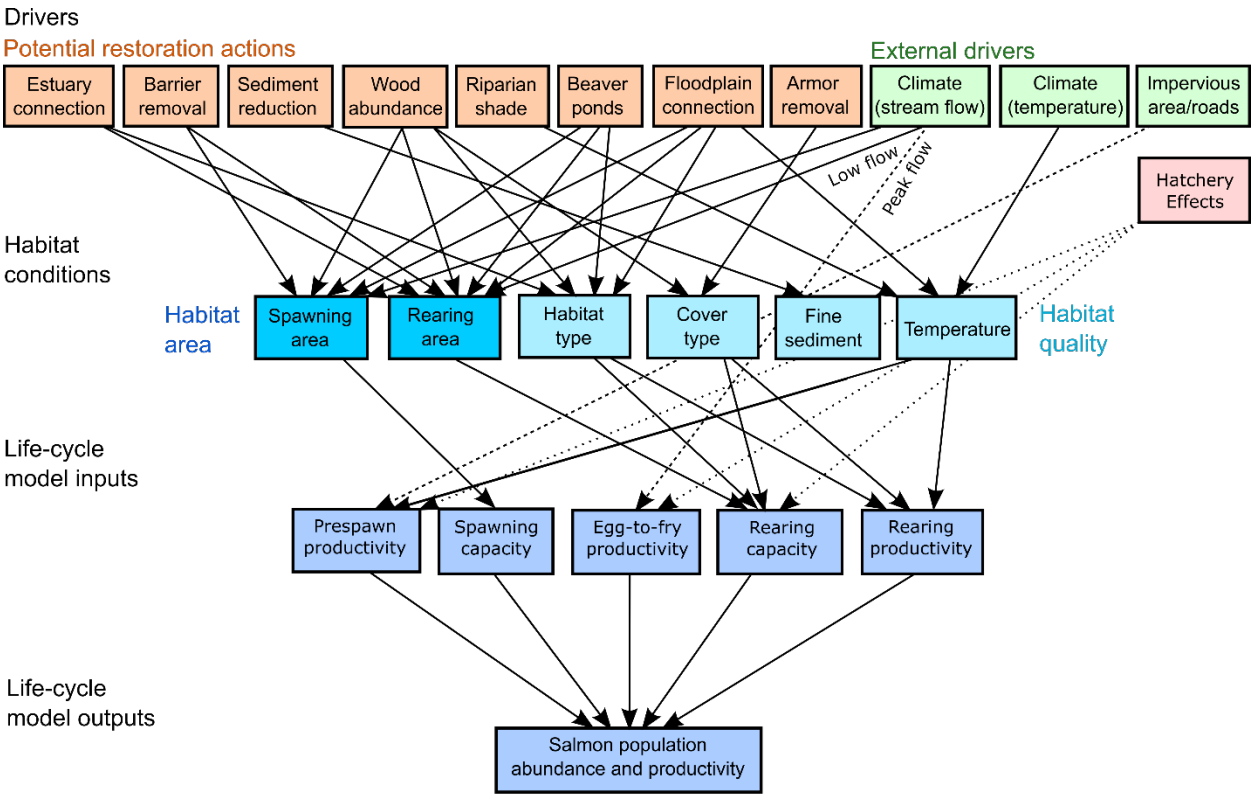

Figure 2-1. Schematic diagram of process linkages represented in the Habitat Assessment and Restoration Planning (HARP) Model. Dashed lines are direct linkages from an external driver to a life-cycle model input (no intermediate habitat change modeled).

The first two steps create the habitat data necessary to assess habitat change from historical to current conditions and to develop diagnostic and restoration scenarios for the life-cycle models. The third and fourth steps translate those habitat condition scenarios into estimates of spawner abundance for each species, subbasin, and scenario modeled. The model can run restoration scenarios for individual restoration action types, combinations of action types, and climate change effects.

In Phase 1 of this project, we quantified restoration potential as the modeled percent change in spawner abundance when a habitat attribute was changed from its current condition to its natural potential (historical) condition, and each habitat attribute was modeled as a separate diagnostic scenario so that we could compare restoration potentials across restoration action types. Climate change effects, hatchery-origin fish, and complex restoration scenarios were not included in Phase 1.

2.1 Summary of Phase 1 Model Results

Estimated losses of beaver ponds and floodplain habitats (compared to historical conditions) were very high in the Stillaguamish River basin, whereas estuary habitat loss was somewhat lower (Beechie et al. 2022). Beaver ponds decreased by 90 to 95%, floodplain marshes and ponds decreased by ~80%, and side channel length decreased by 59% (Table 2-1). Estuary rearing habitat area decreased by 44%.

Migration barrier effects varied among species because their spawning ranges differ. Only 1% of Chinook salmon habitat length and 3% of summer-run steelhead habitat length is above full or partial barriers. By contrast, 20% of coho salmon habitat length and 10% of winter-run steelhead habitat length is above full or partial barriers.

Shade levels have decreased significantly from historical conditions in agricultural and developed areas, resulting in significant increases in modeled stream temperature, with modeled stream temperature increasing more than 2°C in 23% of reaches. Wood loss was assumed to be ubiquitous, reducing both spawning and rearing habitat area and quality. Bank armor was documented only in large rivers (>20m bankfull width), where 9% of bank length is armored.

The Phase 1 diagnostic scenarios suggest that restoration actions to improve coho salmon populations should focus on restoration of beaver pond and floodplain habitats (Figure 2-2), which have predicted restoration potentials of +61 and +83%, respectively (Beechie et al. 2022). (Restoration potential is the modeled percent increase in spawner abundance from current to historical conditions for each action type.) Restoring wood abundance and removing migration barriers had relatively smaller predicted increases in coho spawner abundance (+25% and +14%, respectively). Restoration potentials for the remaining restoration actions were less than +6%.

The HARP Model predicts that steelhead will be most responsive to wood augmentation and floodplain restoration (34% and 31% increase in spawners, respectively), although shade restoration also may benefit steelhead (+14%). All other habitat restoration actions

Table 2-1. Summary of estimated habitat changes in the Stillaguamish River basin.

Habitat type	Habitat Change
Beaver ponds	Decrease of 90-95%
Side channels	Decrease of 59%
Floodplain marshes, ponds	Decrease of ~80%
Estuary rearing habitat area	Decrease of 44%
Percent of habitat length above migration barriers	Coho: 20% Chinook: 1% Winter Steelhead: 10% Summer Steelhead: 3%
Shade and Temperature	Temperature increase >2°C in 23% of reaches
In-stream wood	Wood abundance reduced basin-wide, reducing spawning and rearing capacities for all species
Bank armor	9% of bank habitat armored
Impervious surface and roads	Predicted coho prespawn mortality >20% in small streams near Arlington
Fine sediment	Modest increase in fine sediment levels in small streams in developed or agricultural lands

produced very small (<+3%) modeled increases in spawner abundance for steelhead.

Summer- and fall-run Chinook salmon were less responsive to restoration actions in the Phase 1 HARP Model. Restoration potentials were highest for wood augmentation, bank armor removal, and floodplain reconnection (+17%, +18%, and +22%, respectively). The modeled shade restoration potential was +11%, and all other freshwater restoration actions had essentially no effect. Perhaps surprisingly, estuary restoration only produced a modeled increase in Chinook spawners of 4%. The low modeled estuary restoration potential appeared to be due to the low numbers of fry-sized Chinook juveniles currently reaching the Stillaguamish estuary (Beechie et al. 2022).

2.2 Key Phase 1 Uncertainties

One of the most important uncertainties in the HARP Model is the productivity parameter for the estuary Beverton-Holt function for Chinook fry, although the parameter is less influential in the Stillaguamish basin because so few fry are reaching the estuary and the estuary has excess rearing capacity in its current state. Notably, the modeled response to estuary restoration increases as more Chinook fry enter the estuary, suggesting that the response of the Chinook population to estuary restoration will increase if the basin produces more fry migrants.

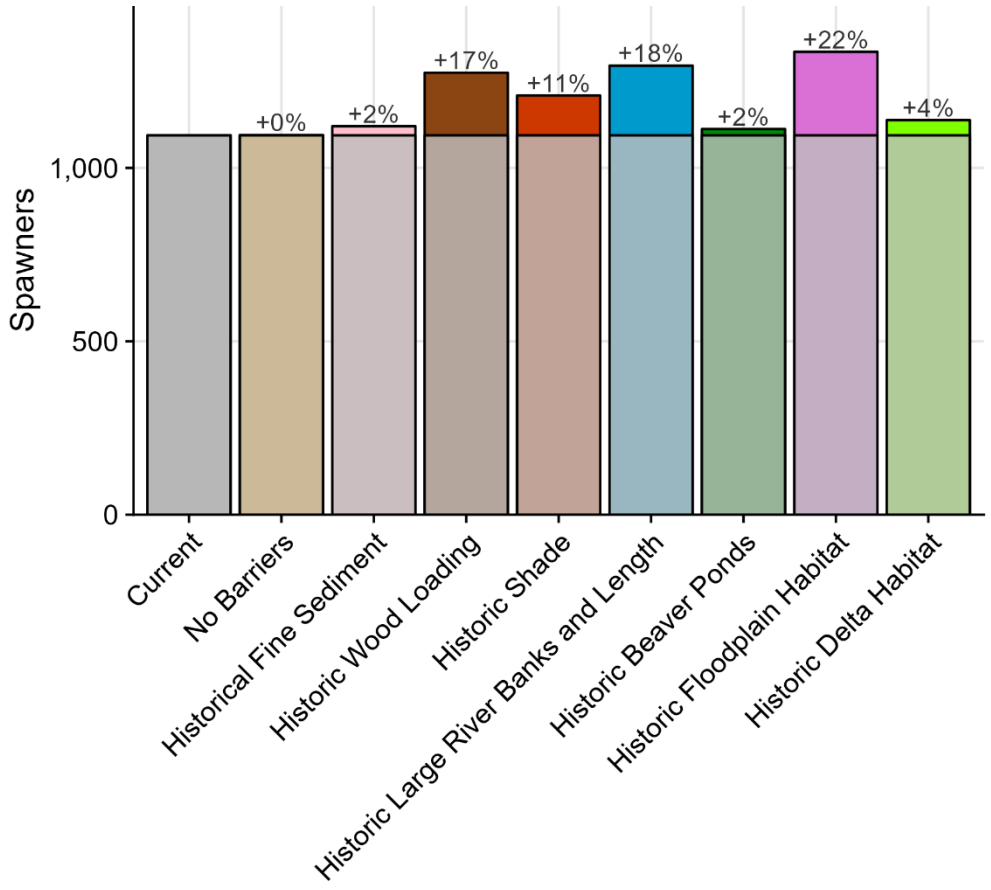

Figure 2-2. Phase 1 spawner abundances for Stillaguamish River Chinook salmon in each diagnostic scenario. The Phase 1 model did not include climate change or hatchery supplementation.

Another factor not included in the Phase 1 model is use of estuary rearing habitat by non-natal juvenile salmonids. We address this uncertainty in the Phase 2 model (Section 3.4.3), by reducing estuary rearing capacity by the proportion of non-natal salmon in the estuary.

Many of the life-stage productivity parameters have relatively high uncertainty, and those parameters can have a large influence on the model results (Jorgensen et al. 2021, Beechie et al. 2023). Of particular importance are the smolt-to-adult return (SAR) rates that we use to calibrate the estuary and nearshore productivity values. As with other models, the HARP Model is very sensitive to estuary and marine survival rates, and increasing confidence in those rates will improve confidence in the model result. This uncertainty is also addressed in the Phase 2 model (Section 3.4.4).

Finally, an improved hydrography layer based on lidar may increase confidence in habitat capacity estimates for small streams used primarily by coho and steelhead. This uncertainty has not been addressed in either model phase.

3. HARP Model Changes in Phase 2

In this project we built upon the Phase 1 analysis by adding climate change effects, alternative restoration strategies, and hatchery effects on natural-origin Chinook salmon in the Stillaguamish basin. The key questions we addressed with the HARP Model are:

1. What are the projected effects of climate change on Stillaguamish Chinook salmon?
2. Which habitat restoration strategies have the greatest potential to benefit Chinook salmon populations under current and future climate conditions?
3. Can current hatchery management strategies contribute to increased Chinook salmon abundance in the future?

To model climate change and habitat restoration strategies, we adjusted specific habitat parameters or functions illustrated in Figure 2-1 to represent either climate change or restoration actions. For example, we estimated changes in future summer stream temperature, summer low flow, and highest one-day average flood flow due to predicted climate change, and those changes in drivers then altered Chinook prespawn mortality (temperature), spawning capacity (low flow), and incubation survival (flood flow) (Section 3.1). The changes in habitat capacity and productivity are inputs to the life cycle model, which then estimates changes in abundance of eggs, juveniles, or adults at each life stage.

The restoration strategies are combinations of actions (top row of Figure 2-1) that can improve habitat quantity or quality, or ameliorate climate change effects (Section 3.2). The model translates those actions and habitat changes into changes in habitat capacity or productivity, which can then increase spawner abundance and salmon population resilience to climate change (Jorgensen et al. 2021, Beechie et al. 2023).

We modeled hatchery fish separately, and they can supplement or compete with wild fish (Section 3.3). Each year broodstock are removed from returning adults and juveniles are out-planted in specific locations. Hatchery-origin adults have lower prespawn survival rates as a function of stream temperature than natural-origin fish (Bowerman et al. 2018), and also have different smolt-to-adult-return rates than natural-origin fish (Zimmerman et al. 2015a, Jim Scott unpublished data).

3.1 Modeled Climate Change Effects

To model climate change effects on freshwater habitats in the Stillaguamish River basin we relied on recent studies that have estimated changes in flood and low flows (Mauger et al. 2021) or stream temperature (Siegel et al., unpublished data). In each case we re-summarized raw model outputs to produce metrics that match the required HARP Model inputs for the current climate (2010-2039), mid-century climate (2040-2069, also referred to as 2050s), and late-century climate (2070-2099, also referred to as 2080s) (Table 3-1).

In the HARP Model, changes in stream flows and temperature affect five life-stage parameters: incubation productivity, subyearling rearing capacity and productivity, and yearling summer rearing capacity and productivity (Table 3-2). Flood flow affects

Table 3-1. Time periods used to model current, mid-century, and late-century flood flow, low flow, and stream temperature.

Era	Central decade	Years included	Number of years
Current	2020s	2010-2039	30
Mid-century	2050s	2040-2069	30
Late-century	2080s	2070-2099	30

Table 3-2. Checklist of life stage capacities (c) and productivities (p) affected by each climate change effect for summer- and fall-run Chinook (p_{incub} = incubation productivity, c_{sub} = subyearling rearing capacity, p_{sub} = subyearling rearing productivity c_{sr} = summer rearing capacity, p_{sr} = summer rearing productivity).

Climate change effect	Prespawn Mortality	Spawning Capacity	Egg Incubation	Sub-yearling Rearing		Yearling Summer Rearing	
			p_{incub}	c_{sub}	p_{sub}	c_{sr}	p_{sr}
Flood flow			X				
Low flow		X		X		X	
Temperature	X				X	X	X

incubation productivity via scour of eggs from redds, low flow affects summer rearing and adult spawning capacity via changes in wetted width, and temperature affects adult prespawn mortality, as well as subyearling and yearling rearing via direct mortality.

3.1.1 Flood Flow Change

Flood flow and low flow statistics were derived from DHSVM modeling results for the Stillaguamish Basin (Mauger et al. 2021). Mauger et al. (2021) published hourly flow predictions for at 18 sites within the basin for 1990-2099 under the Representative Concentration Pathway (RCP) 8.5 emissions scenario using 12 separate global climate models (GCMs) (Appendix B). The RCP 8.5 emissions scenario represents the high end of future greenhouse gas concentrations through the end of the 21st century. We divided the data into the three eras based on water years (Oct 1 – Sept 30, Table 3-1). Within each 30-year era, there were 3,418,584 flow predictions for each of the 18 sites (262,968 hours x 12 GCMs), from which we calculated the annual highest one-day average flood (the greatest mean daily flow value for each water year) for each site, era, and GCM.

We first calculated log Pearson III exceedance (flood flow) probability curves for each 30-year era for each site and GCM. We then calculated the percent change in flow from the current era to the mid- or late-century as a function of recurrence interval for each of the 12 GCMs (e.g., the percent change in 10-year flood flow between the current era and late century for GCM #1) (Figure 3-1, Figure 3-2). This produced 36 flood-flow–recurrence interval relationships at each of the 18 sites. Then we averaged these functions across all of

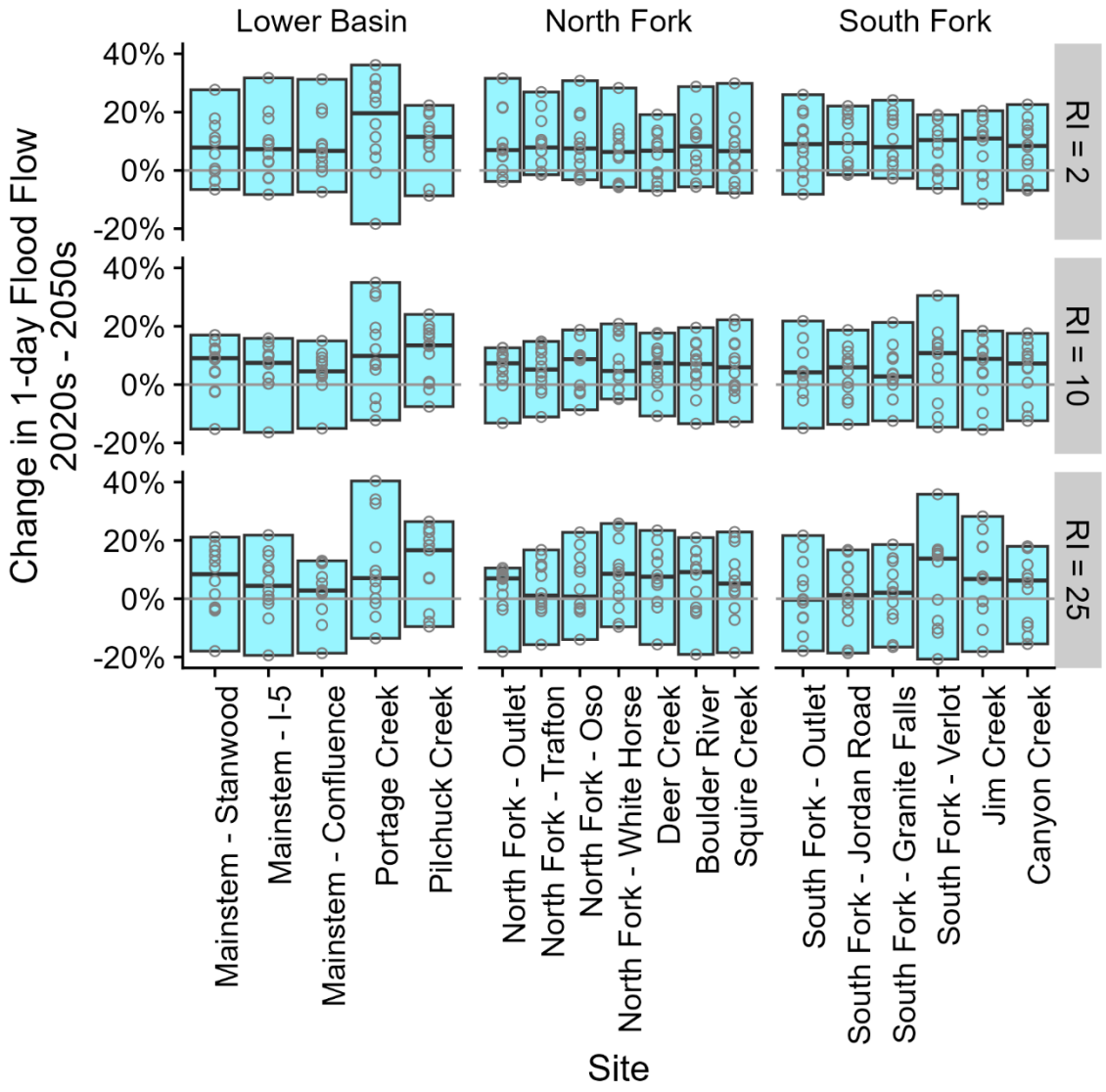

Figure 3-1. Percent increase in 1-day flood flow (at 2, 10, and 25 year return intervals) at 18 sites in the Stillaguamish River basin between the 2020s and 2050s. Open circles represent predicted change using individual GCMs. Blue boxes show the range of values predicted from all 12 GCMs for each site. Dark bars represent median values. Data reanalyzed from Mauger et al. (2021).

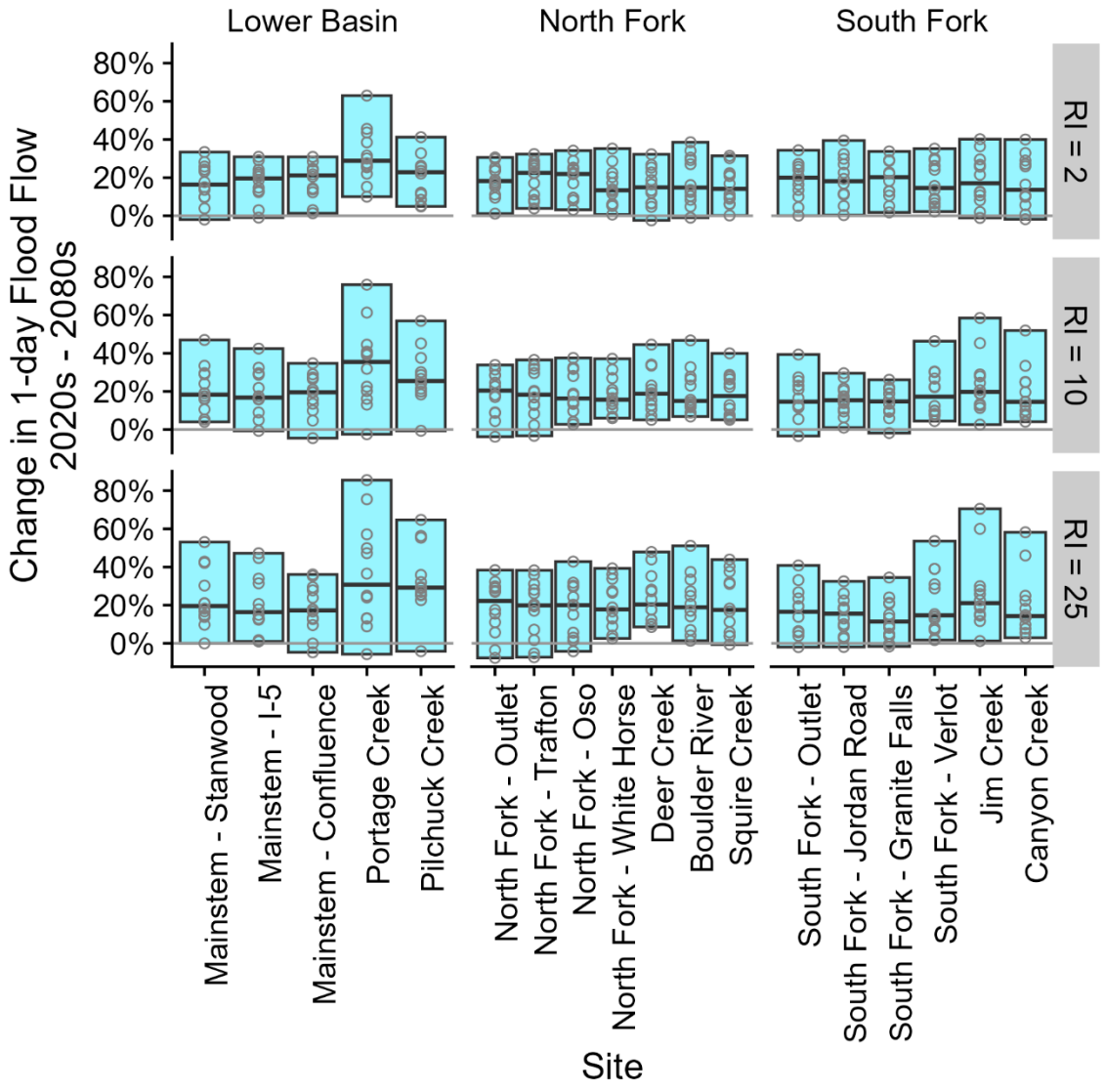

Figure 3-2. Percent increase in 1-day flood flow (at 2, 10, and 25 year return intervals) at 18 sites in the Stillaguamish River basin between the 2020s and 2080s. Open circles represent predicted change using individual GCMs. Blue boxes show the range of values predicted from all 12 GCMs for each site. Dark bars represent median values. Data reanalyzed from Mauger et al. (2021).

the GCMs at each site for each era to create curves representing the ensemble mean percent change in flow at each recurrence interval (Figure 3-3).

Within each site and time period, there was very little difference in the predicted percent change in highest 1-day flood flow across return intervals (Figure 3-3). There was also relatively little variation in predicted percent change among sites. There was a greater

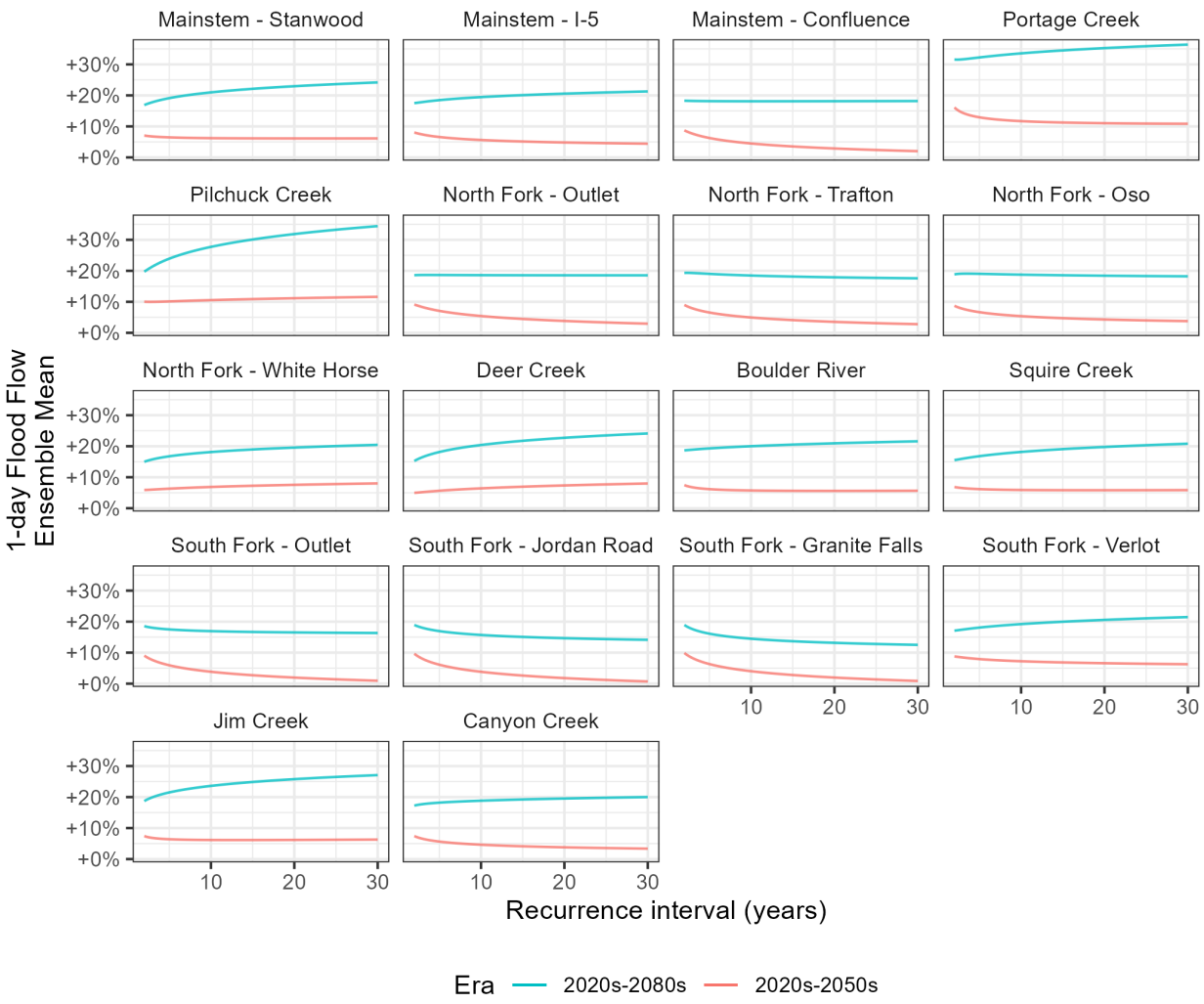

Figure 3-3. Ensemble mean predicted percent change in 1-day flood flow, for 18 sites in the Stillaguamish River basin as a function of recurrence interval. Changes between the 2020s and 2050s are shown in red, and changes between the 2020s and 2080s are shown in teal. (data reanalyzed from Mauger et al. (2021)).

predicted percent change in flood flow from the 2020s to 2080s, at all sites. Some smaller streams (Pilchuck Creek, Portage Creek, Jim Creek) showed greater predicted percent change relative to other sites, but otherwise there was very little spatial pattern to the relationships between flood flow change and recurrence interval.

Given the minor degree of spatial variation in predicted flood flow changes, we used flood flow at the Trafton gage (USGS gage #12167000) as an index of annual basin-wide incubation survival as in prior studies (Zimmerman et al. 2015b, Voloshin et al. 2022). To estimate change in flood flows for each future era in the HARP Model, we averaged predicted percent changes in flood flows at the Trafton gage for the 2, 5, 10, 25, 50, and 100

year return interval floods (Mauger et al. 2021). This yielded a +4.4% increase in flood flow by the 2050s and+18.1% increase by the 2080s. The increased flood flows were then used in the incubation survival function to estimate the increase in egg mortality as a function of increasing flood flow (Nicol et al. 2022).

Voloshin et al. (2022) empirically related egg-to-outmigrant survival to the highest one-day average discharge at USGS gage 12167000.

$$p_{pf} = 0.30154\, e^{-7\times10^{-5}Q_{peak}}$$

Where p_{pf} is egg-to-smolt survival, and Q_{peak} is greatest mean daily discharge (cubic feet per second) between October 1 and January 31 at USGS gage 12167000. In the HARP Model we calculated the highest one-day average discharge as the maximum daily discharge during the entire incubation period (between August 1 and May 10). We used this value to create an incubation productivity multiplier p_{scalar}

$$p_{scalar} = \frac{p_{pf_{era}}}{p_{pf_{med}}}$$

where $p_{pf_{era}}$ is the predicted egg-to-smolt survival based on the adjusted median highest one-day average flow for the modeled era and $p_{pf_{med}}$ is the predicted egg-to-smolt survival based on the observed median highest one-day average flow at USGS gage #12167000 (Table 3-3). We multiplied p_{scalar} by each subbasin's baseline incubation productivity to produce a cumulative incubation productivity for each subbasin.

$$p_{incubation} = p_{fines} \times p_{scalar}$$

Where $p_{incubation}$ is total incubation productivity and p_{fines} is the predicted incubation productivity based on percent fines.

Table 3-3. Era-adjusted one-day average flows and incubation productivity scalars for median highest one-day average flows in each model era.

Era	Era-adjusted median Q_{1-day} (cfs)	Median p_{scalar}
Current	16,850	1
Mid-century	17,591	0.95
Late-century	19,900	0.81

3.1.2 Low Flow Change

Within each 30-year era, we also calculated 7-day annual low flow (the lowest 7-day mean flow) for each of the 18 sites for each year and GCM. We first calculated log Pearson III non-exceedance (low flow) probability curves for each 30-year era for each site and GCM, then calculated the percent change in low flow from the current era to the mid- or late-century as a function of recurrence interval for each of the 12 GCMs (Figure 3-4, Figure 3-5). We then averaged these functions across all of the GCMs at each site for each era to create curves representing the ensemble percent change in flow as a function of recurrence interval (Figure 3-6).

There was substantial variation in the predicted percent change in 7-day average low flow across return intervals, with greater decreases in low flow at the more frequent return intervals (Figure 3-6). That is, the models predict greater decreases in frequently occurring low flows and relatively smaller decreases in more extreme, less frequent low flows.

In addition, there was substantial spatial variation in changes in low flows across the Stillaguamish River basin (Figure 3-6). In the lower basin sites, most GCMs yielded minimal changes in future low flows. In the North Fork Stillaguamish and its tributaries, the majority of GCMs predict flow decreases from the 2020s to 2050s, and nearly all GCMs predict flow decreases from the 2020s to 2080s. The South Fork showed the greatest magnitude in percent low flow change in both mid- and late-century (Figures 3-4 and 3-5).

This spatial variation was associated with drainage basin elevation (Table 3-4, Figure 3-7), with higher-elevation sites generally experiencing greater changes in low flows across all recurrence intervals. We grouped the sites into three low-flow response groups, a "Lower" group containing low-elevation sites with small predicted changes to low flows, a "Middle" group containing moderate-elevation sites with larger predicted changes to low flows, and an "Upper" group containing three high-elevation sites in the upper South Fork Stillaguamish with large predicted changes to low flows (Figure 3-7). We then assigned a response group to each model subbasin based on the mean elevation of its contributing drainage basin (Figure 3-8).

We averaged the percent change in low flow by recurrence interval within each of the three elevation groups and two future time periods to create a total of six functions describing future change in low flow across the basin. We reduced each of these relationships into simple power functions using log-log regression (Figure 3-9, Table 3-5). We modeled relative changes in summer wetted width occurring at half the rate of relative changes in streamflow (Leopold and Maddock 1953, Beechie et al. 2023). Therefore, we adjusted future summer wetted width with the following equation

$$ws_i = ws_{RI2} * \left(\frac{Q_{low,i}\left(1 + a\ RI_i{}^{b}\right)}{Q_{low,RI2}} \right)^{j}$$

where ws_i is the summer wetted width in simulation year j, ws_{RI2} is the summer wetted width in a median year, a and b are constants specific to each model era and response

group (Table 3-5), $Q_{low,i}$ is the simulated low flow, or the climate-specific median low flow when the model is run deterministically, $Q_{low,RI2}$ is the median low flow under current conditions, j is a hydraulic geometry constant (usually denoted as b), and RI_i is the recurrence interval of the simulated low flow. Empirical studies have produced a wide range of hydraulic geometry parameters, which depend on channel size, shape, and roughness (Singh and Zhang 2008). We selected an exponent of 0.5 to represent a value similar to that empirically observed in the Chehalis River basin (Beechie et al. 2023), and within the high end of values observed at other sites.

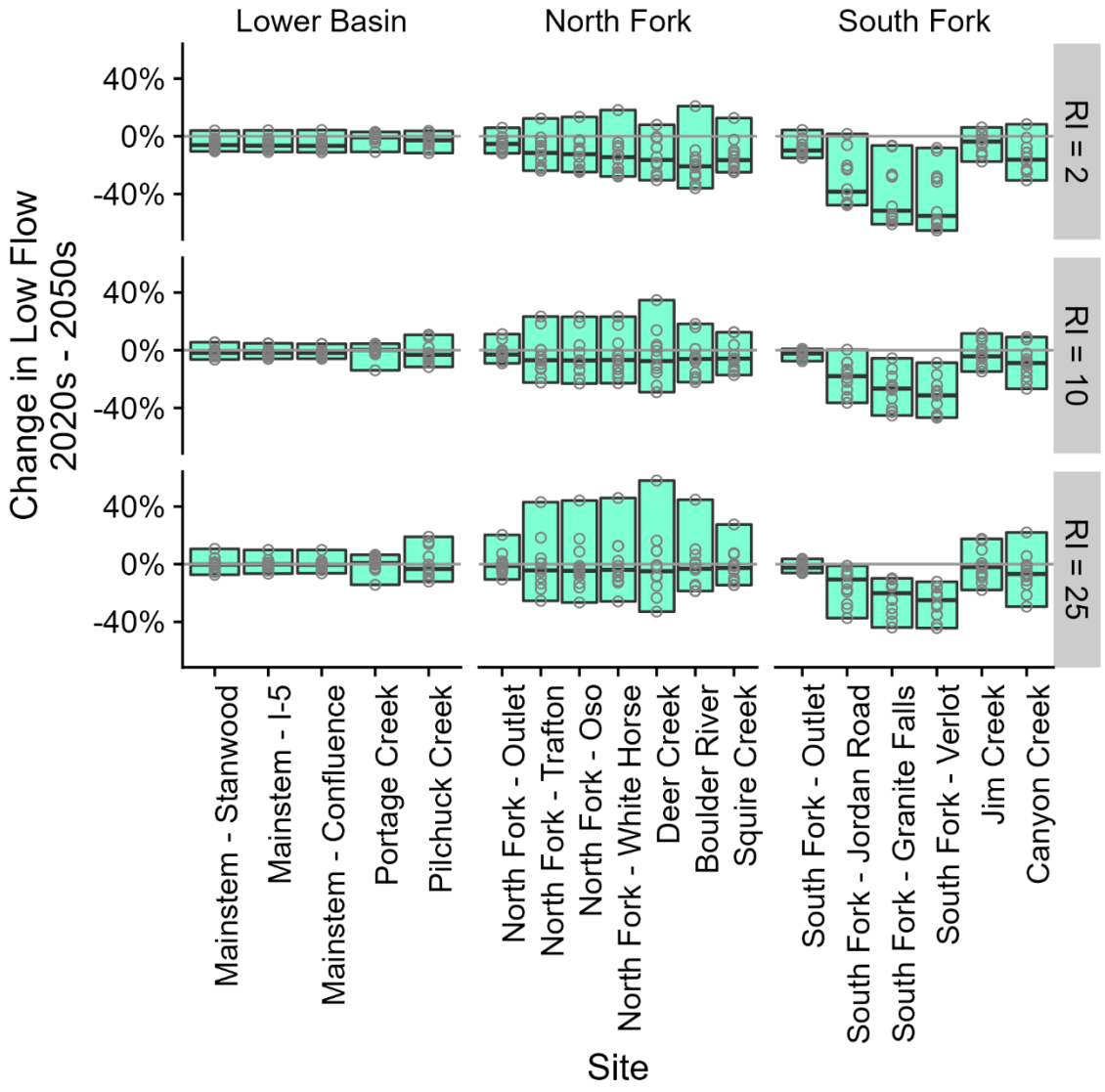

Figure 3-4. Percent decrease in 7-day low flow (at 2, 10, and 25 year return intervals) at 18 sites in the Stillaguamish River basin between the 2020s and 2050s. Open circles represent predicted change using individual GCMs. Teal boxes show the range of values predicted from all 12 GCMs for each site. Dark bars represent median values. Data reanalyzed from Mauger et al. (2021).

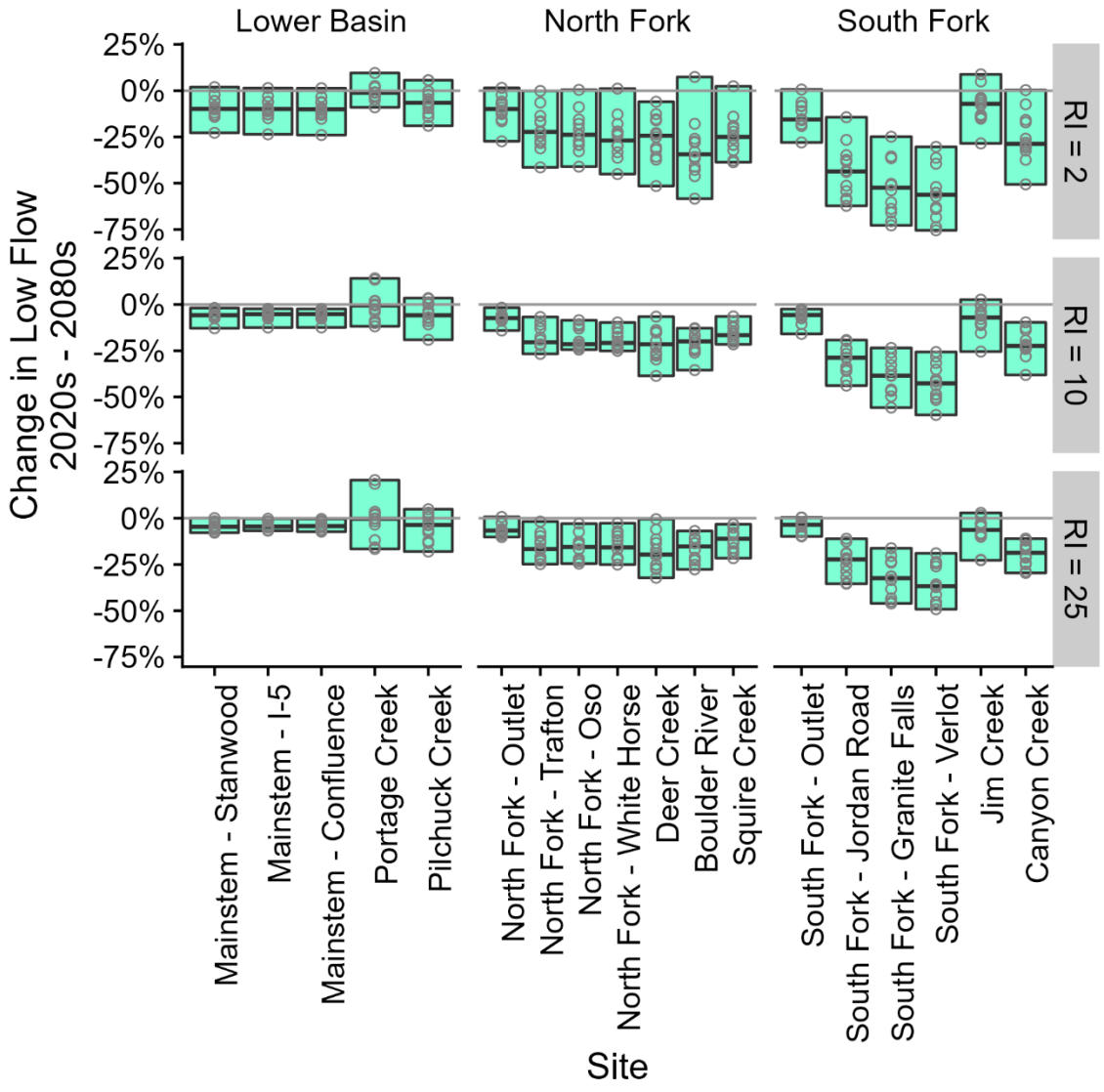

Figure 3-5. Percent decrease in 7-day low flow (at 2, 10, and 25 year return intervals) at 18 sites in the Stillaguamish River basin between the 2020s and 2080s. Open circles represent predicted change using individual GCMs. Teal boxes show the range of values predicted from all 12 GCMs for each site. Dark bars represent median values. Data reanalyzed from Mauger et al. (2021).

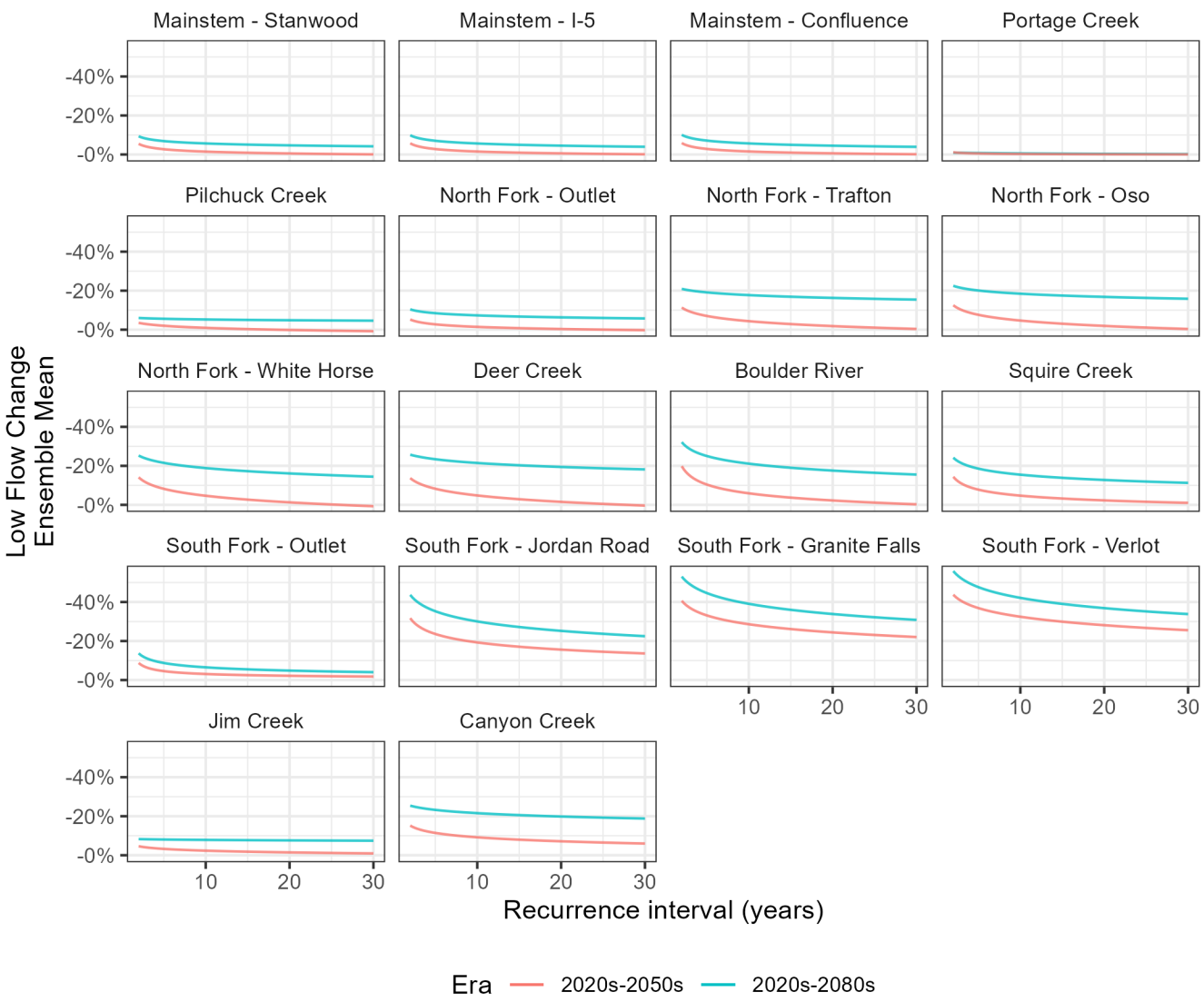

Figure 3-6. Ensemble mean modeled change in 7-day average low flow as a function of recurrence interval. Changes between the 2020s and 2050s are shown in red, and changes between the 2020s and 2080s are shown in teal. Values higher on the Y axis represent larger decreases in annual low flow (data reanalyzed from Mauger et al. 2021).

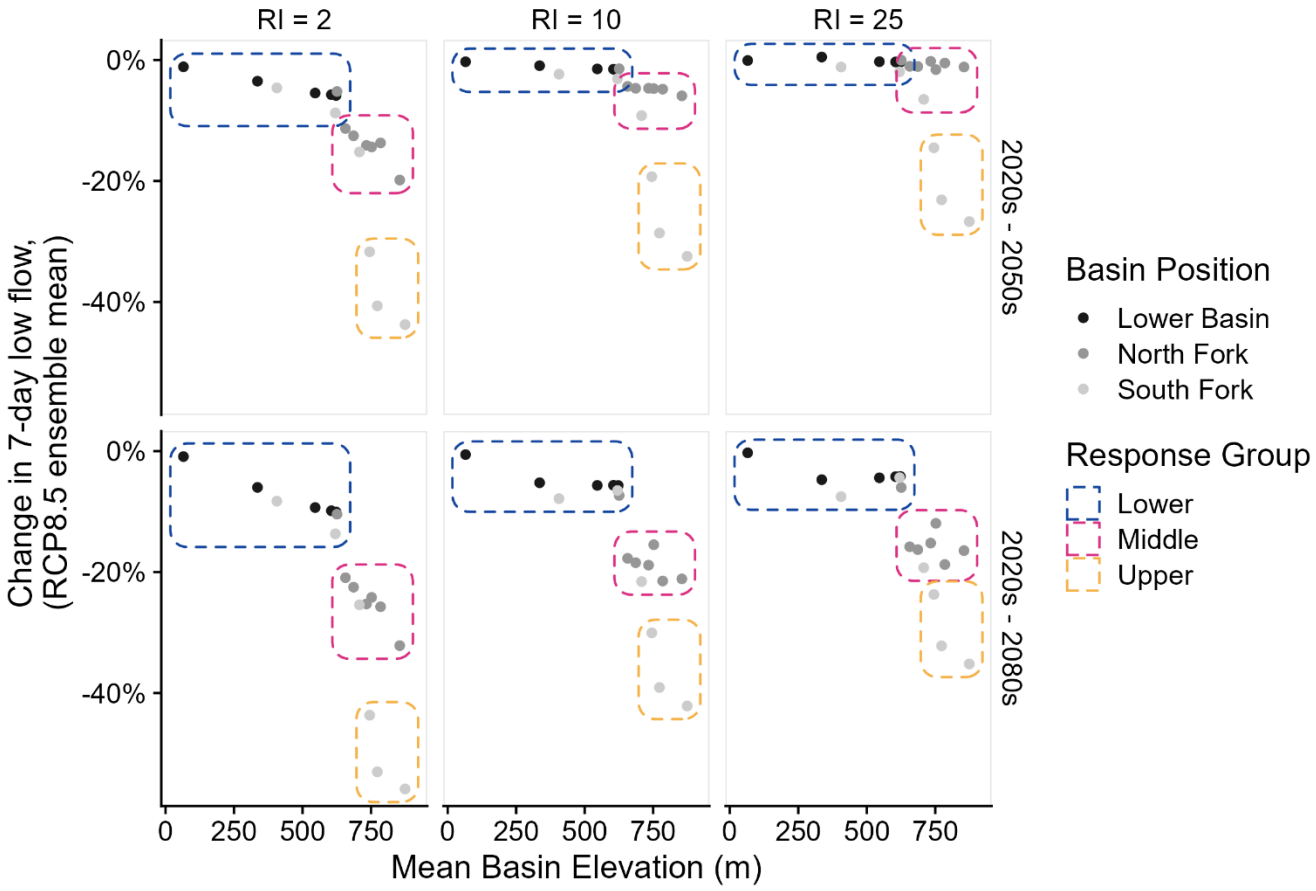

Figure 3-7. Ensemble mean predicted change in 7-day average low flow as a function of mean basin elevation at three different recurrence intervals and two different time periods (2020s-2050s, top and 2020s-2080s, bottom). Basin positions are shown in grayscale, and response groups are outlined by colored boxes. Mean elevations were calculated by delineating individual drainage basins for each flow model site from a conditioned 10-m DEM. Then DEM elevations were averaged within each drainage basin. The pour point for the "Mainstem – Stanwood" site was moved east to the Hat Slough – mainstem confluence to improve watershed delineation on very flat terrain. Flow data reanalyzed from Mauger et al. (2021).

Table 3-4. List of flow prediction sites from Mauger et al. (2021) and associated drainage areas and mean drainage basin elevations calculated from a 10-m NED DEM.

CIG Flow Prediction Site	Drainage Area (km^2)	Mean Drainage Basin Elevation (m)
Mainstem – Stanwood[1]	1,725	546
Mainstem - I-5	1,434	605
Mainstem - Confluence	1,389	622
Portage Creek	48	65
Pilchuck Creek	206	336
North Fork - Outlet	728	626
North Fork – Trafton[2]	678	657
North Fork - Oso	409	686
North Fork - White Horse	209	733
Deer Creek	173	785
Boulder River	68	855
Squire Creek	61	752
South Fork - Outlet	660	620
South Fork - Jordan Road	470	745
South Fork - Granite Falls[3]	304	773
South Fork - Verlot	222	874
Jim Creek	125	406
Canyon Creek	161	708

[1] Corresponds to USGS gage 12170300. The pour point for this site was moved upstream to the confluence of the old mainstem channel and Hat Slough due to watershed delineation issues on very flat topography.
[2] Corresponds to USGS gage 12167000
[3] Corresponds to USGS gage 12161000

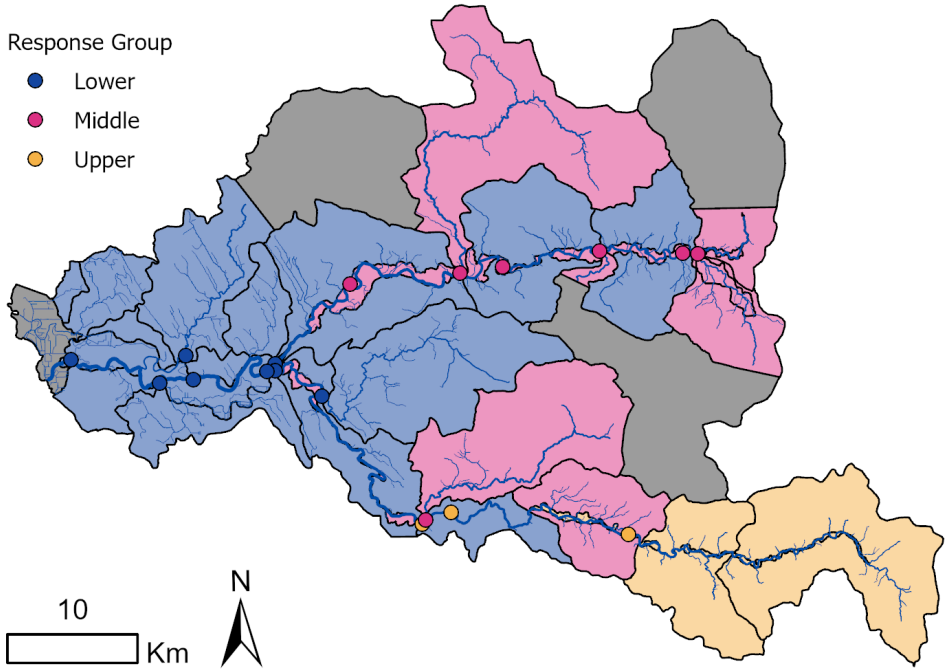

Figure 3-8. Flow prediction sites from Mauger et al. (2021) overlain on HARP Model subbasins. Prediction sites and subbasins draining low-elevation basins in the “Lower” response group are colored blue; the “Middle” elevation response group is colored pink; the “Upper” elevation response group is colored orange.

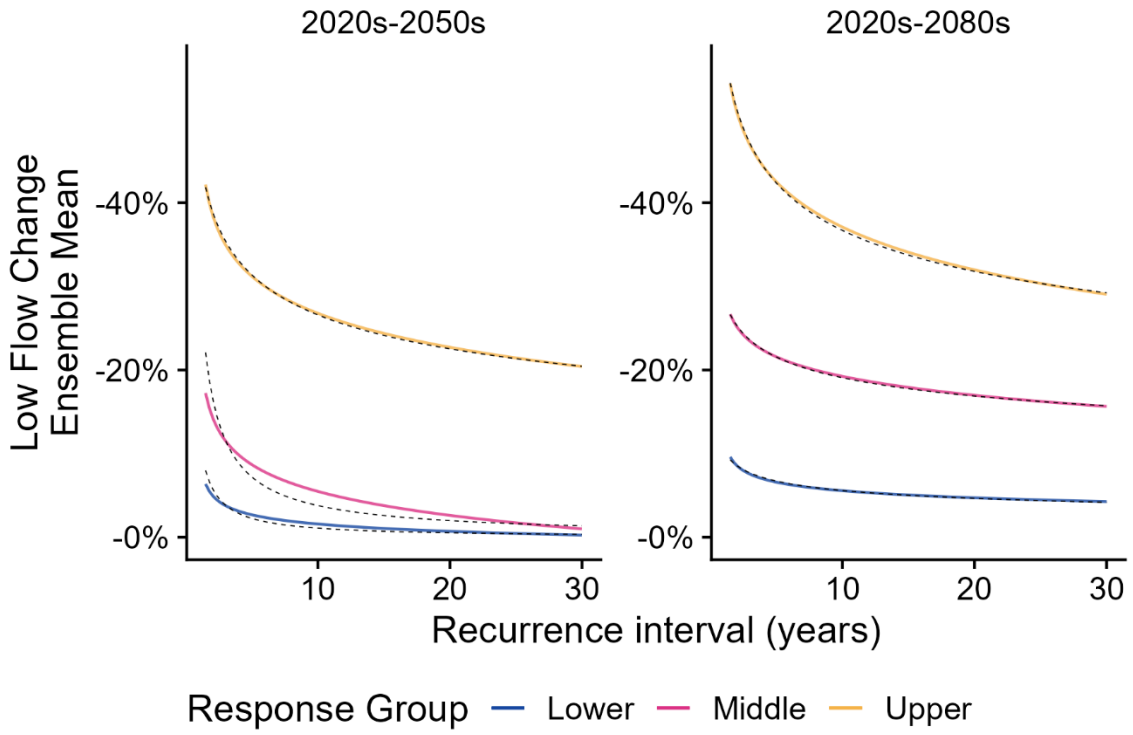

Figure 3-9. Mean change in predicted low flow by response group (colored lines) overlain with simplified best-fit power functions (dotted lines).

Table 3-5. Low flow change model coefficients for a power function in the form $\%\Delta Q_{low} = aRI^b$ where $\%\Delta Q_{low}$ is the percent change in low flow relative to current, RI is the recurrence interval, and *a* and *b* are constants. Predicted changes in discharge and summer wetted width are $\%\Delta Q_{median}$ and $\%\Delta W_{median}$, respectively, for low flows with a 2-year recurrence interval.

Response Group	a	b	$\%\Delta Q_{median}$ $(a*2^b)$	$\%\Delta W_{median}$ $(1+a*2^b)^{0.5}-1$
2020s-2050s				
Lower	-0.122	-1.050	-5.9%	-2.9%
Middle	-0.322	-0.930	-16.9%	-8.5%
Upper	-0.461	-0.239	-39.1%	-19.5%
2020s-2080s				
Lower	-0.103	-0.266	-8.6%	-4.3%
Middle	-0.286	-0.176	-25.3%	-12.7%
Upper	-0.591	-0.207	-51.2%	-25.6%

3.1.3 Stream Temperature Change

Siegel et al. (unpublished data) used a statistical model and 10 downscaled General Circulation Models (GCMs) to produce spatially explicit daily mean stream temperature predictions along variable-length ~1 km reaches for the PNW from 1970 to 2099 under the RCP8.5 emissions scenario. From the data in the Stillaguamish River, we estimated the change in two temperature metrics (maximum 7-day average daily average and June 1-21 average daily average) from the 2020s to the 2050s and 2080s, and then used an empirical correction factor to translate the change in the average temperature metrics to changes in maximum temperature metrics required for the HARP Model (maximum 7-day average daily maximum that affects adult spawners, and June 1-21 average daily maximum that affects late outmigrating juvenile Chinook). Finally, we added the modeled changes in maximum temperature metrics to the modeled current maximum temperature metrics from our Phase 1 analysis (Beechie et al. 2022) to estimate stream temperature in each reach in the mid-century (2050s) and late-century (2080s) scenarios.

The Siegel et al. analysis yielded 109,570 temperature predictions (10,957 days x 10 climate models) for each era at each reach. For each reach and era (2020s, 2050s, and 2080s), we first calculated the maximum 7-day average daily average (max 7-DADA) and June 1-21 average daily average (June 1-21 ADA) within each year for each climate model. We then averaged each metric across the 10 models and 30 years within each era for each reach, yielding an interannual ensemble mean of each temperature metric for each reach and era. That is, each reach in each era has one ensemble mean value for the max 7-DADA and the June 1-21 ADA. Finally, we calculated future temperature change in each reach as the difference between the 2050s or 2080s ensemble mean temperature metric and the 2020s ensemble mean temperature metric.

The Siegel et al. stream network was much coarser than the NHD 1:24,000 hydrography we used for the HARP Model (Figure 3-10), so we transferred estimated changes in the maximum 7-DADA and June 1-21 ADA metrics to the HARP hydrography for those stream reaches that could be paired across the two stream layers. For the many small-to-medium sized streams in the HARP network were not modeled by Siegel et al., we estimated changes in maximum 7-DADA and June 1-21 ADA based on the median of temperature changes for similarly-sized streams modeled by Siegel et al. in the Stillaguamish or Skykomish basins.

Since both temperature metrics were based on daily averages, we applied an empirical correction factor of 1.06 to the maximum 7-DADA and June 1-21 ADA to estimate the equivalent change in the maximum 7-DADM and June 1-21 ADM for the HARP Model (final values in Table 3-6). The correction factor was based on the slope of the relationship between summer (June 1 – September 30) maximum 7DADM and maximum 7-DADA temperature from the NorWeST observed temperature dataset (21,541 daily observations between 2003 and 2013, $r^2 = 0.95$, $p < 10^{-16}$). This gave us the estimated change in the maximum 7-DADM and Jun 1-21 ADM for each reach in the Siegel et al. stream network from the 2020s to the 2050s and 2080s (Figure 3-11).

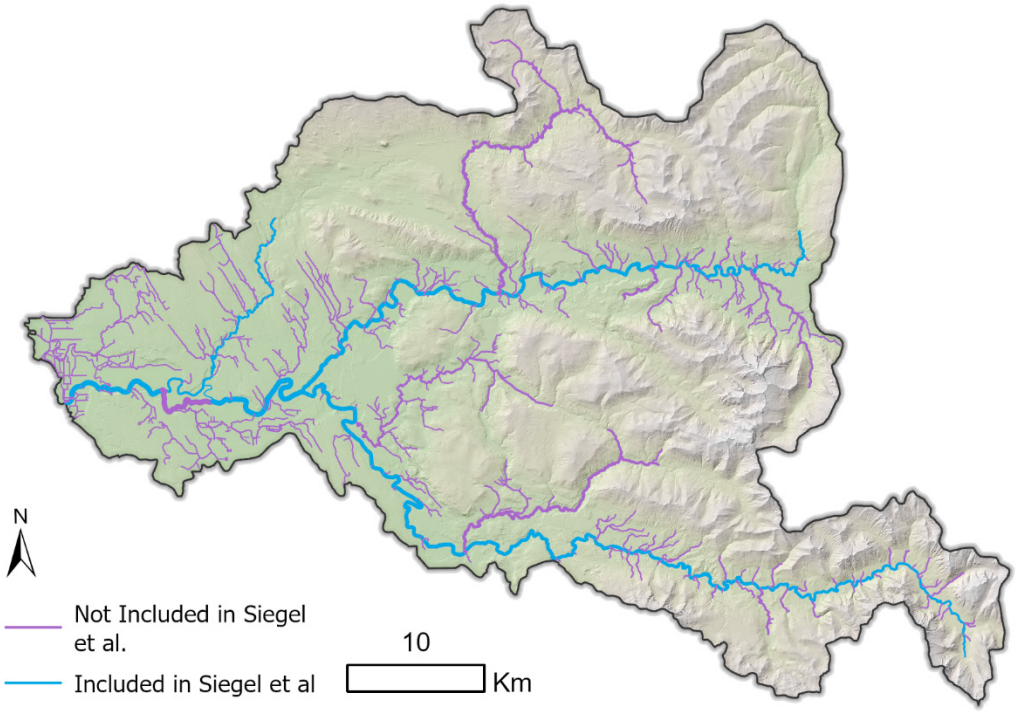

Figure 3-10. Comparison of the Siegel et al. stream network and the HARP Model hydrography. Reaches included in the Siegel et al. analysis are shown in blue. HARP Model reaches not included in the Siegel et al. analysis are shown in purple.

Table 3-6. Estimated values of the change in annual maximum 7-DADM and Jun 1-21 ADM for mid- and late-century for small and medium-sized streams.

	Maximum 7-DADM	**June 1-21 ADM**
Change from current to mid-century (2050s)	+0.85°C	+0.93°C
Change from current to late century (2080s)	+1.73°C	+1.85°C

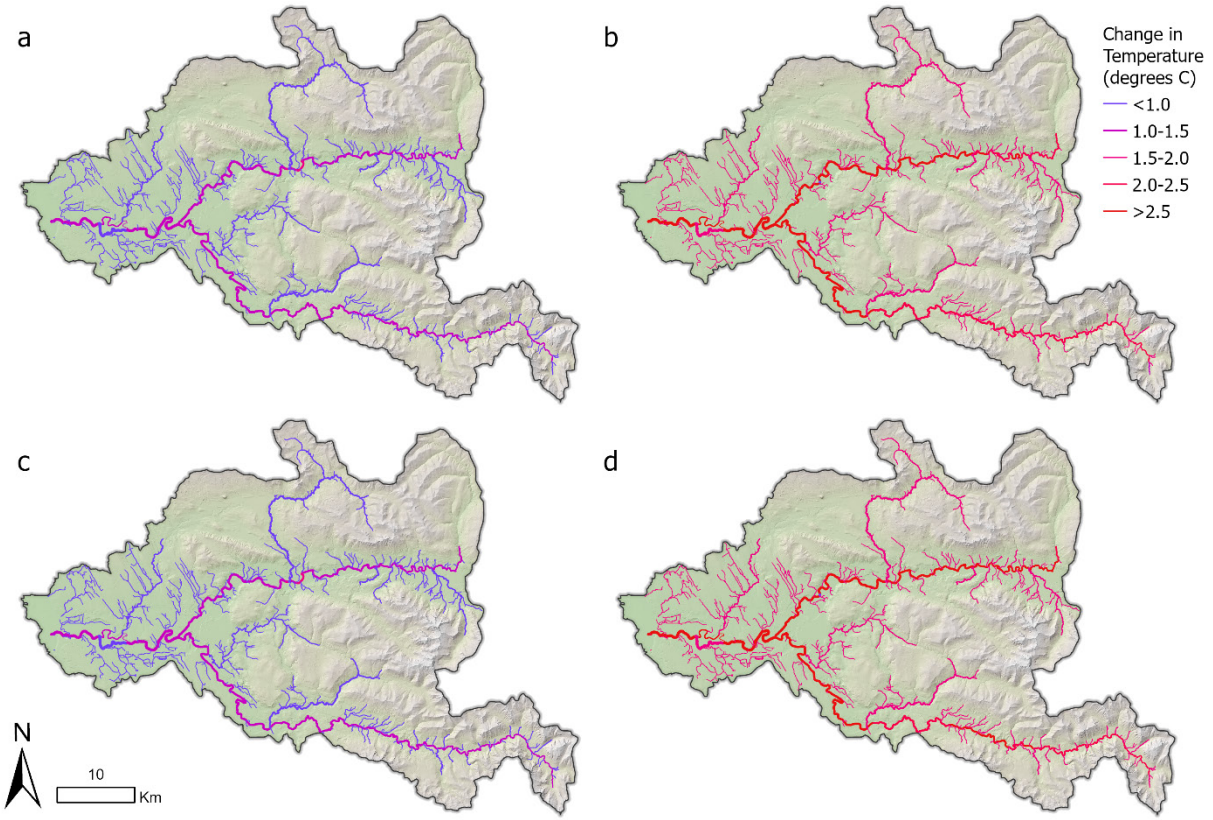

Figure 3-11. Future stream temperature changes used in the no-action scenarios of the HARP Model. (a) Change in maximum 7-DADM between the current and mid-century eras, (b) change in maximum 7-DADM between the current and late-century eras, (c) change in maximum June 1-21 ADM temperatures between the current and mid-century eras (d) change in maximum June 1-21 ADM temperatures between the current and late-century eras.

Once we had estimated changes in the maximum 7-DADM and Jun 1-21 ADM for the 2050s and 2080s for each reach in our attributed hydrography, we added those estimated changes to the current temperatures and subtracted modeled temperature changes due to natural canopy growth (Seixas et al. 2018). Shade and floodplain restoration actions can further reduce modeled temperatures in future scenarios (Beechie et al. 2023).

3.1.4 Stochastic Variation in Flood Flow, Low Flow, and Stream Temperature

To simulate stochastic variation in flood flow, low flow, and stream temperature in the life cycle models, we created stream flow and temperature time series using multivariate auto-regressive state-space (MARSS) models. First, we acquired coincident time series of annual flood and low flow from the USGS stream gage on the North Fork Stillaguamish near Arlington (station ID 12167000) and maximum air temperature from a weather station near the town of Monroe (National Climate Data Center, station ID USC00455525). Each

time series was subset to the incubation ranges per species (Chinook salmon, coho salmon, and steelhead) and consisted of 92 years of data (1930 – 2021). Air temperature data were log-transformed, low flow data were inverse transformed, and flood flow data during the Chinook salmon incubation period were square-root transformed. All data were z-scored prior to analysis. We then fit a MARSS model to a time series of the three variables (i.e., flood flow, low flow, and air temperature), which retains their empirical correlation structure (Holmes et al. 2012, 2020). The MARSS model framework includes both a process model and an observation model to examine trends through time. The process model (equation 1) is an estimate of change in the true, hidden state over time. The observation model (equation 2) describes what we measure, which relates actual observations to the unobservable process equation.

$$\mathbf{x_t} = \mathbf{B}\mathbf{x}_{t-1} + \mathbf{w}_t;\ \mathbf{w_t} \sim \text{MVN}\ (0, \mathbf{Q}) \qquad \text{Eq. 1}$$

$$\mathbf{y}_t = \mathbf{Z}\mathbf{x_t} + \mathbf{v_t};\ \mathbf{v_t} \sim \text{MVN}\ (0, \mathbf{R}) \qquad \text{Eq. 2}$$

In the process model (equation1), $\mathbf{x_t}$ is a *j* x 1 vector of hidden states in year *t.* **B** is a *j* x *j* matrix whose diagonal elements determine the degree of mean-reversion of each state. We set the diagonal elements of the **B** matrix to be unequal among states. The process errors in the *j* x 1 vector $\mathbf{w_t}$ are drawn from a multivariate normal distribution (MVN) with a mean of 0 and variance-covariance matrix **Q.** We set **Q** to be unconstrained. In the observation model (equation 2), $\mathbf{y_t}$ is a *j* x 1 vector of observed flood flow, low flow, and maximum air temperature in year *t.* **Z** is a *i* x *i* matrix that connects each observed time series to their hidden states ($\mathbf{x_t}$). Here, **Z** is an identity matrix. The observation errors in the *i* x 1 vector $\mathbf{v_t}$ are distributed as multivariate normal with a mean of 0 and variance-covariance matrix **R.** We modeled **R** as zero.

The MARSS model was subsequently used to simulate 100 time series of annual flood flow, low flow, and air temperature for 100 years. The simulated air temperature time series was converted to stream temperature using regression coefficients estimated using the NorWeST 7-day average daily maximum stream temperature data in the lower Stillaguamish River (Isaak et al. 2017) ($r^2 = 0.78$, $p = <0.001$):

$$\text{Stream temperature} = \text{Air temperature} * 0.5 + 6.08 \qquad \text{Eq. 3}$$

We then subtracted the mean of all simulated stream temperatures from each simulated stream temperature to create a time series of maximum 7-DADM temperature differences. The differences were also converted into June temperature differences using a regression coefficient from NorWeST stream temperature data (Beechie et al. 2022). These temperature differences were added each year to each reach's stream temperature during a stochastic model run.

Simulated flood flow increases are based on model era (+4.4% for mid-century or +18.1% for late century). We used these values to create an incubation productivity multiplier p_{scalar}:

$$p_{scalar} = \frac{p_{pf_i}}{p_{pf_{med}}}$$

where p_{pf_i} is the predicted egg-to-smolt survival based on the era-adjusted simulated annual flood flow and $p_{pf_{med}}$ is the predicted egg-to-smolt survival based on the observed median highest one-day average flow at USGS gage #12167000. As in the deterministic model, p_{scalar} was used to adjust overall incubation productivity.

We calculated non-exceedance recurrence intervals for each modeled low flow using a log-Pearson III distribution based on observed low flows at USGS gage #12167000 (mean = 5.45, sd = 0.274, skewness = 0.467, all values refer to log-transformed data). Simulated summer wetted widths were adjusted at each reach based on simulated low flow, model era, low flow recurrence interval, and location in the basin using the formula

$$ws_i = ws_{RI2} * \left(\frac{Q_{low,i}\left(1 + a\ RI_i^{\ b}\right)}{Q_{low,RI2}}\right)^k$$

Where ws_i is the summer wetted width in simulation year i, ws_{RI2} is the wetted width in a median year (as used in the current model era when the model is run deterministically), a and b are constants specific to each model era and response group (Table 3-5), $Q_{low,i}$ is the simulated low flow, $Q_{low,RI2}$ is the median low flow under current conditions, k is a hydraulic geometry constant set to 0.5, and RI_i is the recurrence interval of the simulated low flow.

3.1.5 Time Series Simulation

In Phase 2 for the stochastic model runs, we simulated 100 separate 100-year time series of annual habitat conditions for each combination of modeled climate condition (2020s, 2050s, or 2080s) and restoration scenario (No Action, diagnostic scenario, or custom scenario). We ran each time series through the life-cycle model to produce 10,000 years of simulated abundances for each climate condition-scenario pair (450,000 total). When the HARP Model is run stochastically, the same stochastic time series is used for model burn-in (50-150 years) and full model run. Examples of the resulting variation in spawner abundances are shown in Figure 3-12 and Figure 3-13.

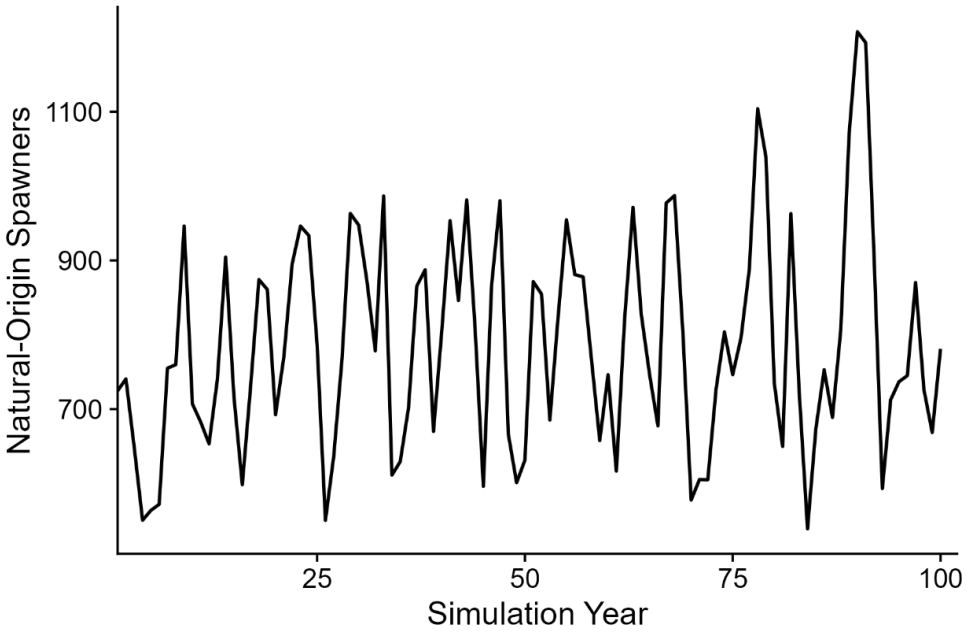

Figure 3-12. Annual variation in spawner abundance for a single 100-year iteration of the stochastic life-cycle model for Chinook salmon in the Stillaguamish River basin under current climate conditions, without habitat restoration.

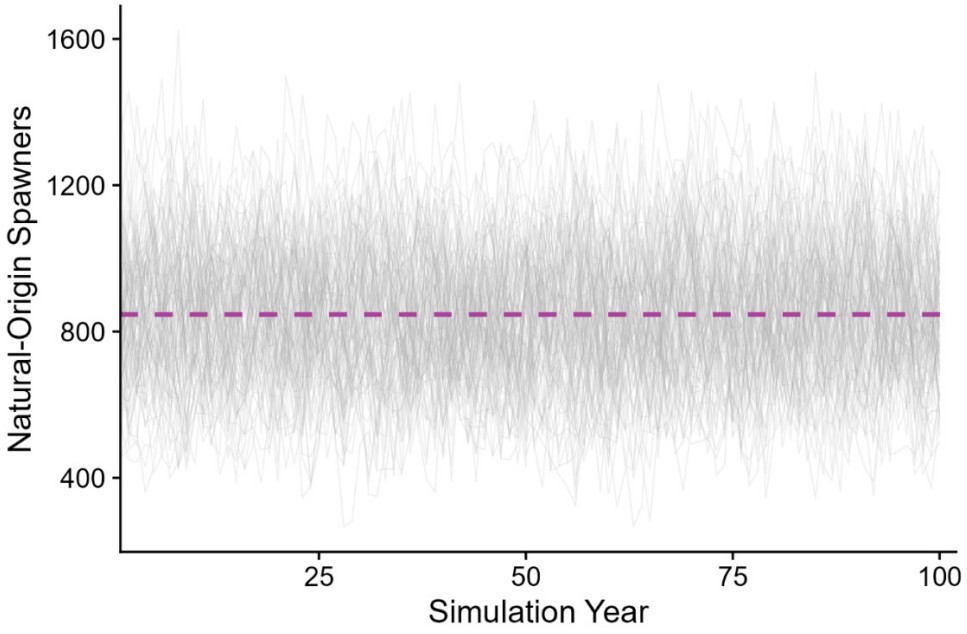

Figure 3-13. Annual variation in spawner abundance for 100 iterations (100 years each) of the stochastic life-cycle model for Chinook salmon in the Stillaguamish River basin under current climate conditions, without habitat restoration. Thin gray lines are the 100 iterations of 100-year time series. Dashed purple line is the median spawner abundance across all simulations and years.

3.2 Modeled Restoration Scenarios

Our approach to developing restoration strategies was to first develop draft scenarios based on the diagnostic scenario results, and then to have local stakeholders review and refine those strategies based on local knowledge and feasibility of implementation for each action type. Each restoration strategy identifies restoration actions and intensities for each subbasin, so that each restoration strategy is tailored to local restoration potential for each action type in every subbasin. Restoration intensity ranges from 0 to 1, indicating the percentage of the difference between natural potential and current condition to be restored. An intensity of 0 indicates no restoration effort for that action type, and non-zero intensity indicates that restoration effort for that action type moves life-stage habitat capacity and productivity the specified percentage from the current condition toward the natural potential condition. For example, an intensity of 0.5 indicates that half of restoration potential will be realized. With respect to restoration implementation, this can be interpreted as restoring half of the stream length to its full natural potential, restoring 100% of the stream length to half of its natural potential, or some combination of the two.

3.2.1 Development of Restoration Scenarios

We developed a Shiny application to display subbasin diagnostic results and other habitat information to facilitate development of the restoration strategies. The most important data display was the result of the diagnostic scenario results for each individual subbasin, which we used to select which restoration action types to focus on in each subbasin. We ran the diagnostic scenarios in each subbasin separately, holding all habitat conditions in other subbasins at the current condition. This allowed us to examine the variation in restoration potential across action types and subbasins.

Based on the subbasin diagnostic results, we developed four alternative restoration strategies using different rule sets and climate time periods (Table 3-7). For each strategy Chinook salmon was the focal species, and action types and restoration intensities were based on the subbasin diagnostic results. Two were based on results of the diagnostic scenario results under current climate conditions (Chinook 1a and Chinook 2a). We also created strategies using the diagnostic analysis run under the 2080s climate (Chinook 1b and Chinook 2b) to identify actions that most increase resilience to climate change. Thresholds of restoration potential and selection of restoration intensities are somewhat arbitrary, but they are designed to illustrate the potential benefit of alternative restoration strategies for Chinook salmon. In addition to the four rule-based strategies, the Stillaguamish Technical Advisory Group (TAG) created two strategies representing low and high levels of restoration intensity, based in part on the HARP Model results and in part on anticipated feasibility of restoration. The final restoration scenarios and maps of the spatial distribution of each action type are in Appendix C.

Table 3-7. Rule sets for developing four alternative draft restoration strategies for Chinook salmon. For all strategies the barrier removal intensity is 1 if restoration potential is >10%.

Draft Strategy	Climate Era	Rule Set
Chinook 1a	2020s	• Restoration potential 10%-40%: 25% intensity • Subbasin restoration potential ≥40%, or total population increase >5%: 75% intensity
Chinook 1b	2080s	• Restoration potential 10%-40%: 25% intensity • Subbasin restoration potential ≥40%, or total population increase >5%: 75% intensity
Chinook 2a	2020s	• Restoration only in Lower Stillaguamish mainstem, NF Stillaguamish 1, SF Stillaguamish 1 • Subbasin restoration potential ≥10%, or total population increase >5%: 75% intensity
Chinook 2b	2080s	• Restoration only in Lower Stillaguamish mainstem, NF Stillaguamish 1, SF Stillaguamish 1 • Subbasin restoration potential ≥10%, or total population increase >5%: 75% intensity

3.2.2 Restoration Scenario Data Structure

The input data format for restoration scenarios is illustrated in Table 3-8 (draft strategy Chinook 1a) and Table 3-9 (draft strategy Chinook 1b), with restoration actions and intensities defined for each subbasin. The rows in each table are subbasins and the columns are restoration action types. Each cell in the table contains a restoration intensity value for subbasin-action combination. For example, a value of 0.75 in the cell for wood augmentation in the Lower Stillaguamish subbasin indicates that the scenario will model restoring 75% of the Chinook salmon restoration potential for wood augmentation. Each draft restoration scenario file can be read into the HARP Model to estimate the potential increase in spawner abundance for Chinook salmon, steelhead, and coho salmon.

Table 3-8. Input data structure for restoration actions and intensities by subbasin. Example excerpted from draft strategy Chinook 1. MB = migration barrier removal, FS = fine sediment reduction, WA = wood augmentation, SH = shade restoration, AR = armor removal, BP = beaver pond restoration, FP = floodplain reconnection.

Subbasin	MB	FS	WA	SH	AR	BP	FP
Lower Stillaguamish	-	-	0.75	-	0.75	-	-
NF Stillaguamish 1	-	-	-	0. 75	-	-	0.75
NF Stillaguamish 2	-	-	-	0.25	-	-	0. 25
NF Stillaguamish 3	-	-	-	-	-	-	0. 25
NF Stillaguamish 4	-	-	-	-	-	-	0. 25
Pilchuck Creek	-	-	0.25	0. 75	-	-	0. 75
Canyon Creek	-	-	0. 25	0.25	0. 25	-	0. 25
Harvey Armstrong	-	-	-	-	-	-	-
Portage Creek	-	-	-	-	-	-	-

Table 3-9. Input data structure for restoration actions and intensities by subbasin. Example excerpted from draft strategy Chinook 1b. MB = migration barrier removal, FS = fine sediment reduction, WA = wood augmentation, SH = shade restoration, AR = armor removal, BP = beaver pond restoration, FP = floodplain reconnection.

Subbasin	MB	FS	WA	SH	AR	BP	FP
Lower Stillaguamish	-	-	0.75	-	0.75	-	-
NF Stillaguamish 1	-	-	-	-	-	-	-
NF Stillaguamish 2	-	-	-	0.25	-	-	0. 75
NF Stillaguamish 3	-	-	-	0.25	-	-	0. 75
NF Stillaguamish 4	-	-	-	0.25	-	-	0. 75
Pilchuck Creek	-	-	-	-	-	-	-
Canyon Creek	-	-	0. 75	0.75	0.25	-	0. 75
Harvey Armstrong	-	-	-	-	-	-	-
Portage Creek	-	-	-	-	-	-	-

3.3 Modeled Hatchery Effects

There are two integrated Chinook salmon hatcheries in the Stillaguamish River basin, a summer-run hatchery on Harvey Creek (a tributary to the North Fork Stillaguamish) and a fall-run captive broodstock hatchery on Brenner Creek (a tributary to the South Fork Stillaguamish near Granite Falls). We modeled each hatchery separately, with broodstock removed from natural- and hatchery-origin spawners in each year and juveniles released into the river at specific locations each year. Figure 3-14 illustrates how hatchery fish were integrated into the Chinook life-cycle model, and Table 3-10 summarizes details of the modeled hatchery actions and effects.

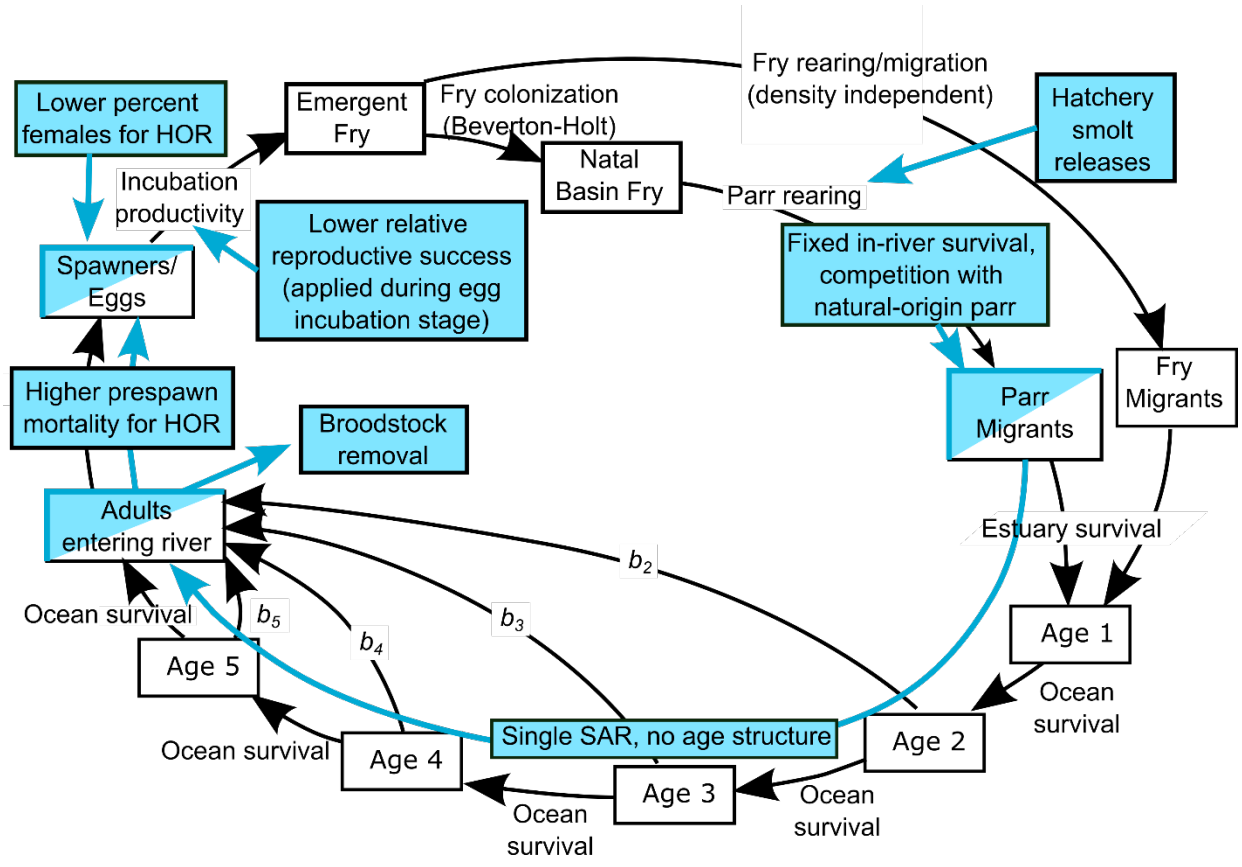

Figure 3-14. Diagram of hatchery effects included in the Phase 2 HARP Model. Blue boxes and blue lines indicate modeled hatchery practices and life stages of hatchery outplants. Blue and white boxes are life stages with mixed hatchery-origin and natural-origin fish. White boxes and black lines represent natural-origin fish (including progeny of hatchery-origin fish that spawned in the river).

Table 3-10. Summary of Chinook hatchery actions and effects included in the Phase 2 HARP Model for the Stillaguamish River basin. See text for more detail on each component.

Action or effect	Description of Modeled Effect	
	North Fork – Harvey Creek	**South Fork – Brenner Creek**
Broodstock removal	Remove 70 natural-origin and 70 hatchery-origin returning adults each year	Not modeled (removal of 400 juveniles from outmigrant population each year is negligible)
Juvenile releases	Add 180,000 parr distributed across NF Mainstem 3, NF Mainstem 2, NF Mainstem 1, and Lower Mainstem subbasins in each year	Add 60,000 parr distributed across SF Mainstem 1 and Lower Mainstem subbasins in each year
In-river survival of hatchery parr	Empirical estimate: 72% of released hatchery juveniles (both hatcheries) survive to parr migrant at the smolt trap	
Competition with natural origin parr	Hatchery juveniles interact with natural juveniles in NF Mainstem 3, NF Mainstem 2, NF Mainstem 1, and Lower Mainstem subbasins, reducing density-dependent survival of natural-origin parr	Hatchery juveniles interact with natural juveniles in SF Mainstem 1 and Lower Mainstem subbasins, reducing density-dependent survival of natural-origin parr
Marine survival	Lower smolt-to-adult return (SAR) for hatchery-origin fish than for natural-origin fish ($SAR_{hatchery}$ = 0.23; $SAR_{natural}$ = 0.38)	
Prespawn mortality	Hatchery-origin spawners have higher temperature-induced prespawn mortality than natural-origin spawners	
Spawning distribution	Empirical estimate: Hatchery-origin adults return to subbasins in proportions informed by carcass survey data, and compete with wild spawners for available spawning capacity	
Relative Reproductive Success (RRS)	Hatchery-origin female returns that spawn in the wild have lower reproductive success (RRS); for simplicity we apply the entire RRS adjustment (0.73) to survival during the egg incubation stage	

3.3.1 Broodstock Collection and Juvenile Releases

Adult broodstock for the Harvey Creek Hatchery are seined from the North Fork Stillaguamish River from late July through September, taking up to 150 summer-run adults per year from pools in North Fork Mainstem Subbasins 2 and 3 (National Marine Fisheries Service 2019). Collections have averaged 141 adults between 1992 and 2021 (minimum = 89, maximum = 181). Fish are spawned when mature, and juveniles are raised in the hatchery to approximately 8 cm in length and then transported to the Whitehorse Hatchery rearing ponds (Rkm 45 on the North Fork Stillaguamish River) where they are volitionally released (late March to mid-June). After mid-June the remaining juveniles are forced to leave the pond (National Marine Fisheries Service 2019). The summer-run release target is 220,000 juveniles per year, but the average hatchery release from brood years 2014-2020 was 179,720.

For the Brenner Creek Hatchery, up to 400 Chinook smolts are seined from the South Fork Stillaguamish River from early March through July, with a target of up to 200 fall-run smolts kept to raise in the hatchery to spawning adults (National Marine Fisheries Service 2019). All smolts are genetically tested and fish other than fall-run are returned to the river. When fall-run adults are captured in the North Fork Stillaguamish River during seining for summer-run adults, those fall-run adults are added to the Brenner Creek broodstock. Fish are spawned when mature, and juveniles are raised in the hatchery until volitional release into Brenner Creek and then to South Fork Mainstem 1 subbasin (near Granite Falls) between late April and early June (National Marine Fisheries Service 2019). The fall-run release target is 200,000 juveniles per year, but the average hatchery release from brood years 2014-2020 was 59,832. Prior year releases were less than 13,000.

In the HARP Model, we remove 140 adult Chinook salmon each year from the North Fork Stillaguamish and its tributaries. We remove 70 hatchery-origin fish and 70-natural-origin fish each year regardless of modeled run size. The seventy natural-origin broodstock fish are removed in quantities proportional to the size of the returning natural-origin spawner population in each subbasin. That is, if subbasin #3 were to receive 50% of the returning natural-origin fish in a given year, 35 fish would be removed from that subbasin as broodstock. Likewise, the seventy hatchery-origin fish are removed proportionally to the size of the returning hatchery-origin run in each North Fork subbasin. This method is intended to simulate random fishing of natural-origin and hatchery-origin individuals during upstream migration. We do not simulate removal of South Fork juveniles for the Brenner Creek hatchery program because the juvenile broodstock target (400 fish) is very small compared to the number of outmigrants.

We do not explicitly model broodstock fecundity or hatchery survival in the model. Rather, we insert 180,000 juvenile Chinook parr into the North Fork Stillaguamish and 60,000 juvenile Chinook parr into the South Fork Stillaguamish each year. Hatchery juveniles are distributed equally among all mainstem subbasins downstream of the release site to simulate outmigration and competition with natural-origin parr. For the Harvey Creek hatchery, 25% of the released parr are inserted into each of the following subbasins: Lower Mainstem Stillaguamish, North Fork Stillaguamish 1, North Fork Stillaguamish 2, and North

Fork Stillaguamish 3. For the Brenner Creek hatchery, 50% of the released parr are inserted into the Lower Mainstem Stillaguamish and 50% into South Fork Stillaguamish 1.

Each year, two groups of 2,500 to 3,000 hatchery-origin juveniles are trucked directly to the lower river for use in smolt trap efficiency trials (Voloshin et al. 2022). We do not explicitly model this alternate migration path in the HARP Model.

In Model 1 (with temperature-related prespawn mortality, Section 3.3.5), expected returns of natural-origin Chinook salmon to the North Fork Stillaguamish drop substantially in the 2050s and 2080s. The drop is enough that removing 70 adults from the river as broodstock would likely become impractical. We ran the model under the no-action scenario under 10 different North Fork hatchery operation intensities ranging from 10% of the current broodstock removal and smolt production to 100% of the current broodstock removal and smolt production. For each model and time period, we identified the greatest North Fork hatchery operation intensity where broodstocking would remove no more than 20% of North Fork natural-origin returners in the median simulation year. Maximum hatchery operation intensities vary between Model 1 and Model 2 because Model 2 (without temperature-related prespawn mortality, Section 3.3.5) produces more returning salmon (Table 3.11). We used these North Fork operation intensities for all climate simulations, except ones in which we varied hatchery operation intensity (Section 4.3) or marine survival (Section 5.4).

3.3.2 Juvenile Competition and Survival in Freshwater

In the HARP Model Chinook salmon juveniles of multiple subpopulations can occupy the same mainstem reaches during rearing and outmigration. Summer-run hatchery-origin juveniles can compete with natural-origin juveniles in the mainstem North Fork and lower mainstem downstream of the White Horse rearing ponds (located in North Fork Stillaguamish 3 subbasin). Fall-run hatchery-origin juveniles can compete with natural-

Table 3.11. Percent of hatchery current hatchery broodstock take by climate scenario and Model version. Model 1 includes temperature-related prespawn mortality whereas Model 2 does not (Section 3.3.5).

Climate Period	With Prespawn Mortality (Model 1)	Without Prespawn Mortality (Model 2)
2020s	100% of current effort	100% of current effort
2050s	70% of current effort	100% of current effort
2080s	30% of current effort	90% of current effort

origin juveniles in the lower South Fork mainstem and lower mainstem downstream of Brenner Creek (located in the South Fork Stillaguamish 1 subbasin).

Because we have estimates of hatchery parr releases and hatchery-origin parr passing the smolt trap, we used an empirical estimate of in-river survival for hatchery-origin juvenile Chinook (Jim Scott, unpublished data). Based on 10 years of data (2006-2015), the average estimated in-river survival for hatchery-origin juvenile Chinook parr is 72%.

Under mid- and late- century climate conditions, hatchery-origin freshwater juvenile survival is slightly reduced based on modeled median June 1-21 temperatures under the no-action scenario. We adjust freshwater survival in reaches exceeding 18°C using the same equation that we used for natural-origin spawners.

In this model structure, the survival estimate of hatchery fish is density-independent and does not respond to habitat restoration. However, we do allow hatchery-origin parr to affect the density-dependent survival of natural-origin parr since hatchery fish outmigrate during natural-origin parr rearing period (Voloshin et al. 2022). We use the relative proportions of hatchery-origin and natural-origin juveniles to adjust rearing capacity for natural-origin parr in each subbasin using the following formula.

$$c_{adj} = c_{habitat} \frac{n_{N.O.fry} \times p_{rear}}{n_{N.O.fry} \times p_{rear} + n_{H.O.parr}}$$

where c_{adj} is the adjusted capacity, $c_{habitat}$ is the intrinsic capacity of the habitats in the subbasin, $n_{N.O.fry}$ is the number of natural-origin fry that have migrated into the subbasin, p_{rear} is the 8-week density-independent rearing productivity for the subbasin, and $n_{H.O.parr}$ is the number of hatchery-origin parr in the subbasin. Note that this interaction only occurs mainstem subbasins that contain or are downstream of hatchery release sites (NF Mainstem 3, NF Mainstem 2, NF Mainstem 1, SF Mainstem 1, and Lower Mainstem).

3.3.3 Juvenile Competition in the Estuary

While Chinook salmon juveniles of multiple subpopulations can also occupy the estuary at the same time, parr-sized hatchery-origin Chinook spend little time in the estuary relative to estuary rearing fry. Therefore, we do not model competition in the estuary. If there are differences in estuary survival between hatchery- and natural-origin Chinook smolts in the estuary, those differences are subsumed into the empirical estimates of smolt-to-adult return rates (Section 3.3.4).

3.3.4 Differential Marine Survival

A number of studies have shown that hatchery-origin salmon have lower smolt-to-adult return (SAR) rates than natural-origin fish (Zimmerman et al. 2015a, Chasco et al. 2021). For this project, WDFW used coded wire tag data for Stillaguamish hatchery-origin and natural-origin Chinook salmon to estimate SAR values (Jim Scott, unpublished data). SAR rates for hatchery-origin returns (HOR) were lower than SAR rates for natural-origin

returns (NOR) for both total run and escapement (Table 3-12). We used the escapement SAR rate to estimate hatchery effects on marine survival of Chinook salmon in the Stillaguamish River basin, which includes all harvest.

3.3.5 Hatchery-origin Returns to Spawning Grounds

The majority of hatchery-origin returns in the Stillaguamish basin spawn in the wild rather than returning to the hatchery rack. WDFW carcass survey data show that most hatchery-origin Chinook spawn in subbasin N.F. Stillaguamish Mainstem 3 (56% of HOR total), followed by N.F. Stillaguamish 2 (26%), and less than 10% in each of the other subbasins (Table 3-13). We modeled the spatial distribution of hatchery-origin returns based on the proportion of marked fish that have been surveyed by WDFW in each subbasin. Hatchery-origin spawners in the North Fork Stillaguamish were 44% female, whereas the natural-origin spawners were 50% female. Sex ratios were held constant across years. While there are a few years of data in the South Fork there were only 42 HOR individuals in the sample (76% female). Due to the low South Fork sample size, we also used the North Fork sex ratios for the South Fork because the North Fork dataset was a longer time series with many more fish in the sample. Hatchery-origin spawners averaged 55% of total spawners from 2002 to 2021 (WDFW and Stillaguamish Tribe, unpublished data).

3.3.5 Temperature Effect on Prespawn Mortality

Spring Chinook salmon spawners are generally quite sensitive to high summer stream temperatures because they enter rivers in spring and hold through the hottest part of the summer prior to spawning in late summer through the fall (Bowerman et al. 2018, 2021). In the Stillaguamish River basin, South Fork Chinook are fall-run fish, which begin entering the river in mid-August and begin spawning in September, whereas North Fork Chinook are summer-run fish, which begin entering the river in early June and begin spawning in mid–August. The fall-run population (South Fork) is arguably adapted to avoid migrating during high summer temperatures, whereas a large percentage of the summer-run

Table 3-12. Average smolt-to-adult return (SAR) rates for hatchery-origin and natural-origin Chinook salmon in the Stillaguamish River basin for outmigrant years 2007-2016 (Jim Scott, WDFW, unpublished data). Total run SAR rate does not include harvest mortality (North Pacific or terminal area).

	Total run SAR	Escapement SAR
Hatchery-origin returns	0.52%	0.23%
Natural-origin returns	0.59%	0.38%

Table 3-13. Spatial distribution of marked carcasses in the North Fork and South Fork Stillaguamish River from 2013 to 2022. Two subbasins that had only 1 record of marked carcasses were excluded.

	Number of marked individuals	Percent of total number of marked individuals
North Fork Hatchery Returns		
Mainstem North Fork Stillaguamish 01	23	3.2%
Mainstem North Fork Stillaguamish 02	189	26.2%
Mainstem North Fork Stillaguamish 03	405	56.1%
Mainstem North Fork Stillaguamish 04	37	5.1%
Squire Creek	8	8.3%
Boulder River	60	1.1%
North Fork Total	*722*	
South Fork Hatchery Returns		
Mainstem South Fork Stillaguamish 01	25	61.0%
Mainstem South Fork Stillaguamish 02	2	4.9%
Jim Creek	14	34.1%
South Fork Total	*41*	

population (North Fork) must also hold in the river through the period of highest temperatures (generally in July and August). Because there is uncertainty in the degree to which Stillaguamish Chinook spawners experience temperature-related prespawn mortality, we ran two versions of the HARP Model, one with temperature-related prespawn mortality (Model 1) and one without (Model 2).

Model 1

Hatchery-origin Chinook spawners are more sensitive to stream temperature during their prespawn holding and migration period than are natural-origin spawners (Bowerman et al. 2018, 2021). The linear model that predicts prespawn mortality for mixed hatchery-origin and natural-origin spring Chinook salmon spawners in the Willamette basin is

$$ln\left(\frac{PSM}{1-PSM}\right) = -9.053 + (0.387 \cdot 7DADM) + (0.029 \cdot PHOS)$$

or

$$PSM = \frac{1}{1 + e^{-(-9.053+(0.387 \cdot 7DADM)+(0.029 \cdot PHOS))}}$$

where *PSM* is prespawn mortality, *7-DADM* is the maximum 7-day average daily maximum temperature, and *pHOS* is percent hatchery-origin spawners (Bowerman et al. 2018). Within the range of *7-DADM* for the Stillaguamish River basin (12° to 29°C), *PSM* would be 2% to 92% for mostly natural-origin spawners and 14% to 99% for mostly hatchery-origin spawners (Figure 3-15). However, in many other basins the difference in prespawn mortality between hatchery-origin and natural-origin spring Chinook spawners is much less than in the Willamette basin (Bowerman et al. 2021). Therefore, we chose to modify the prespawn mortality equation so that hatchery-origin prespawn mortality was consistent with a large number of Chinook salmon populations in the Columbia basin, rather than with the Willamette population (which appears to have more extreme prespawn mortality than other basins).

To calculate prespawn mortality of natural-origin adults, we set *pHOS* equal to 0, yielding the equation:

$$PSM = \frac{1}{1 + e^{-(-9.053+(0.387 \cdot 7DADM))}}$$

For hatchery-origin spawners we replaced the *pHOS* expression with a value set by trial and error to visually approximate the prespawn mortality curve for Upper Columbia hatchery-origin spring-run Chinook salmon in Bowerman et al. (2021) (final value is 0.87):

$$PSM = \frac{1}{1 + e^{-(-9.053+(0.387 \cdot 7DADM)+(0.87))}}$$

We used this equation to represent prespawn morality for hatchery-origin spawners in the Stillaguamish River basin (Figure 3-15).

Model 2

Because Model 1 may overestimate the effect of temperature on prespawn mortality (especially for the fall-run), we also ran a model version without prespawn mortality related to temperature. This model essentially assumes that the Stillaguamish populations are adapted to avoid high temperatures that would cause mortality (either in migration timing or by finding cool water refuges for holding), *and* that they can adjust their spawning timing or holding locations in the future to continue avoiding high temperatures. This alternative may underestimate temperature effects for the summer-run (North Fork) population, but may be more accurate for the fall-run (South Fork) population.

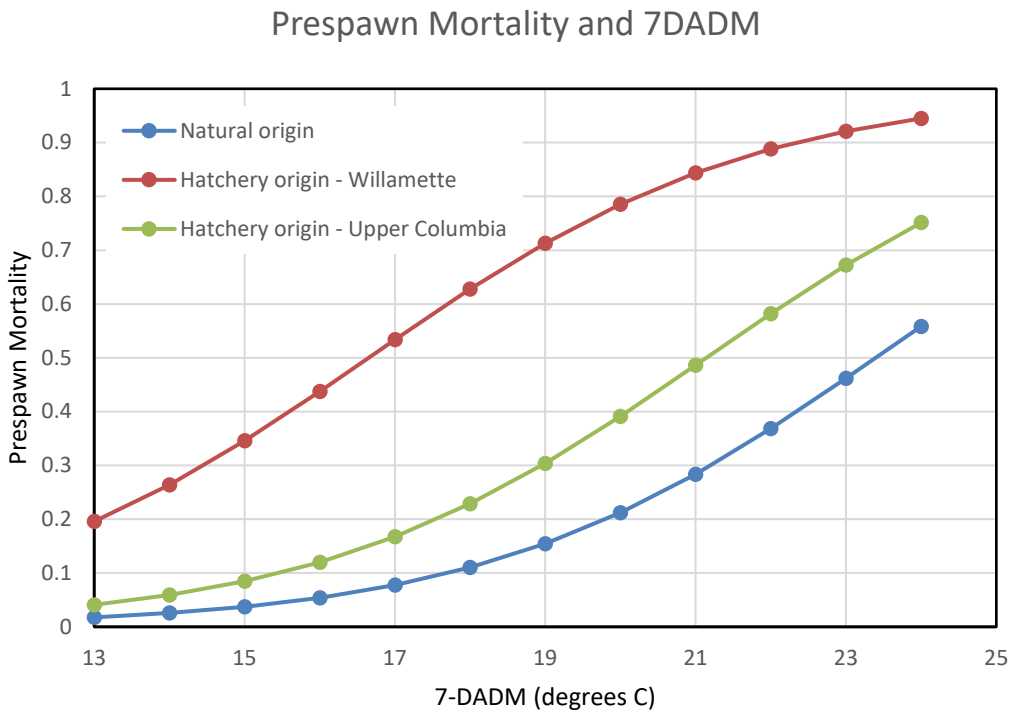

Figure 3-15. Modeled prespawn mortality of Chinook salmon adults as a function of 7-DADM for natural-origin and hatchery-origin spawners, based on the function developed for the Willamette River basin (red and blue lines) (Bowerman et al. 2018). The green line for hatchery origin spawners in the Stillaguamish River basin is similar to that for Upper Columbia spring-run Chinook salmon (shown in Figure 5 in Bowerman et al. 2021). We do not use the function for Willamette hatchery-origin spawners (red line) in this study.

3.3.6 Relative Reproductive Success

Hatchery-origin fish spawning in the wild generally have lower reproductive success (returning adults per spawner) than natural-origin spawners (Christie et al. 2014), and the ratio of hatchery-origin adults per spawner to natural-origin adults per spawner is termed Relative Reproductive Success (RRS). In the HARP Model we applied the RRS value to all progeny of first generation hatchery females spawning in the wild, so that adult returns from HO spawners was 73% of that of NO spawners (data from Christie et al. 2014). For simplicity, we applied this value during the incubation period in the model, based on a finding in the Wenatchee River that reduced RRS likely occurred between spawning and early juvenile rearing (Christie et al. 2014). We applied the RRS in the incubation stage because that stage is density independent, and the calculation is straightforward (0.73 x incubation survival).

3.4 Other Model Changes

3.4.1 Total Rearing Period and Residence Time

Based on Chinook salmon outmigrant data for the Snohomish River basin (Tulalip Tribes, unpublished data), we shortened the Chinook parr-rearing residence time to 9 weeks, and increased the total rearing period to 18 weeks. This effectively doubled the rearing capacity from the Phase 1 model. In both models we estimated subyearling rearing capacity as a function of daily maximum fish density, mean residence time, and the temporal extent of the rearing period to account for multiple groups of fish moving through the same habitats (Jorgensen et al. 2021):

$$c = d \cdot A \cdot \frac{t}{r}$$

where, c is capacity (# of fish), d is maximum daily density (fish/ha), A is habitat area (ha), t is the extent of the rearing period (weeks), and r is the mean residence time (weeks). In the Phase 2 model, we used a total rearing period (t) of 18 weeks and mean residence time in the natal subbasin (r) of 9 weeks, so c is $d \cdot A \cdot 2$.

3.4.2 Adjustments to Chinook Rearing Distribution

Based on stakeholder input, we made two small adjustments to the juvenile rearing distribution. We added juvenile rearing to the lower one mile of Church Creek, and to the lower portion of Portage Creek up to the I-5 crossing. Both river segments are contained in the Lower Mainstem subbasin, so the changes effectively increase Chinook rearing capacity in that subbasin.

3.4.3 Reduced Estuary Rearing Capacity

Estuary rearing capacity is effectively reduced by juvenile salmonids from other basins occupying estuary habitat, especially from the Skagit and Snohomish River basins (Beamer et al. 2016, Hayes et al. 2019, McKinney 2023). In the Stillaguamish estuary we accounted for this using the equation

$$c_{adj} = c_{habitat} \times f_{S.O.fry}$$

where c_{adj} is the adjusted capacity, $c_{habitat}$ is the intrinsic capacity of the estuary, $f_{S.O.fry}$ is the fraction of fry in the Stillaguamish estuary that originated in the Stillaguamish basin. We used a value of 60% for $f_{S.O.fry}$ based on preliminary genotyping results of Stillaguamish estuary Chinook (McKinney 2023). For diagnostic purposes, we also calibrated and ran the model with several other values of $f_{S.O.fry}$ ranging from 20% to 100% (Appendix D).

While we know that the proportion of natal-basin fish varies spatially across individual river deltas (Beamer et al. 2016, Hayes et al. 2019, McKinney 2023), we cannot exactly predict the proportion of natal-basin fish that will occupy newly restored estuary habitats. Moreover, we cannot predict whether habitat restoration or other factors will cause more

rapid increases in Stillaguamish fry migrants (or, conversely, in non-natal juveniles). Therefore, we assumed that the proportions of natal and non-natal fish using the estuary remain constant under all scenarios.

3.4.4 SAR Changes

We received updated data for SAR rates (marine survival) of natural-origin and hatchery-origin Chinook salmon in the Stillaguamish River basin for subyearlings outmigrating between 2007-2016 (Jim Scott, WDFW, unpublished data) (Table 3.10). These survival values represent the total survival of fish between the smolt trap and spawning grounds. The survival calculations rely on annual transgenerational genetic mark-recapture (tGMR) analysis of fin clips collected during late-season spawning surveys. Since spawning surveys in the Stillaguamish are conducted late in the season and may not include carcasses from early-season mortalities, we redefined model SAR rates to include all life stages between the smolt trap and late season spawning grounds. In other words, our model SAR rates includes three separate components: estuarine and nearshore survival, marine survival, and freshwater prespawn survival.

We did not have direct measurements of marine survival for Chinook salmon that outmigrate from the Stillaguamish River as yearlings, but marine survivals have been studied for yearling and subyearling spring Chinook outmigrants in the Skagit basin (Welch et al. 2021). In the Skagit basin, the median yearling SAR rate is 1.55x greater than of the median subyearling SAR rate, so we multiplied the Stillaguamish natural-origin subyearling SAR rate by 1.55 to estimate a SAR rate for yearling outmigrants from the Stillaguamish basin, yielding a subyearling survival estimate of 0.58%. We assumed all yearling outmigrants were of natural origin.

3.4.5 Recalibration of Four Life-Stage Parameters

For the HARP Model in the Stillaguamish basin, four unknown Chinook life stage parameters were calibrated to known data: fry-migrant in-river survival (p_f), the percentage of parr that outmigrate as subyearlings rather than remaining in the river to become yearlings ($percent_{sub}$), early marine survival rate plus harvest (p_{PSp}) for parr migrants, and early marine survival rate plus harvest (p_{PSy}) for yearling migrants. Note that we originally calibrated the early marine survival rates when harvest was not included in the SAR, and early marine (Puget Sound) survival was roughly approximated by SAR rate divided by the annual ocean survivals. With harvest included in the SAR rate, the same calibration results in a parameter that includes both early marine survival and harvest. After installing the climate change and hatchery components of the model, we recalibrated those four parameters. Revised values are p_f = 0.13, $percent_{sub}$ = 0.94, p_{PSp} = 0.016, and p_{PSy} = 0.020. Calibration methods are in Appendix E.

4. Results

The HARP Model simulates effects of habitat change from historical to current conditions, as well as effects of future restoration actions, climate change, and hatchery supplementation. All results presented here include stochastic variation in flood flows, low flows, and stream temperatures in the habitat model, as well as the two Chinook hatchery programs in the life-cycle model. Spawner abundances represent the median value of all stochastic model runs.

4.1 Diagnostic and Restoration Scenarios

The diagnostic scenario results compare median modeled spawner abundance under each diagnostic scenario against the median modeled no-action spawner abundance, and the percent change between the two is the *restoration potential* for that action type. The Model 1 diagnostic scenario results suggest the same beneficial action types for Stillaguamish Chinook salmon as highlighted in our Phase 1 results: floodplain reconnection, wood augmentation, bank armor removal, and shade (Figure 4-1). Floodplain reconnection and wood augmentation have the highest restoration potentials at 22% and 19%, respectively, whereas bank armor removal and shade have smaller restoration potentials of 15% and 11%, respectively. The Model 2 results show very little response to either shade (0%) or floodplain reconnection (4%) (Appendix F) because there is no effect of temperature on prespawn mortality. The highest restoration potentials for Model 2 are wood augmentation (17%) and bank armor removal (22%). Estuary restoration potential is +9% in both Model 1 and Model 2.

The custom restoration scenarios developed in collaboration with local stakeholders produced potential increases in spawner abundance ranging from 9% to 35% using Model 1 (Figure 4-2). Of all single-action diagnostic and custom restoration scenarios, Chinook 1a and Chinook 2a produced the largest increases in modeled spawner abundance with 34% to 35% estimated increase in spawner abundance. The TAG 2 scenario produced a similar modeled increase of 30% while the TAG 1 scenario produced a more modest increase of 9%. The Model 2 results are broadly similar, except that predicted increases in natural-origin spawner abundance are slightly lower for each restoration scenario (Appendix F). Under current climate conditions, all scenarios except TAG1 have predicted spawner increases of 27% to 29%.

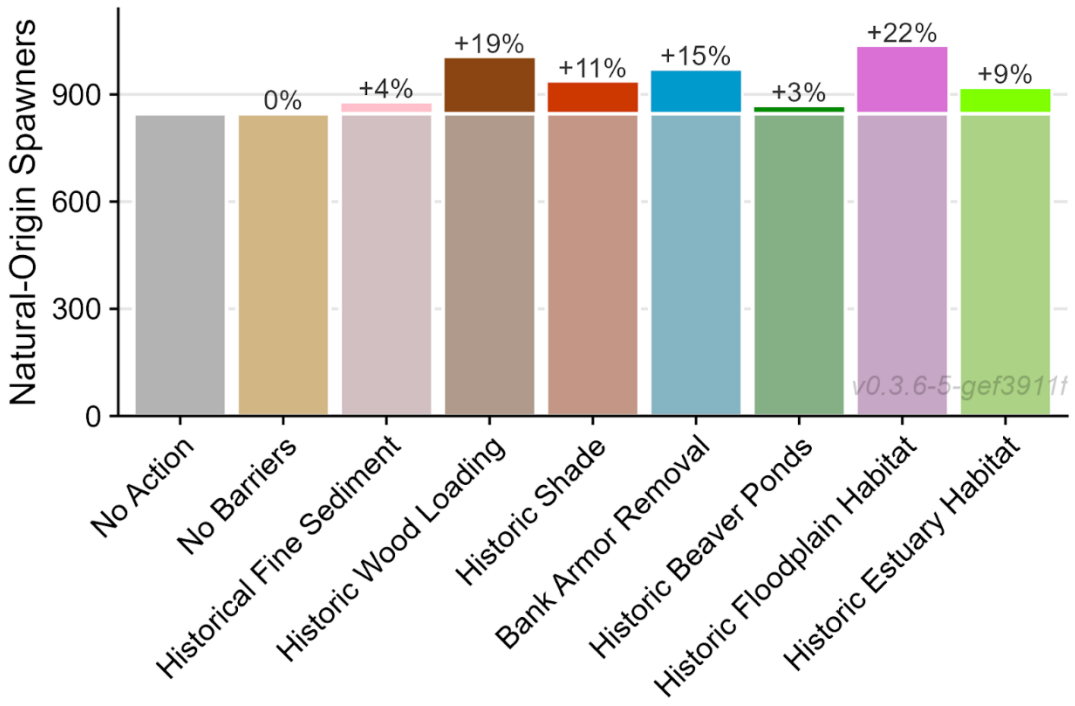

Figure 4-1. Modeled median 2020s spawner abundances under each diagnostic scenario.

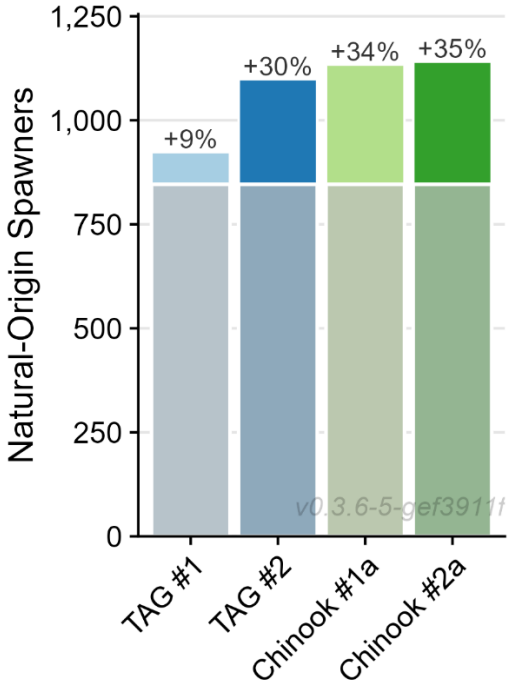

Figure 4-2. Modeled median 2020s spawner abundances under each restoration scenario.

4.2 Climate Change Effects

4.2.1 Projected Climate Change Effects without Restoration Actions

Modeled natural-origin spawner abundance decreased by 65% from current climate to the 2080s in no-action scenarios (i.e., no freshwater or estuary habitat restoration) (Figure 4-3). Moreover, the mid-century and late-century climate change effects reduce abundance for all life-stages included in the life-cycle model (Table 4-1). Under mid-century climate conditions life-stage abundances decrease by 25% – 42%, and by the late century life stage abundances decrease by 60% - 82%. Fry migrants have the greatest reduction in abundance (-42% in the 2050s and -82% in the 2080s) and parr migrants have the smallest reductions in abundance (-25% in the 2050s and -60% in the 2080s). Model 2 (without temperature-related prespawn mortality) predicts a natural-origin spawner abundance decline of 33% in the no-action scenario (Appendix F), indicating that the degree to which prespawning adults are sensitive to temperature is a key uncertainty in the model. Model 2 projected life-stage abundance decreases are much smaller than the Model 1 projected decreases, ranging from 0% to -15% in mid-century and -8% to -49% in the late century.

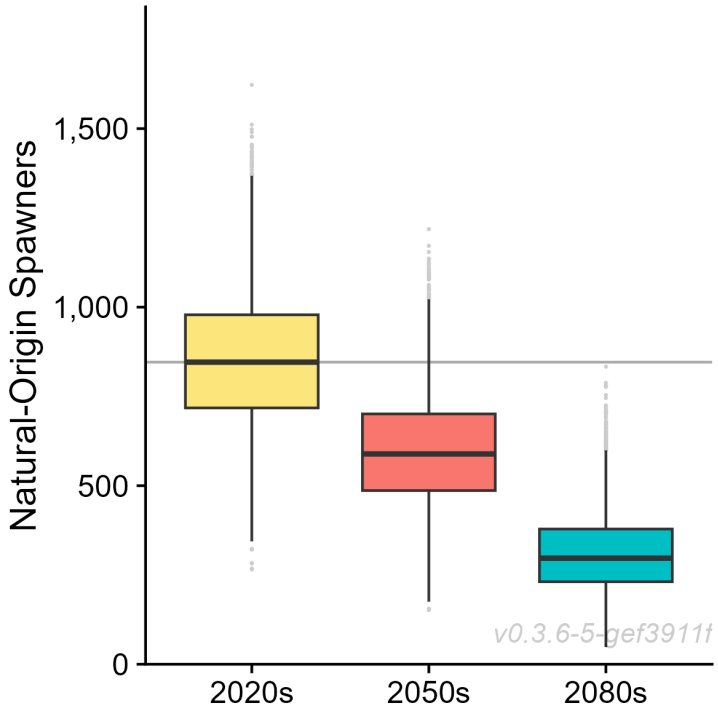

Figure 4-3. Modeled natural-origin spawner abundances under current (2020s), mid-century (2050s), and late-century (2080s) climate conditions without habitat restoration (no-action scenario). Thick black lines show median natural-origin spawner abundance.

Table 4-1. Percent change in median modeled abundances for six Chinook salmon life stages under 2050s and 2080s climate conditions for Model 1 (with temperature-related prespawn mortality) and Model 2 (no temperature-related prespawn mortality) under the no-action scenario, relative to modeled 2020s abundances. PSM in Table headings refers to prespawn mortality.

	Model 1 (with PSM)		Model 2 (without PSM)	
Life Stage	**2050s**	**2080s**	**2050s**	**2080s**
Eggs	- 32%	-66%	-7%	-23%
Emergent fry	-34%	-72%	-13%	-41%
Fry migrants	-42%	-82%	-15%	-49%
Parr migrants	-25%	-60%	-11%	-32%
NOR spawners	-30%	-65%	-11%	-33%
HOR spawners	-38%	-73%	-0%	-8%

Current habitat and climate conditions produce higher modeled spawner densities (4–12 fish/km) in the middle and upper mainstem North Fork, Boulder River, Squire Creek, upper Deer Creek, Jim Creek, and the upper mainstem South Fork, which mostly agrees with empirical redd survey data (WDFW, unpublished data). However, the spatial distribution of spawners will likely shift upstream in the future, with few to no spawners in the lower North and South Forks by the 2080s (Figure 4-4). Modeled spawner densities decrease in all reaches across the Stillaguamish basin under mid (2050s) or late-century (2080s) climate conditions. Mid-century climate conditions reduce modeled spawner density throughout most of the Stillaguamish in the 2050s and 2080s, and sub-populations in the lower mainstem North Fork and Pilchuck Creek are projected to be extirpated by the 2080s without habitat restoration. The highest projected spawner densities in the 2080s (4–8 fish/km) are in the upper South Fork mainstem and Boulder River.

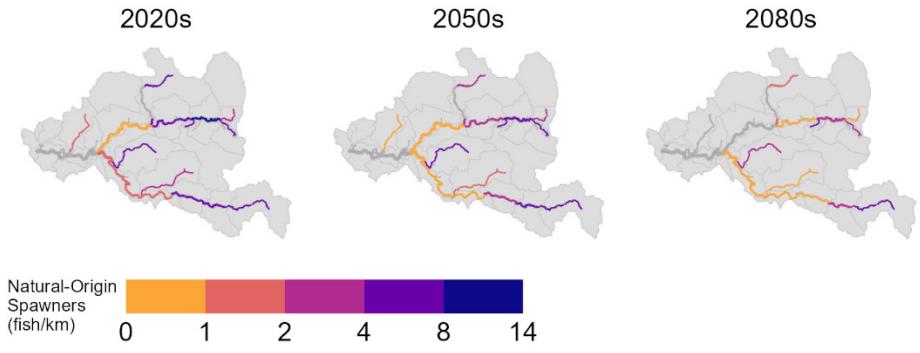

Figure 4-4. Modeled median natural-origin spawner densities (spawners per kilometer of spawning habitat) under current (2020s), mid-century (2050s), and late-century (2080s) climate conditions without habitat restoration. Gray lines indicate reaches without spawners and reaches in subbasins with fewer than 2 modeled spawners.

The Model 2 results project the highest spawner densities in the lower Stillaguamish mainstem under current climate conditions (Appendix F), which is not consistent with current observations. Spawner densities shift upstream somewhat by the 2080s, but unlike the Model 1 results, moderate to high spawner densities are sustained in the lower mainstem, North Fork 1, and South Fork 1 reaches into the late century.

4.2.1 Restoration Scenarios and Climate Change

Restoration potentials for the single-action diagnostic scenarios differ among climate periods, with some restoration scenarios yielding greater percent increases relative to the no-action scenario under future climate conditions (Figure 4-5). However, the total restoration benefit, measured in number of natural-origin spawners, is reduced for all scenarios under future climate conditions. Floodplain reconnection has the largest effect on Stillaguamish Chinook in all time periods (22%-51%), and restoration potential for floodplain reconnection in the late century is at least 22% more than all other single-action diagnostic scenarios. Wood augmentation and shade restoration also become increasingly important under 2080s climate conditions, with modeled restoration potentials increasing from 19% to 29% and 11% to 24%, respectively. Bank armor removal maintains roughly the same spawner response throughout all time periods (14-15%).

In contrast, the Model 2 results show that shade restoration and floodplain reconnection have little benefit now or in the 2050s or 2080s (Appendix F), and wood augmentation and bank armor removal produce roughly the same percentage increase natural-origin spawner abundance in all three climate scenarios.

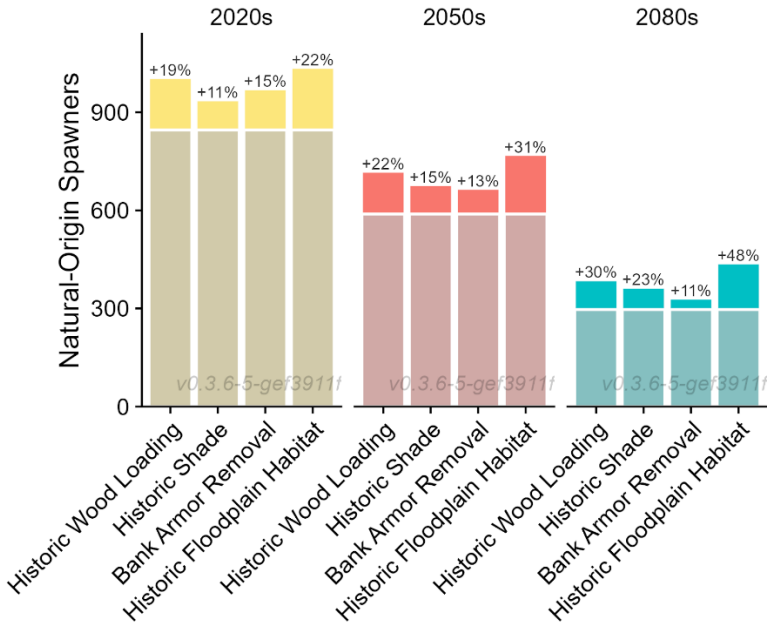

Figure 4-5. Modeled median spawner abundances under four single-action diagnostic scenarios under current (2020s), mid-century (2050s), and late-century (2080s) climate conditions. No-action abundances are indicated by shaded bars for each climate condition.

Five of the six restoration scenarios combining multiple actions produce at least 30% increases in modeled spawner abundance under current climate conditions, and most produce larger percent increases under future climate conditions (Figure 4-6). However, total modeled abundance is projected to be lower than current abundance by late century even with habitat restoration. The modeled percent increase in spawner abundance for the TAG 1 scenario declined from 9% to 7% by late century, and the modeled spawner abundance increase for the TAG2 scenario ranges from 28%-30% across all three time periods. Chinook 1a and 2a show modest increases in the mid-century (35% and 36%, respectively) and late-century (36% and 37%, respectively). For Model 2 under late-century climate conditions, all scenarios except TAG1 have predicted increases between 26% and 29%, and natural-origin spawner abundance is slightly lower than the current spawner abundance (Appendix F).

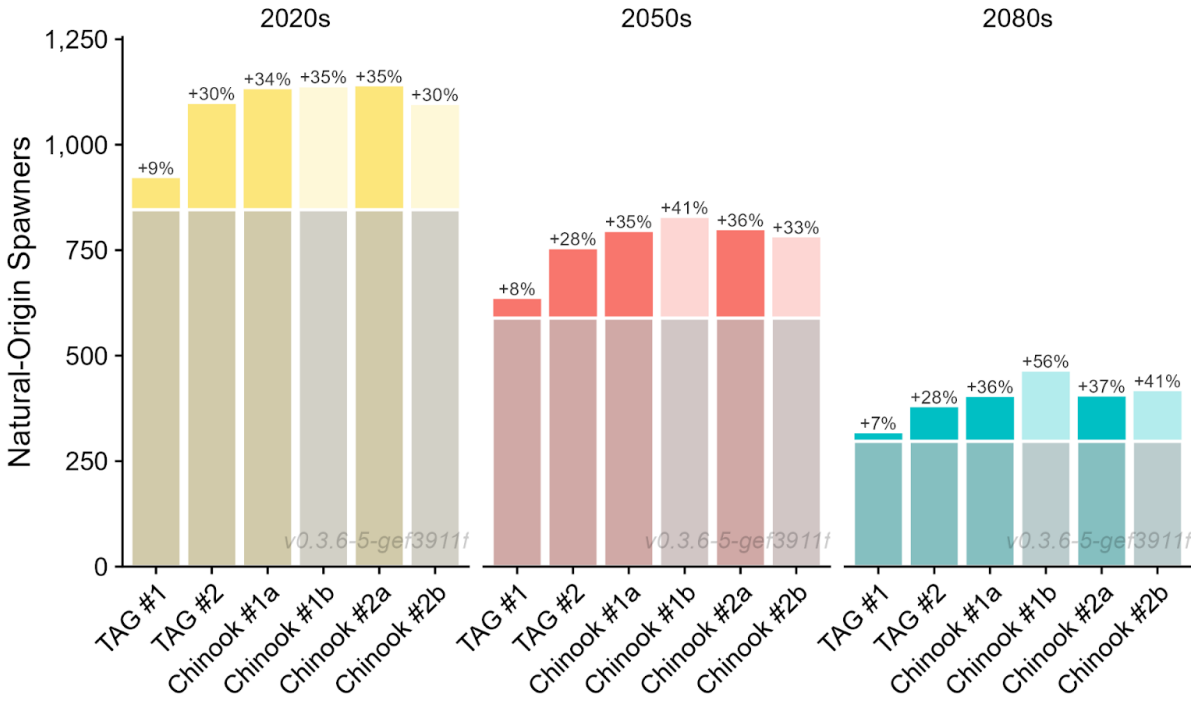

Figure 4-6. Modeled spawner abundances under six custom restoration scenarios under current (2020s), mid-century (2050s), and late-century (2080s) climate conditions. Scenarios Chinook 1b and Chinook 2b, which were designed specifically for late-century conditions, are shown in pastels. No action abundances are indicated by shaded bars for each climate condition.

The Chinook 1b and Chinook 2b scenarios (which are based 2080s diagnostic scenarios) provide the most restoration potential in the late century. In particular, Chinook 1b produces the highest spawner response of all custom restoration and single-action diagnostic scenarios with 56% restoration potential in the late-century. This strategy also produces the highest spawner response in the mid-century (41%). Chinook 2b produces a similar response to Chinook 1a and Chinook 2a in the mid-century (33%) but produces a greater percent change relative to the no-action scenario in the late-century (41%).

The response of natural-origin spawners to the custom restoration scenarios under future climate conditions also varies spatially (Figure 4-7). Under current climate conditions, the additional spawners resulting from custom restoration scenarios are distributed basin-wide, with the highest densities of additional spawners predominantly in the North Fork Stillaguamish. In the mid and late-century, however, the spatial distribution of the

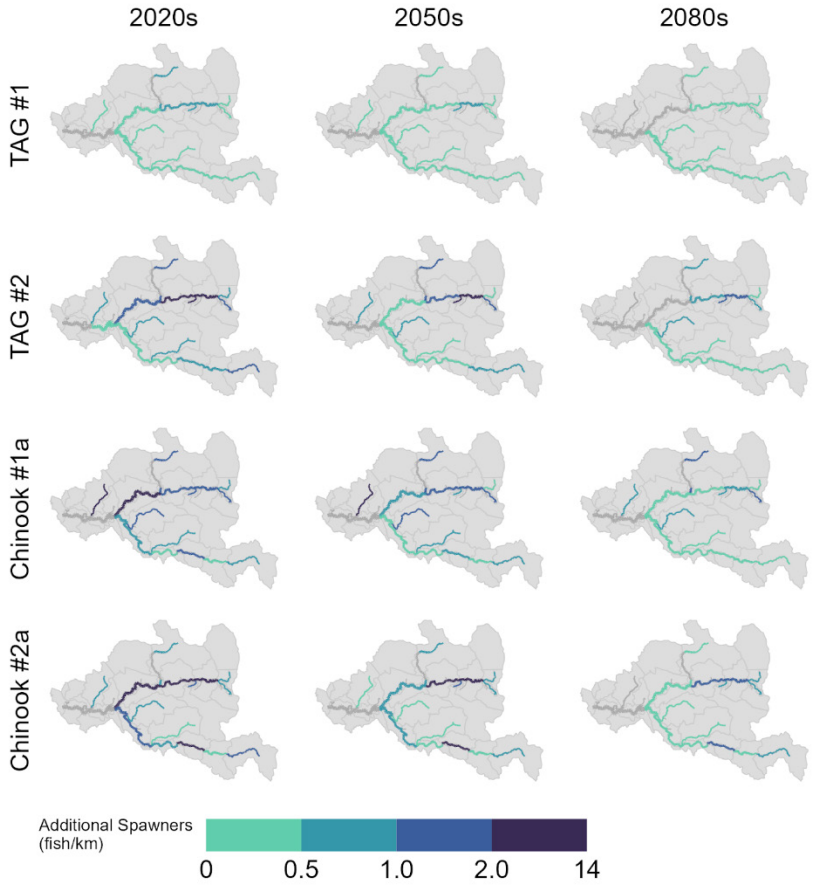

Figure 4-7. Increases in natural-origin spawner density (spawners per kilometer of spawning habitat) gained from restoration under current (2020s), mid-century (2050s), and late-century (2080s) climate conditions. Density changes are relative to each era's no-action condition. Gray lines indicate reaches without spawners and reaches in subbasins with fewer than 2 spawners.

additional spawners is contracted to smaller reaches of the upper North Fork Stillaguamish and the densities decrease. Chinook 2a shows the widest distribution of additional spawners including natural-origin fish returning at high densities in the lower South Fork Stillaguamish and two reaches in the middle and upper South Fork Stillaguamish.

4.3 Hatchery Influences

Under current Stillaguamish Chinook hatchery management strategies, the HARP Model projects declines in both natural-origin and hatchery-origin spawners under mid- and late-century climate conditions (Figure 4-8). However, the reduction of hatchery-origin spawners in each time period is substantially less than the natural-origin spawners, primarily because we assume that hatcheries continue to produce the same number of juvenile outmigrants per adult spawner, whereas juvenile outmigrants per natural-origin spawner is expected to decrease as flood flows and stream temperatures increase.

As climate change reduces the number of modeled natural-origin spawners through time, the proportion of natural-origin fish removed for broodstock (pNOB) increases because the broodstock removal remains constant (Figure 4-9). If current broodstock practices in the North Fork Stillaguamish are continued (that is, removal of roughly 70 natural-origin returners from the North Fork Stillaguamish each year), the median proportion of natural-origin spawners removed from North Fork subbasins increases from 19% currently to 25% in the mid-century and 38% in the late-century.

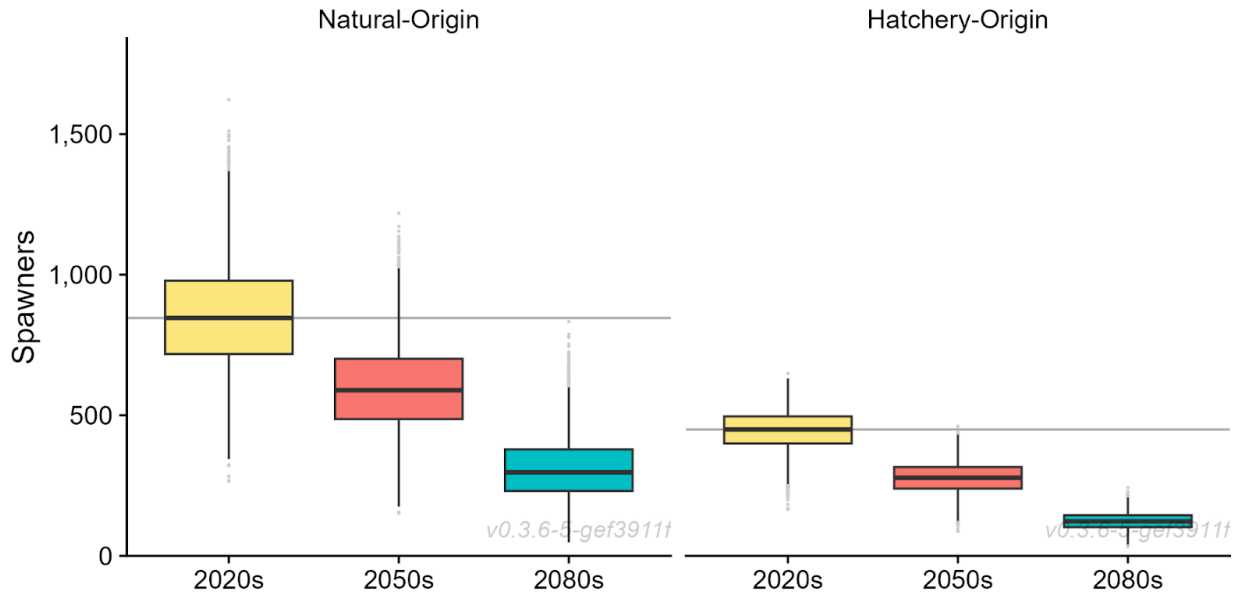

Figure 4-8. Modeled natural-origin (left) and hatchery-origin (right) spawner abundances under current (2020s), mid-century (2050s), and late-century (2080s) climate conditions without habitat restoration. Thick black lines are the median spawner abundance.

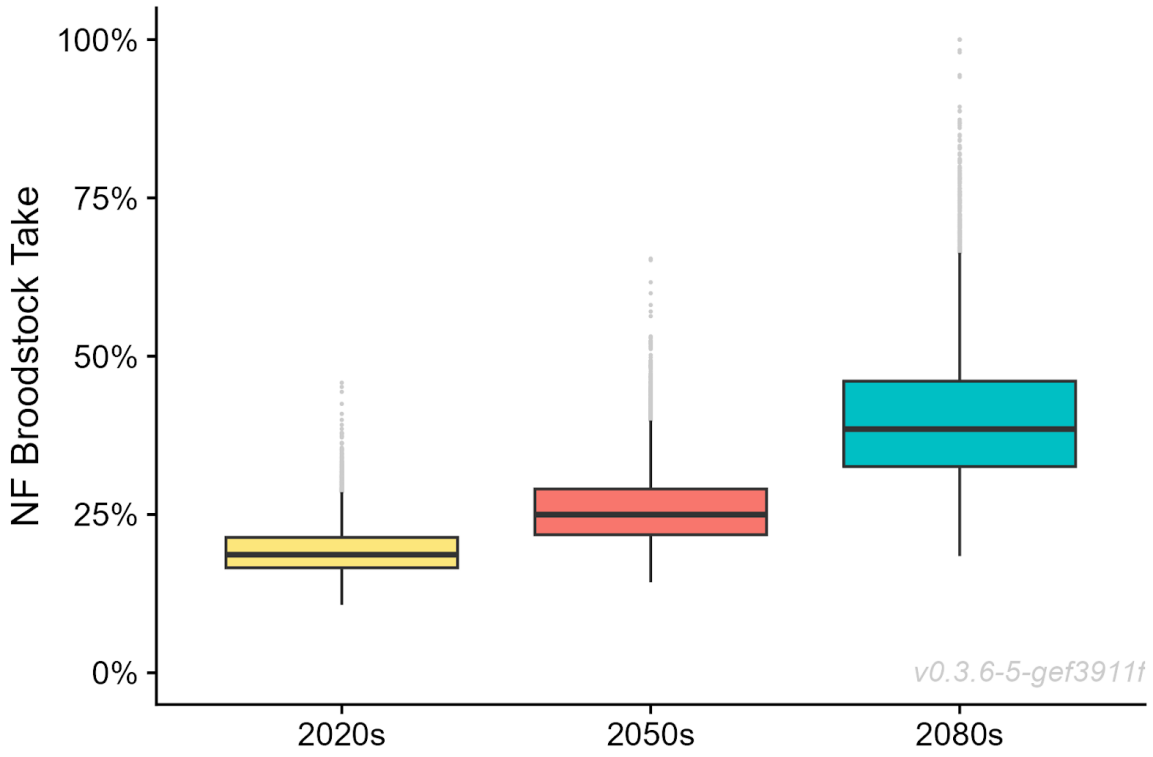

Figure 4-9. Modeled percent of the North Fork Stillaguamish natural-origin run required to be taken as broodstock to maintain a pNOB of 0.5 and 140 total broodstock at the Harvey Creek Hatchery under current (2020s), mid-century (2050s), and late-century (2080s) climate conditions without habitat restoration. Thick black lines are the median percent broodstock removal.

Given the estimated reduction in both natural- and hatchery-origin spawners under future climate conditions, we modeled the potential effects of a range of hatchery production strategies and the potential response of natural-origin spawners, hatchery-origin spawners, and the proportion of natural-origin fish removed for broodstock. If North and South Fork Stillaguamish hatchery smolt releases and North Fork Stillaguamish broodstock removal increased relative to the current strategy, the model suggests that median abundances of natural-origin spawners would decrease under all climate conditions (Figure 4-10, top row), up to a modeled maximum reduction of -9% to -11% under a hypothetical doubling of all hatchery strategies. This is mainly a reflection of the increased percentage of natural-origin spawners removed as broodstock, which reduces natural-origin spawner abundance. However, competition between juvenile hatchery-origin fish and juvenile natural-origin fish also plays a role. Conversely, a reduction in hatchery production to 20-30% of current levels could increase abundance of natural-origin spawners by up to 4%. These trends are similar across all modeled climate conditions; however, the magnitude of natural-origin spawner abundance change decreases through time.

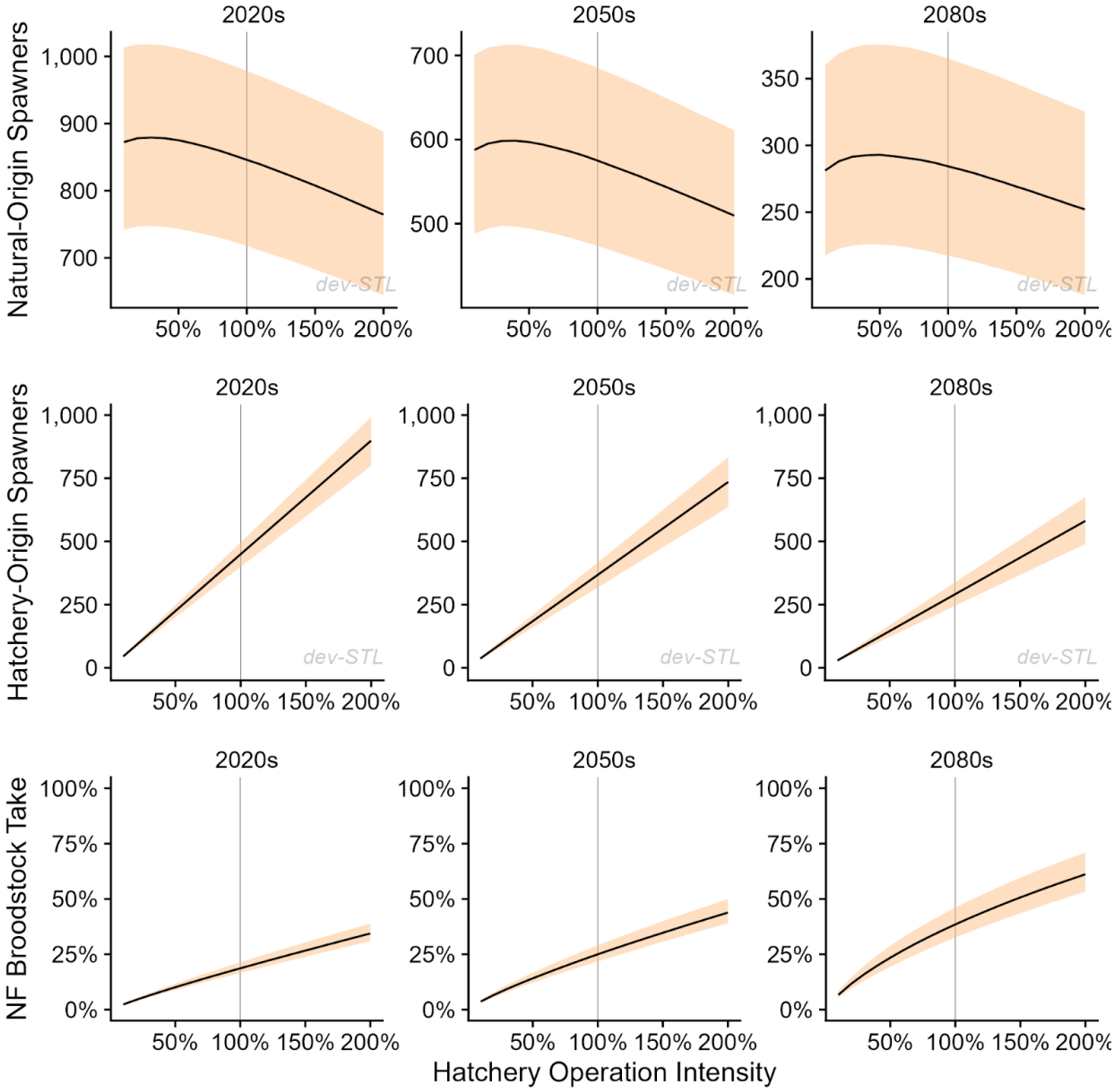

Figure 4-10. Modeled response of natural-origin spawner abundance (top row), hatchery-origin spawner abundance (middle row), and percent broodstock take (bottom row) for lower hatchery operation intensity (10% of current broodstock take and juveniles released, x axis) to higher intensity (200% of current broodstock take and juveniles released, x axis) in the three climate periods (2020s, 2050s, and 2080s, columns). Current intensity is 100% on the x-axis (gray vertical line). Black lines show median values and shaded regions show interquartile (25th-75th percentile) ranges.

While the abundance of hatchery-origin spawners responds positively to increased hatchery production, the magnitude of the response decreases in each climate time period

(Figure 4-10, middle row). If hatchery operations were to increase while maintaining a pNOB of 0.5 for the Harvey Creek hatchery operation, the overall proportion of North Fork natural-origin returners removed for broodstock will increase as well, especially in the late century (Figure 4-10, bottom row). Under 2020s climate conditions, a hypothetical doubling of hatchery operations would increase the percent of natural-origin North Fork spawners removed for broodstock from a median of 19% to 34%. Under 2050s climate conditions, doubling hatchery operations would increase the median removal fraction from 25% to 44%. Under 2080s climate conditions, doubling hatchery operations would increase the median removal fraction from 38% to 61% (Figure 4-10, bottom row).

Percent Natural Influence (PNI) decreases for North Fork subpopulations with worsening climate conditions and with increasing hatchery operation intensity (Figure 4-11). At current hatchery operation intensity, the model produces a median PNI of 0.50 under 2020s climate conditions, a median PNI of 0.47 under 2050s climate conditions, and a median PNI of 0.43 under 2080s climate conditions. With a hypothetical doubling of hatchery operations, the model produces a median PNI of 0.42 under 2020s climate conditions, 0.40 under 2050s climate conditions, and 0.38 under 2080s climate conditions. Conversely, a hypothetical reduction in hatchery operations could increase PNI. Under a hypothetical reduction of hatchery operations to 20% of current levels, modeled median PNI is 0.75 under 2020s conditions, 0.71 under 2050s conditions, and 0.63 under 2080s conditions. We did not calculate PNI for South Fork subpopulations because pNOB is not well-described for the relatively young Brenner Creek hatchery operations.

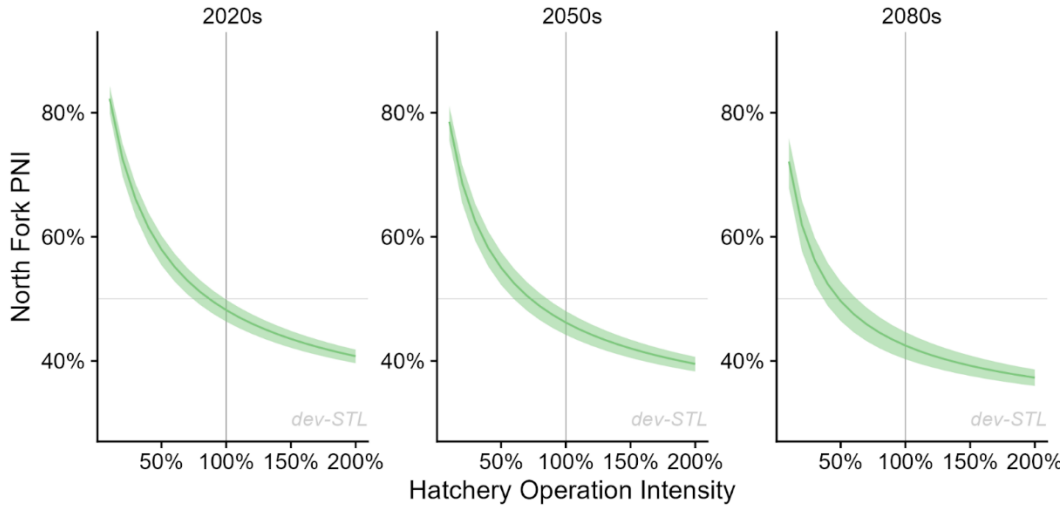

Figure 4-11. Modeled PNI (y axis) as a function of modeled hatchery operation intensity (x axis) under three climate conditions (2020s, 2050s, and 2080s). The x-axis is the percent of current smolt release numbers from both hatcheries and current broodstock removal for Harvey Creek operations, with 100% intensity (gray vertical line) representing current operations. Green lines show median values and shaded regions show interquartile (25th-75th percentile) ranges. PNI of 50% is shown by a horizontal gray line.

Model 2 estimates a smaller decline in natural-origin fish, and North Fork broodstocking practices become much more sustainable as they take a smaller proportion of the total North Fork natural-origin returns. Also, hatchery returns remain constant because they are no longer influenced by warming temperatures in the model.

4.4 Marine Survival

When the HARP Model is run using the current observed SAR rates, the modeled population sizes for both natural-origin and hatchery-origin spawners approximately match observed spawner abundances. This low survival rate constrains current population size, and it might also limit population responses to habitat restoration. However, survival rates in the 1970s were well above 2%, then declined steadily to less than 1% by 1990, where the rates have remained since (Welch et al. 2021). To examine the effect of marine survival rate on population size and modeled population responses to restoration, we ran the model with a range of SAR values that have been observed in the past few decades (0.36-0.8) and found that increasing SAR rates from the median observed value of 0.38% (natural-origin subyearlings) can dramatically increase modeled abundance (Figure 4-12).

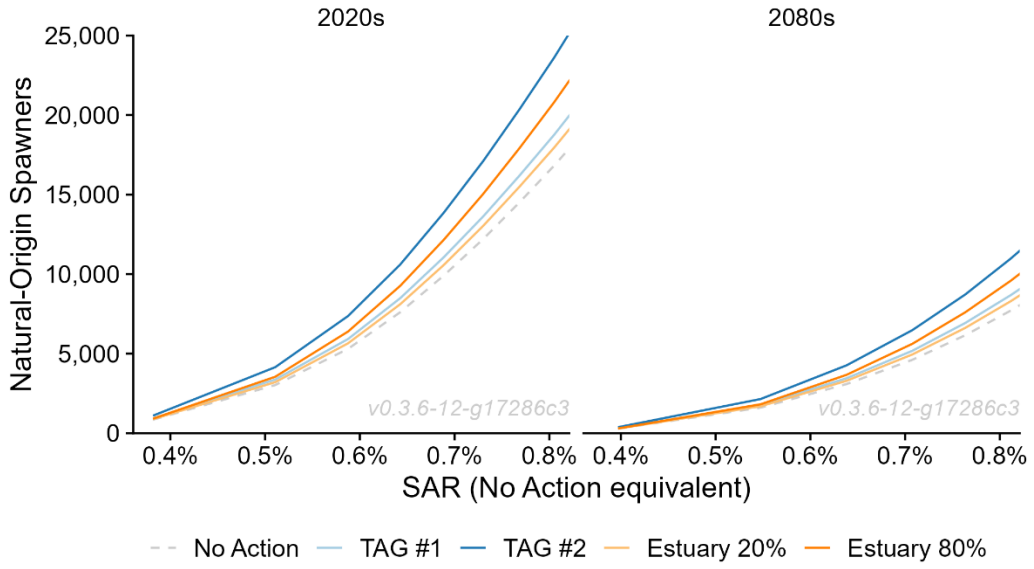

Figure 4-12. Median number of modeled natural-origin spawners as a function of a marine survival under four restoration scenarios and two climate conditions. The no-action scenario is shown as a dotted gray line, TAG scenarios are shown in blue, and orange lines represent two additional restoration scenarios where only the estuary is restored. Estuary restoration intensity in the two estuary restoration scenarios matches restoration intensity in the two TAG scenarios (TAG #1" = 20%" and "TAG #2" = 80%). Subyearling natural-origin marine survivals, yearling natural-origin marine survivals, and hatchery-origin marine survivals were adjusted simultaneously and proportionally in each simulation.

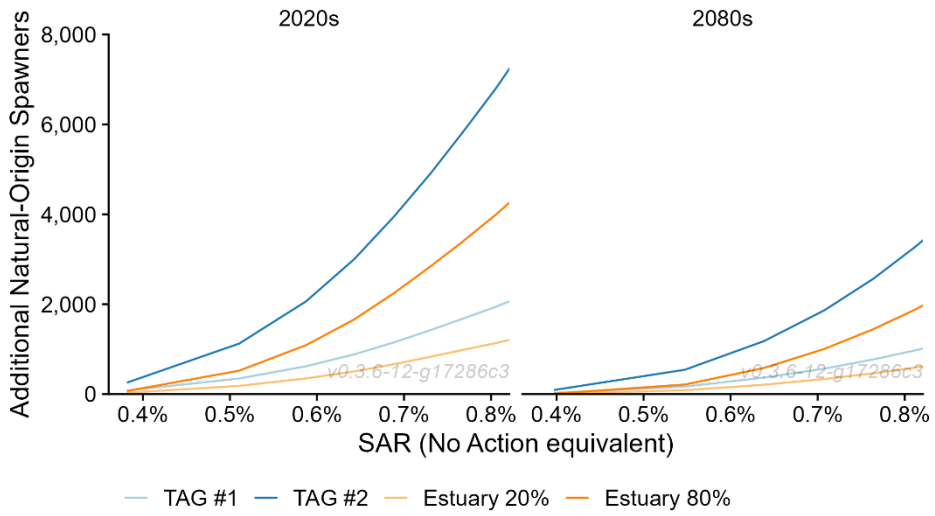

Figure 4-13. Modeled increase in natural-origin spawner abundance (difference between the median number of spawners in a restoration scenario and the median number of spawners in the no-action scenario) as a function of marine survival under four restoration scenarios and two climate conditions.

Even a modest increase in SAR rate to 0.6% could increase abundance of natural-origin spawners nearly 10 fold (Figure 4-12), and could also help realize greater freshwater benefits from restoration actions (Figure 4-13). While an increase to 0.6% is a 67% increase from the current SAR rate with harvest, it is near the current SAR rate without harvest (0.59%) and far less than SAR rates in the 1970s (>2%, Welch et al. 2021).

4.5 Life-cycle Model Sensitivity

The one-at-time life-cycle model sensitivity analysis suggests that Stillaguamish Chinook salmon abundance is very sensitive to subyearling rearing capacity and productivity, as well as adult prespawn survival (Figure 4-14). However, there is little room for improvement in these parameters (10% to 25% over current levels), and the projected population response is commensurately low. This is consistent with the diagnostic and restoration strategy results, which show that restoration actions to increase rearing habitat quality (wood augmentation, armor removal) and reduce stream temperature (shade, floodplain reconnection) produce the largest response in spawner abundance. In contrast, spawning capacity and yearling summer rearing capacity have much more room to improve, but they produce very little response in modeled abundance. This indicates that the population is not limited by spawning capacity, and the low response to summer rearing capacity reflects the fact that less than 1% of juvenile outmigrants in the Stillaguamish are yearlings.

The preceding results for hatchery management also suggest there may be little opportunity to increase natural-origin spawner abundance through hatchery practices

(Figure 4-10, top row). However, there are no genetic effects in the hatchery model, and parameter uncertainty is relatively high because there are no local data on hatchery influences on prespawn mortality, hatchery- natural-origin competition, or relative reproductive success. In contrast, the marine survival analysis indicates that the population is perhaps most sensitive to the SAR parameter, which is currently very low relatively to historical levels. Increasing the SAR value to 0.6 (still much lower than SAR in the 1970s) could dramatically increase natural-origin spawner abundance.

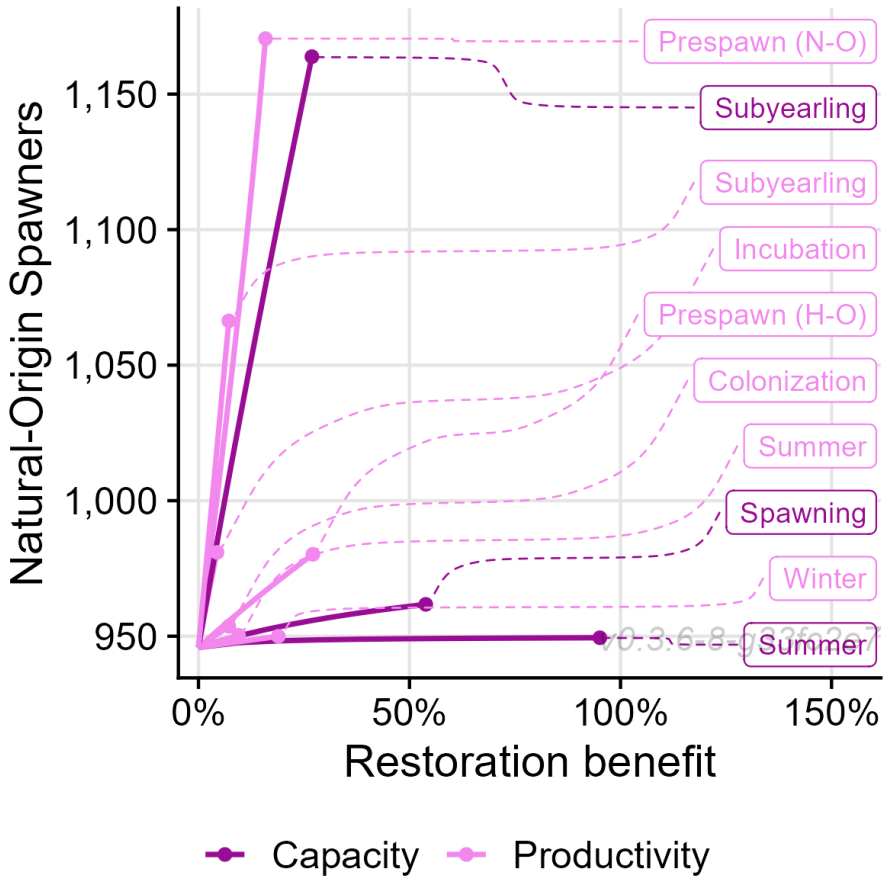

Figure 4-14. One-at-a-time sensitivity analysis of life-stage parameters. The baseline (0% on the x-axis) is the modeled natural-origin spawner abundance with current habitat conditions. The x axis is percent increase in a capacity or productivity parameter from the current condition up to the maximum (historical) value of the parameter, and the y axis is modeled natural-origin spawner abundance.

5. Discussion

We continued development of the HARP Model for Stillaguamish River Chinook salmon by incorporating climate change effects, hatchery-origin Chinook salmon, and multi-action restoration scenarios. Our results suggest that future climate conditions will dramatically reduce abundances of natural-origin Chinook salmon in the absence of habitat restoration, and that a range of medium to high-intensity restoration strategies could elicit positive responses in natural-origin Chinook salmon – either by improving spawner abundances under current climate conditions or by mitigating some of the climate-associated losses under future conditions. The model does not suggest that hatchery operations could offset the effects of climate change on natural-origin spawner abundances.

5.1 Climate Change Uncertainties

The HARP Model 1 results (with temperature-related prespawn mortality) suggest that, without habitat restoration, climate change will likely reduce Stillaguamish Chinook spawner abundances in the future (-65% natural origin spawners by the 2080s), and that some life stages will be increasingly vulnerable to extreme events such as high stream temperatures or higher flows. The Model 2 results without temperature-related prespawn mortality predict a much lower sensitivity to climate change (-33% by the 2080s). Both models predict the largest decreases in emergent fry and fry migrants (Table 4-1), suggesting that the basin may be increasingly underseeded in the future. Fewer fry migrants will reduce density dependence during estuary rearing, potentially reducing the effect of estuary restoration on Chinook survival in the future. Moreover, a reduction in the fry outmigrant life history type could make the population more vulnerable to impacts that would primarily affect longer-residing parr outmigrants, as most of the population would be susceptible to factors affecting parr survival (e.g., reduced food availability or higher temperatures).

5.1.1 Use of RCP 8.5 Emissions Scenario

Our climate change effects are estimated solely using the RCP 8.5 emissions scenario, which represents high greenhouse gas concentrations. This scenario is considered the best projection of near- to mid-term climate change, as its projected emissions are most consistent with recent trends (Schwalm et al. 2020). However, RCP 8.5 begins to estimate somewhat high emissions by the 2050s, and estimated emissions are much higher than the other RCPs by the 2080s. Alternative emissions scenarios (e.g., RCP 6, RCP 4.5) have estimated potential greenhouse gas concentrations that are lower than expected emissions by 2050, and those scenarios would produce different climate change results, especially in the late-century time period (2080s). Additionally, we used the ensemble mean of the RCP 8.5 GCMs, but the range of predictions among GCMs is quite large. Overall, the majority of predicted temperature changes across all RCP-GCM combinations are lower than the one we used, which would result in less dire predictions of Chinook salmon abundance in the future.

5.1.2 Effects of Increasing Stream Temperature

The HARP Model results suggest that Stillaguamish Chinook salmon are particularly sensitive to high temperatures during adult migration and holding in the river, but our prespawn survival function is based on relationships developed in the Willamette and upper Columbia Rivers where temperatures are hotter and returning adults undertake longer and more complex migrations to return to their natal basins. We have no local prespawn mortality data with which to develop a local empirical function relating high stream temperature to prespawn mortality. This uncertainty could affect the scale and spatial pattern of climate sensitivity, and decrease the modeled effect of the shade restoration and floodplain reconnection actions (Appendix F).

Shifts in phenology not captured by the HARP Model could also improve Chinook salmon resilience to climate change. For example, later run timing could shorten the amount of time that returning Chinook salmon spend in warm water and reduce temperature-related prespawn mortality. Such a shift in migration and spawning timing could occur for the fall-run population in the South Fork, which enter the river in August or later. In that case, phenotypic plasticity or genetic adaptation is plausible, resulting in a gradual shift toward later migration timing in response to increasing temperature. Phenological shifts are less likely for summer-run population in the North Fork, which begin entering the river in June, hold in the river through the hottest part of the summer, and begin spawning during August when temperatures are still high. Despite an expectation that such a selective pressure might eliminate spawning during high temperatures, temperature-related prespawn mortality occurs in many viable Chinook populations (Bowerman et al. 2018, 2021). Presumably, high survival in subsequent life stages is sufficient to sustain an early spawning population despite some level of prespawn mortality.

There is also the possibility that thermal refuges could partially mitigate the effects of rising stream temperatures, but we did not have the survival data needed to include those potential effects in the model. An interesting observation for some Skagit River spring-, summer-, and fall-run populations is a trend toward later spawning over the last 2-6 decades (Austin et al. 2020), even though spring- and summer-run adults enter the river prior to summer high temperatures. This may suggest that Chinook adults are able to find thermally suitable holding areas to survive the summer high temperatures, and then move to spawning areas as temperatures decline in the fall. Data on thermal anomalies in the Stillaguamish are available (Leonetti et al. 2015), so it may be possible to study adult Chinook holding locations and prespawn mortality to determine whether Chinook are finding cool water refuges and whether prespawn mortality is a significant problem for this population.

5.1.3 Effects of Increasing Peak Flow

It is expected that, given sufficient floodplain space, channels should increase in width and depth in response to increasing flows (Goode et al. 2013), although sediment transport is also expected to increase (Verhaar et al. 2011). Theoretically this would mean that Chinook spawners would shift laterally or upstream to find spawning areas that are similar to those

they select today, and that spawning-site peak flows and redd scour would not exceed current levels. While this could completely offset effects of increasing peak flows (a possibility suggested in (Goode et al. 2013)), past trends in Puget Sound Chinook indicate the opposite—that population productivity has declined as winter flow variability has increased (Ward et al. 2015). In Puget Sound rivers, peak flows during egg incubation are increasing faster than low flows at which spawning occurs (there were no trends in mean winter flow), which suggests that spawners may be confined to a smaller area of the channel and redds are subsequently exposed to higher flood flows (Ward et al. 2015). Likewise, flow predictions for the Stillaguamish predict decreasing low flows during spawning months for summer-run Chinook salmon and increasing high flows during incubation (Mauger et al. 2021). Such an increase in flow variability would produce a peak-flow effect on redd scour regardless of channel adjustment, and mortality for a given flow could increase rather than decrease. On the other hand, if Ward et al. are not correct and channel adjustment does occur, there is the possibility that there will be little or no effect of increasing peak flow (Goode et al. 2013).

5.1.4 Effects of Decreasing Low Flow

A large percentage of Stillaguamish Chinook parr-migrants rear in the river in spring, with most leaving in May or early June. Therefore, the end-of-stage capacity for parr rearing would logically be controlled by the May/June wetted width. We did not have May or June observed wetted widths, but we did have estimates of March and August wetted width, and we selected the August width so that we did not overestimate capacity. However, both May and June flows are projected to decrease significantly in the future (similar to the August flow (Mauger et al. 2021)), suggesting that a decrease in May-June parr rearing capacity is likely to be similar in magnitude to the change late summer rearing capacity. On the other hand, if warming temperatures result in short incubation time and earlier emergence and outmigration, parr migrants may be able to leave the river prior to the period of decreased low flows (April or earlier, Mauger et al. 2021).

5.1.5 Climate Change and the Marine Environment

In this project we only modeled climate change effects on stream flow and temperature in the freshwater environment. However, climate change is also expected to impact estuarine and nearshore habitats via changes in salinity, temperature, and inundation regimes (sea level rise), and marine habitats via changes in marine temperatures, ocean circulation, and marine food webs (Crozier et al. 2021, Sobocinski et al. 2021). Such changes may contribute to either declines or increases in survival, and restoration and management actions affecting estuarine and early marine survival may also help increase marine survival.

5.2 Restoration Strategies

The model results suggest that a range of restoration strategies may benefit Stillaguamish Chinook salmon under current climate conditions. Several of the restoration scenarios produced similar responses in spawner abundance in the current climate, suggesting that

various restoration strategies can benefit this population in the absence of climate change effects. These restoration scenarios range from basin-wide efforts to those solely focused in mainstem reaches, and they also range in the number and types of restoration actions included (i.e., some strategies focus primarily on floodplain reconnection and shade restoration, whereas others also include bank armor removal, wood augmentation, and fine sediment reduction). Notably, the most feasible restoration scenario given current constraints to land acquisition and restoration (TAG 1) produced only a small response in natural-origin spawners due to lower intensity of restoration effort. Other scenarios with higher restoration intensity produce larger modeled increases in spawner abundance, suggesting that more restoration effort will be required to produce a modest increase in natural-origin Chinook salmon spawner abundance.

Our results also suggest that high intensity restoration effort will be essential to ameliorating future climate change effects on Stillaguamish Chinook salmon. Floodplain reconnection appears to be especially important as it may help reduce future elevated stream temperatures in mainstem reaches, and could improve prespawn survival and juvenile rearing productivity in the late century. While floodplain reconnection may partially compensate for future reduced summer rearing and spawning capacity via decreased low flows, the temperature reduction may not offset effects of substantial low flow decreases in the upper South Fork mainstem reaches. Floodplain reconnection may also ameliorate some impacts of projected increases in flood peaks on egg-to-fry survival (Nicol et al. 2022, Beechie et al. 2023), although this effect was not explicitly included in our analysis.

Nearly all mainstem and tributary subpopulations use the lower river for migration or rearing, and efforts that improve habitat in these reaches may have positive effects on spawner abundances throughout the basin. In these lower mainstem reaches, the HARP Model indicates that important restoration actions include floodplain reconnection and shade restoration to decrease stream temperature, and to a lesser extent bank armor removal and wood augmentation to increase juvenile rearing habitat capacity. Therefore, comprehensive restoration projects in the lower river may not only help restore lower river spawning populations, but also contribute to increased spawner abundance in up-river subpopulations.

The Phase 1 HARP Model results indicated that, for Chinook salmon, estuary restoration has very low restoration potential because the current number of outmigrating Chinook fry is far below the modeled Stillaguamish estuary capacity. Those results indicate that estuary restoration will be most effective when paired with other strategies that increase fry production. However, the model's estuary restoration actions also assume that restored habitat will be occupied by the same proportion of natal-basin and non-natal fish as the rest of the estuary. In reality, the occupancy of any newly restored habitat will likely vary based on location and change over time at both long and short timescales. Therefore, actual restoration potentials could be above modeled restoration potentials if the newly restored habitat is used preferentially by Stillaguamish-origin juveniles, or if the newly restored habitat is of better quality than other estuary habitats.

To address multiple stressors on Chinook salmon populations and increase resilience to climate change, a restoration strategy that increases life history diversity may be critical as populations with a diverse portfolio of life histories may fare best in a future climate (Schindler et al. 2010, Greene et al. 2010, Sobocinski et al. 2021). Such restoration strategies will likely include actions that both ameliorate climate change effects and increase habitat diversity for threatened species (Beechie et al. 2013). In our analysis, the two strategies that most increased resilience to climate change were strategies 1b and 2b, which were developed by running the diagnostic scenarios under the 2080s climate. Those strategies ameliorate climate change effects where possible, and create the largest spawner abundance increases in late century. However, the model suggests life history diversity may still be reduced in the future because there are fewer spawners even with restoration in late century, and that may result in decline of the fry migrant life-history type.

5.3 Hatchery Supplementation

Based on the model results, Stillaguamish natural-origin Chinook salmon do not appear to benefit from increased hatchery production under current or future climate scenarios. While hatchery operations increase the total number of returning fish, the current level of hatchery supplementation appears to reduce the number of natural-origin spawners under both current and future climate conditions. However, the model also indicates that hatchery supplementation may provide a small benefit to natural-origin spawners if broodstock take and juvenile releases were reduced from current levels.

Under current climate conditions, basin-wide pHOS and North Fork PNI are at or near recommended thresholds for "contributing" populations with integrated hatchery programs (HSRG 2009, 2020). However, under 2050s and 2080s climate conditions, the median basin-wide pHOS rises beyond the recommended upper threshold of 0.30, and median North Fork PNI drops below the recommended lower threshold of 0.50. (Medians are across all simulations and years, without habitat restoration.) Both metrics indicate increasing hatchery influence on the Stillaguamish Chinook salmon population with climate change if hatchery broodstock removal and juvenile releases continue at current levels. Additionally, Harvey Creek broodstock practices may become logistically challenging or impossible with dwindling numbers of North Fork spawners.

Finally, hatchery effects were modeled as a function of spatial segregation of hatchery-origin and natural-origin adult spawning in particular reaches, removal of NOR adults for broodstock, lower relative reproductive success for progeny of hatchery-origin adults spawning in the wild, and competition among hatchery- and natural-origin juveniles. The effects of hatchery supplementation do not account for genetic effects, either past or future. While genetic effects could affect survival rates of natural-origin Chinook salmon, we don't have sufficient data to include such effects in the HARP Model.

5.4 Influence of Marine Survival

Our analysis suggests that the low smolt-to-adult-return (SAR) rate for Stillaguamish Chinook may limit the potential benefits of habitat restoration, and that effects of

freshwater habitat restoration could be substantially higher if marine survival increased. While neighboring populations likely experience shared nearshore and ocean conditions, Stillaguamish Chinook have the lowest median contemporary SAR (0.36%) of Whidbey Basin Chinook populations. For comparison, the Skagit, Skykomish, and Snoqualmie River SAR rates are 0.45%, 0.53%, and 1.32%, respectively (Lisi and Anderson 2022). A marginal increase in marine survival could provide substantial benefits to Stillaguamish Chinook salmon, although management actions to improve marine survival have not yet been identified.

Puget Sound Chinook salmon have experienced declines in marine survival from 2% in the early 1970s to <0.5% in over the last decade (Welch et al 2022), and other studies have shown that SAR is influenced by a range of factors including predation, ocean conditions, competition, forage fish abundance, anthropogenic impacts, and harvest (Sobocinski et al. 2021). However, only a few of these can be influenced by management actions. One important factor within Puget Sound that affects marine survival is abundance of forage fish (juvenile herring) when juvenile Chinook salmon enter the nearshore environment (Chamberlin et al. 2017, 2021). Specifically, where there is high abundance of small juvenile herring (relative to the size of juvenile Chinook salmon) growth of Chinook salmon is higher in the early marine rearing stage (Chamberlin et al. 2017). Therefore, management of herring populations to increase foraging opportunities for Chinook salmon may be an important management action to increase SAR. However, forage fish were only modestly correlated with Chinook marine survival in a correlation analysis (Sobocinski et al. 2021), indicating some uncertainty in this potential cause.

Other studies suggest that marine survival may also be affected in Puget Sound by high numbers of hatchery releases in years with abundant juvenile pink salmon (even years) (Kendall et al. 2020, Claiborne et al. 2021), availability of zooplankton prey (Beauchamp et al. 2018), or by increased predation on juvenile and adult Chinook salmon by marine mammals (Chasco et al. 2017). Indeed, the number of Chinook salmon adult equivalents eaten by harbor seals, stellar sea lions and California sea lions increased from an estimated 18,800 in 1970 to 161,600 in 2015, while killer whale consumption of Chinook salmon remained relatively constant at ~83,000 over that time period. By comparison, commercial and sport fishing harvest in Puget Sound has been ~30,000 adult Chinook since 2010 (Chasco et al. 2017).

Sobocinski et al. (2021) pointed out that there is no single obvious cause of reduced SAR, and that Puget Sound factors such as seal and herring abundance were weakly correlated with Chinook marine survival. Moreover, they speculated that the overall weak relationship between Puget Sound predictor variables and Chinook salmon marine survival may suggest that large-scale ocean factors may be more important. However, another study found no correlation among ocean indicators and marine survival in Salish Sea Chinook salmon populations (Ruff et al. 2017). While neither study found direct evidence of influential ocean factors, Sobocinski et al. (2021) noted that a shift in ocean regime was observed during the 1980s, which corresponds with the timing of the steep decline in marine survival. Several other studies have found a relationship between chum salmon marine survival and abundance of pink salmon in the ocean (not in Puget Sound), which

appears to result from the two species overlapping in the ocean (Anderson et al. 2021, Litz et al. 2021). However, an effect of competition in the ocean has so far not been observed in Chinook salmon.

5.5 Other Model Limitations

The HARP Model only simulates restoration actions for which we can model the associated restored habitat condition, and there may be non-modeled or incompletely modeled restoration actions that could still improve salmon habitat in conjunction with modeled restoration actions. For example, we do not have historical fine sediment records describing streambed sediment composition, nor do we have extensive data describing current sediment composition. Therefore, three of the four statistical models predicting fine sediment levels were a function of immutable landscape variables, and only one model (for streams smaller than 30 m bankfull width) included a mutable landscape variable (Beechie et al. 2022). The models for larger rivers did not include any mutable variables, so modeled historical and current fine sediment conditions were the same for large rivers (>30 m bankfull width). This result is consistent with other studies indicating that fine sediment levels were primarily controlled by immutable landscape variables (Anlauf et al. 2011b, 2011a). However, it is not consistent with current perceptions of fine sediment levels in the lower North and South Forks of the Stillaguamish River, where it is believed that high supply of fine sediment from the Oso and Gold Basin landslides has increased fine sediment levels. Additional work planned in 2023 aims to improve understanding of current fine sediment conditions in large rivers of the basin, and to help determine whether large landsides are important influences on fine sediments in spawning gravels.

We also exclude certain biological processes from the model due to lack of data, such as seasonal growth rates and effects on survival in later stages. Despite the availability of growth models to simulate growth given seasonal stream temperatures and food availability, we have not found a way to estimate reach-level and seasonal food availability, and therefore have not been able to include a growth component in the model. An additional challenge for incorporating processes such as growth into the HARP Model the disaggregated Beverton-Holt structure of life stages. This model form requires an end-of-stage capacity for each life stage, as well as a single life-stage productivity (density-independent survival). Most modeled processes or habitat factors in the model are translated into scalars that modify life-stage capacities and productivities, which would also be required to translate the results of any growth model into Beverton-Holt parameters for each life stage.

6. Conclusions

The goals of this project were to use the HARP Model to evaluate potential effects of climate change on Stillaguamish Chinook salmon, identify restoration actions and strategies that will most increase spawner abundance and resilience to climate change, and evaluate if hatchery practices could help offset climate change effects. Based on the HARP Model results, we arrived at five main conclusions.

1. The HARP Model 1 version (with temperature-related prespawn mortality) suggests that Stillaguamish Chinook salmon are very vulnerable to climate change, and their vulnerability likely stems from temperature effects on prespawn mortality and flood flow effects on incubation survival. However, an alternative model with no temperature-related prespawn mortality (Model 2) suggests a much less severe future for these populations. Moreover, the potential for channel adjustment and phenological shifts may further ameliorate potential effects of climate change on stream flow and temperature.
2. A restoration strategy that emphasizes five key actions (floodplain reconnection, wood augmentation, bank armor removal, shade restoration, and estuary reconnection) is likely to most benefit Chinook salmon under current climate conditions. Notably, several or all of these actions can be included in a single project. Strategies with increased emphasis on floodplain reconnection appear to most increase resilience to climate change, as they provide larger increases in modeled spawner abundance in the late-century climate.
3. Lack of fry migrants currently limits benefits of estuary restoration. Because fry migrant abundance is very low relative to estuary rearing capacity, expanding estuary rearing capacity through habitat restoration does not generate a significant increase in modeled spawner abundance.
4. Extremely low marine survival since the 1980s limits population size and effect of restoration actions. Since the 1980s, marine survival has dropped from over 2% to 0.36% (for natural-origin spawners, including harvest). Increasing marine survival could substantially increase population size and the population response to restoration actions. For comparison, the marine survival rate for natural-origin spawners without harvest is estimated at 0.59%.
5. Current hatchery practices do not increase abundance of natural-origin Chinook in the current climate, nor in any future climate scenario. The model suggests that reducing hatchery production to about 25% of current production may produce a small increase in natural-origin Chinook spawner abundance in all climate scenarios. However, modeled percent hatchery-origin spawners (pHOS) would increase under mid- and late-century climate conditions. At the same time, maintaining a constant adult broodstock from a smaller natural-origin population would substantially increase the percentage of natural-origin adult returns taken for hatchery broodstock, further reducing natural origin spawners in the future.

These conclusions suggest that it may be challenging to increase spawner abundance of Stillaguamish Chinook salmon through habitat restoration in the future, primarily because marine survival is extremely low and climate change is expected to decrease spawner abundance. However, we only modeled the most extreme greenhouse gas emissions scenario (RCP 8.5), which currently appears to be the most accurate projection of mid-century climate change but may overestimate emissions in the late-century. Hence, maintaining an emphasis on floodplain and estuary restoration actions may ultimately be an important component of increasing resilience to climate change. Further research into to causes of early marine mortality in Puget Sound may also identify management actions that can help increase marine survival. Finally, the HARP Model does not suggest that hatchery supplementation can offset effects of climate change.

References

Anderson, A. J., A. M. Claiborne, M. Agha, and M. N. C. Litz. 2021. Puget Sound Chum Salmon Growth Linked to Competitor Abundance, Climate Indices, and Copepod Species Richness. Transactions of the American Fisheries Society 150:707–729.

Anlauf, K. J., W. Gaeuman, and K. K. Jones. 2011a. Detection of Regional Trends in Salmonid Habitat in Coastal Streams, Oregon. Transactions of the American Fisheries Society 140:52–66.

Anlauf, K. J., D. W. Jensen, K. M. Burnett, E. A. Steel, K. Christiansen, J. C. Firman, B. E. Feist, and D. P. Larsen. 2011b. Explaining spatial variability in stream habitats using both natural and management-influenced landscape predictors. Aquatic Conservation: Marine and Freshwater Ecosystems 21:704–714.

Austin, C. S., T. E. Essington, and T. P. Quinn. 2020. In a warming river, wild Chinook salmon spawn later but hatchery-origin conspecifics do not. Canadian Journal of Fisheries and Aquatic Sciences.

Beamer, E., C. Greene, E. Brown, K. Wolf, C. Rice, and R. Henderson. 2016. An Assessment of Juvenile Chinook Salmon Population Structure and Dynamics in the Nooksack Estuary and Bellingham Bay Shoreline, 2003-2015. Report to City of Bellingham under 2013 Interlocal Agreement (Contract #2014-0102, Slkgit River System Cooperative, La Conner, WA.

Beauchamp, D. A., N. Elder, M. Wittmond, L. Wetzel, M. Hoy, K. Stenberg, A. Lind-Null, and K. A. Larsen. 2018. Effects of Seasonal Availability and Energy Content of Key Prey on Growth Performance during Critical Periods for Juvenile Chinook Salmon. U.S. Geological Survey, Salish Sea Marine Survival Project Report Number SSMSP35, Seattle, WA.

Beechie, T., H. Imaki, J. Greene, A. Wade, H. Wu, G. Pess, P. Roni, J. Kimball, J. Stanford, P. Kiffney, and N. Mantua. 2013. Restoring salmon habitat for a changing climate. River Research and Applications 29:939–960.

Beechie, T. J., C. Fogel, C. Nicol, J. C. Jorgensen, B. L. Timpane-Padgham, and P. M. Kiffney. 2023. How does habitat restoration increase salmon population resilience to climate change? Ecosphere.

Beechie, T. J., O. Stefankiv, B. Timpane-Padgham, A. Goodman, and M. Lowe. 2022. Habitat Assessment and Restoration Planning (HARP) Model for the Snohomish and Stillaguamish River Basins. NOAA Contract Report NMFS-NWFSC-CR-2022-xx, Seattle, WA.

Bowerman, T. E., M. L. Keefer, and C. C. Caudill. 2021. Elevated stream temperature, origin, and individual size influence Chinook salmon prespawn mortality across the Columbia River Basin. Fisheries Research 237:105874.

Bowerman, T., A. Roumasset, M. L. Keefer, C. S. Sharpe, and C. C. Caudill. 2018. Prespawn Mortality of Female Chinook Salmon Increases with Water Temperature and Percent Hatchery Origin. Transactions of the American Fisheries Society 147:31–42.

Chamberlin, J., E. Petrou, W. Duguid, R. Barsh, F. Juanes, J. Qualley, and L. Hauser. 2021. Phenological diversity of a prey species supports life-stage specific foraging opportunity for a mobile consumer. ICES Journal of Marine Science 78:3089–3100.

Chamberlin, J. W., B. R. Beckman, C. M. Greene, C. A. Rice, and J. E. Hall. 2017. How relative size and abundance structures the relationship between size and individual growth in an ontogenetically piscivorous fish. Ecology and Evolution 7:6981–6995.

Chasco, B., B. Burke, L. Crozier, and R. Zabel. 2021. Differential impacts of freshwater and marine covariates on wild and hatchery Chinook salmon marine survival. PLOS ONE 16:e0246659.

Chasco, B., I. C. Kaplan, A. Thomas, A. Acevedo-Gutiérrez, D. Noren, M. J. Ford, M. B. Hanson, J. Scordino, S. Jeffries, S. Pearson, K. N. Marshall, and E. J. Ward. 2017. Estimates of Chinook salmon consumption in Washington State inland waters by four marine mammal predators from 1970 to 2015. Canadian Journal of Fisheries and Aquatic Sciences 74:1173–1194.

Christie, M. R., M. J. Ford, and M. S. Blouin. 2014. On the reproductive success of early-generation hatchery fish in the wild. Evolutionary Applications 7:883–896.

Claiborne, A. M., L. Campbell, B. Stevick, T. Sandell, J. P. Losee, M. Litz, and J. H. Anderson. 2021. Correspondence between scale growth, feeding conditions, and survival of adult Chinook salmon returning to Puget Sound and coastal Washington: Implications for forecasting. Progress in Oceanography 198:102443.

Crozier, L. G., B. J. Burke, B. E. Chasco, D. L. Widener, and R. W. Zabel. 2021. Climate change threatens Chinook salmon throughout their life cycle. Communications Biology 4:1–14.

Gablonsky, J. M., and C. T. Kelley. 2001. A Locally-Biased form of the DIRECT Algorithm. Journal of Global Optimization 21:27–37.

Goode, J. R., J. M. Buffington, D. Tonina, D. J. Isaak, R. F. Thurow, S. Wenger, D. Nagel, C. Luce, D. Tetzlaff, and C. Soulsby. 2013. Potential effects of climate change on streambed scour and risks to salmonid survival in snow-dominated mountain basins. Hydrological Processes 27:750–765.

Greene, C. M., J. E. Hall, K. R. Guilbault, and T. P. Quinn. 2010. Improved viability of populations with diverse life-history portfolios. Biology Letters 6:382–386.

Hayes, M. C., S. Hodgson, C. S. Ellings, W. D. Duval, and S. P. Rubin. 2019. Seasonal Use of a Nonnatal Marine Basin by Juvenile Hatchery Chinook Salmon. Marine and Coastal Fisheries 11:437–453.

HSRG. 2009. Columbia River Hatchery Reform System-Wide Report. Hatchery Scientific Review Group.

HSRG. 2020. Developing Recovery Objectives and Phase Triggers for Salmonid Populations. Hatchery Scientific Review Group.

Johnson, S. G. 2022, July 19. stevengj/nlopt. C.

Jorgensen, J. C., C. Nicol, C. Fogel, and T. J. Beechie. 2021. Identifying the potential of anadromous salmonid habitat restoration with life cycle models. PLOS ONE 16:e0256792.

Kendall, N. W., B. W. Nelson, and J. P. Losee. 2020. Density-dependent marine survival of hatchery-origin Chinook salmon may be associated with pink salmon. Ecosphere 11:e03061.

Leonetti, F. E., K. J. Terpstra, and B. J. Dittbrenner. 2015. Temperature anomalies in the Stillaguamish River mapped from 2001 thermal infrared imagery. Snohomish County Public Works, Surface Water Management, Everett, WA.

Leopold, L. B., and T. Maddock. 1953. The Hydraulic Geometry of Stream Channels and Some Physiographic Implications. U.S. Government Printing Office.

Lisi, P., and J. Anderson. 2022. Synchrony of Freshwater and Marine Survival among Chinook Salmon Populations in Puget Sound. Washington Department of Fish and Wildlife, Olympia, WA.

Litz, M. N. C., M. Agha, A. M. Dufault, A. M. Claiborne, J. P. Losee, and A. J. Anderson. 2021. Competition with odd-year pink salmon in the ocean affects natural populations of chum salmon from Washington. Marine Ecology Progress Series 663:179–195.

Mauger, G. S., J. Robinson, R. J. Mitchell, J. Won, and N. Cristea. 2021. Climate Change and Flooding in Snohomish County: New Dynamically -Downscaled Hydrologic Model Projections. Climate Impacts Group, University of Washington., Seattle, WA.

McKinney, G. J. 2023. DNA-Based Population-of-Origin Assignments of Juvenile Chinook Salmon From Stillaguamish Estuary Habitats. Washington Department of Fish and Wildlife, Olympia, WA.

National Marine Fisheries Service. 2019. Final Environmental Assessment for Four Salmon Hatchery Programs in the Stillaguamish River Basin. National Marined Fisheries Service, West Coast Region, Seattle, WA.

Nicol, C. L., J. C. Jorgensen, C. B. Fogel, B. Timpane-Padgham, and T. J. Beechie. 2022. Spatially overlapping salmon species have varied population response to early life history mortality from increased peak flows. Canadian Journal of Fisheries and Aquatic Sciences 79:342–351.

Powell, M. J. D. 1994. A Direct Search Optimization Method That Models the Objective and Constraint Functions by Linear Interpolation. Pages 51–67 *in* S. Gomez and J.-P. Hennart, editors. Advances in Optimization and Numerical Analysis. Springer Netherlands, Dordrecht.

Ruff, C. P., J. H. Anderson, I. M. Kemp, N. W. Kendall, P. A. Mchugh, A. Velez-Espino, C. M. Greene, M. Trudel, C. A. Holt, K. E. Ryding, and K. Rawson. 2017. Salish Sea Chinook salmon exhibit weaker coherence in early marine survival trends than coastal populations. Fisheries Oceanography 26:625–637.

Schindler, D. E., R. Hilborn, B. Chasco, C. P. Boatright, T. P. Quinn, L. A. Rogers, and M. S. Webster. 2010. Population diversity and the portfolio effect in an exploited species. Nature 465:609–612.

Schwalm, C. R., S. Glendon, and P. B. Duffy. 2020. RCP8.5 tracks cumulative CO2 emissions. Proceedings of the National Academy of Sciences of the United States of America 117:19656–19657.

Seixas, G. B., T. J. Beechie, C. Fogel, and P. M. Kiffney. 2018. Historical and future stream temperature change predicted by a lidar-based assessment of riparian condition and channel width. Journal of the American Water Resources Association 54:974–991.

Singh, V. P., and L. Zhang. 2008. At-a-station hydraulic geometry relations, 1: theoretical development. Hydrological Processes 22:189–215.

Sobocinski, K. L., C. M. Greene, J. H. Anderson, N. W. Kendall, M. W. Schmidt, M. S. Zimmerman, I. M. Kemp, S. Kim, and C. P. Ruff. 2021. A hypothesis-driven statistical approach for identifying ecosystem indicators of coho and Chinook salmon marine survival. Ecological Indicators 124:107403.

Verhaar, P. M., P. M. Biron, R. I. Ferguson, and T. B. Hoey. 2011. Implications of climate change in the twenty-first century for simulated magnitude and frequency of bed-material transport in tributaries of the Saint-Lawrence River. Hydrological Processes 25:1558–1573.

Voloshin, A., C. Scofield, and J. Griffith. 2022. Mainstem Stillaguamish River Smolt Trapping Project: 2021 Annual Report. Stillaguamish Tribe of Indians, Natural Resources Department, Arlington, WA.

Ward, E. J., J. H. Anderson, T. J. Beechie, G. R. Pess, and M. J. Ford. 2015. Increasing hydrologic variability threatens depleted anadromous fish populations. Global Change Biology 21:2500–2509.

Welch, D. W., A. D. Porter, and E. L. Rechisky. 2021. A synthesis of the coast-wide decline in survival of West Coast Chinook Salmon (Oncorhynchus tshawytscha, Salmonidae). Fish and Fisheries 22:194–211.

Zimmerman, M. S., J. R. Irvine, M. O'Neill, J. H. Anderson, C. M. Greene, J. Weinheimer, M. Trudel, and K. Rawson. 2015a. Spatial and Temporal Patterns in Smolt Survival of Wild and Hatchery Coho Salmon in the Salish Sea. Marine and Coastal Fisheries 7:116–134.

Zimmerman, M. S., C. Kinsel, E. Beamer, E. J. Connor, and D. E. Pflug. 2015b. Abundance, survival, and life history strategies of juvenile Chinook salmon in the Skagit River, Washington. Transactions of the American Fisheries Society 144:627–641.

Appendix A. Model Spatial Structure

Subbasin numbers and names are shown in Figure A-1 and Table A-1. Subbasin boundaries were based on Endangered Species Act subbasins, then modified to add mainstem floodplain subbasins and remove areas without anadromous salmonids. Spawning and rearing distributions of Chinook salmon are shown in Figure A-2. Release sites of hatchery-origin juvenile Chinook salmon are shown in Figure A-3.

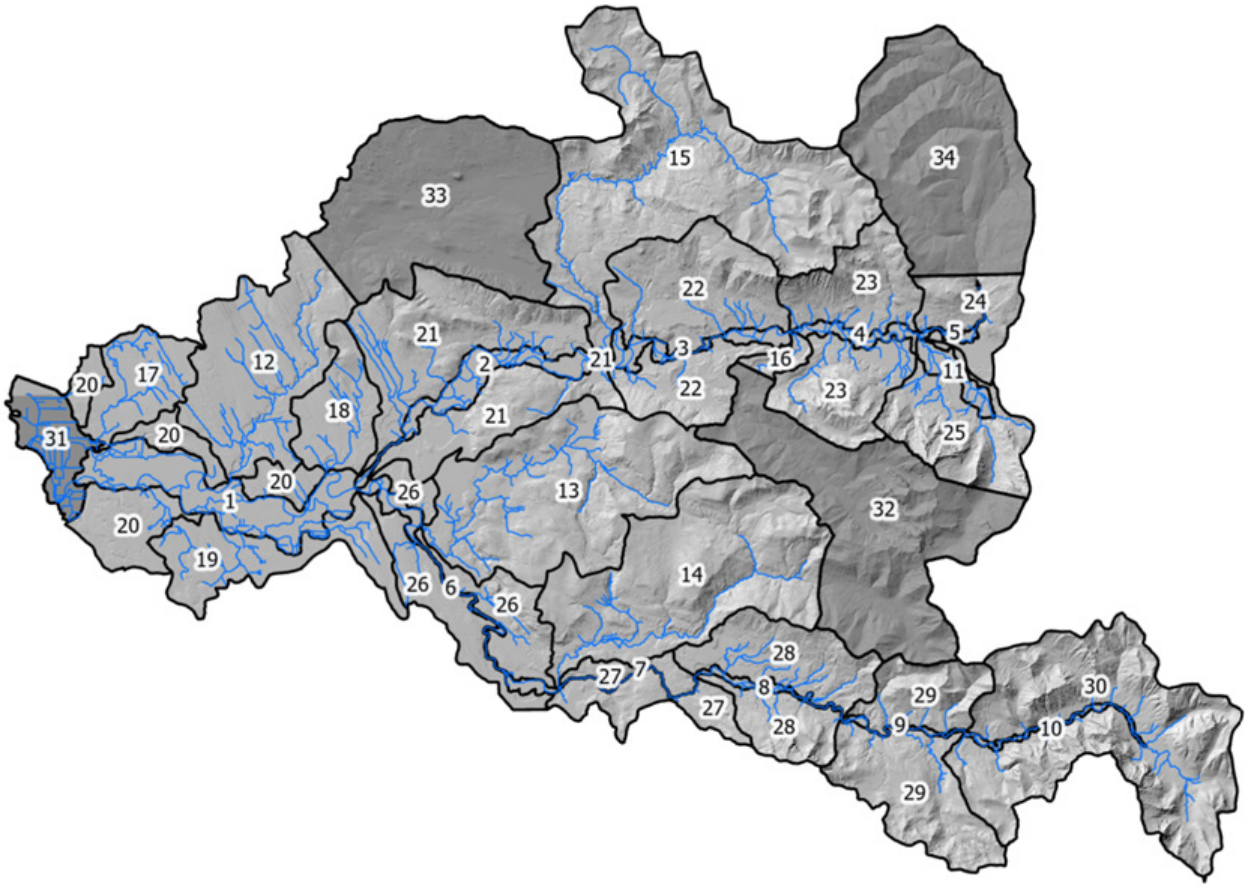

Figure A-1. Freshwater subbasin boundaries used in the HARP Model analysis. Dark gray areas are subbasins without anadromous salmonids and the Stillaguamish estuary.

Table A-1. List of basin numbers and names for the Stillaguamish River basin.

Subbasin number	Subbasin Name	Location
1	Lower Mainstem Stillaguamish	Norman Rd. to confluence of NF and SF
2	Mainstem North Fork Stillaguamish 1	Confluence to Deer Creek
3	Mainstem North Fork Stillaguamish 2	Deer Creek to Boulder River
4	Mainstem North Fork Stillaguamish 3	Boulder River to Squire Creek
5	Mainstem North Fork Stillaguamish 4	Above Squire Creek
6	Mainstem South Fork Stillaguamish 1	Confluence to Canyon Creek
7	Mainstem South Fork Stillaguamish 2	Robe Canyon
8	Mainstem South Fork Stillaguamish 3	Robe Canyon to Twenty–two Creek
9	Mainstem South Fork Stillaguamish 4	Twenty–two Creek to Mallardy Creek
10	Mainstem South Fork Stillaguamish 5	Above Mallardy Creek
11	Squire Creek	Mouth to end of Squire Creek Rd.
12	Pilchuck Creek	Lower Pilchuck Creek
13	Jim Creek	Entire subbasin
14	Canyon Creek	Entire subbasin
15	Deer Creek	Entire subbasin
16	Boulder River	Confluence to NW-SE bend
17	Church Creek	Entire subbasin
18	Harvey Armstrong Creek	Entire subbasin
19	Upland Portage Creek	Entire subbasin
20	Upland Lower Stillaguamish	Tributaries to Lower Stillaguamish 1
21	NF Stillaguamish 1 tribs	Confluence to Deer Creek
22	NF Stillaguamish 2 tribs	Deer Creek to Boulder River
23	NF Stillaguamish 3 tribs	Boulder River to Squire Creek
24	NF Stillaguamish 4 tribs	Above Squire Creek
25	Squire Creek	Upland Squire Creek
26	SF Stillaguamish 1 tribs	Confluence to Canyon Creek
27	SF Stillaguamish 2 tribs	Robe Canyon
28	SF Stillaguamish 3 tribs	Robe Canyon to Twenty–two Creek
29	SF Stillaguamish 4 tribs	Twenty–two Creek to Mallardy Creek
30	SF Stillaguamish 5 tribs	Above Mallardy Creek

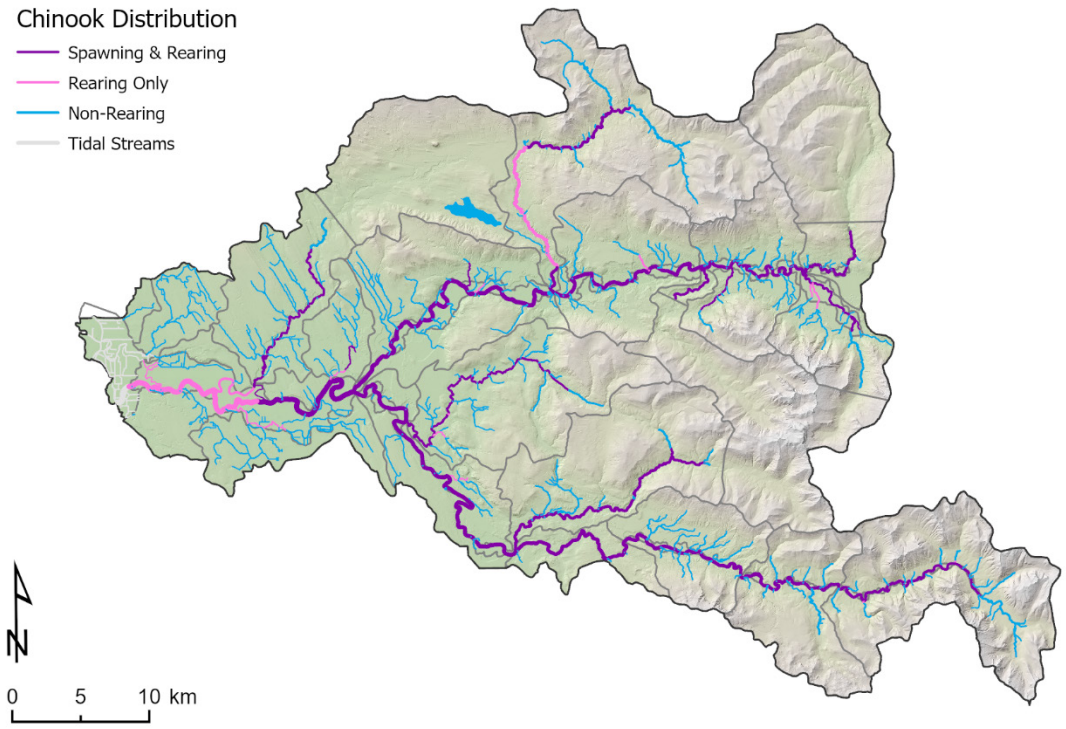

Figure A-2. Spawning and rearing distribution of Chinook salmon used in the HARP Model analysis. Tidally-influenced streams are shown in light gray. Subbasins boundaries are shown in dark gray. Several large lakes are shown for reference. The widths of the stream lines on the map do not represent the true widths of the streams.

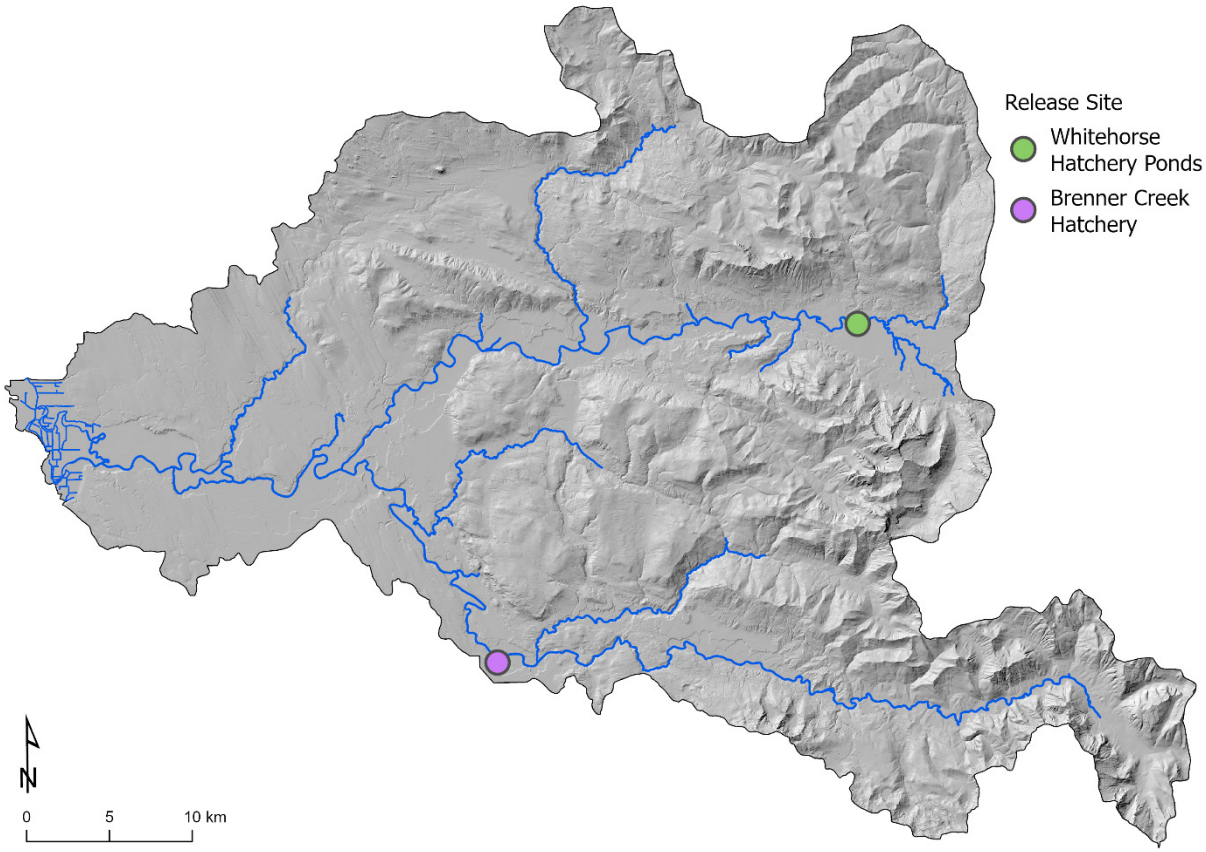

Figure A-3. Release sites of hatchery-origin juvenile Chinook salmon for the North Fork Stillaguamish River (Whitehorse Hatchery Ponds) and the South Fork Stillaguamish River (Brenner Creek Hatchery).

Appendix B. General Circulation Models Used in the Stillaguamish HARP Analysis

Table B-1. GCMs used to model flood flow, low flow, and stream temperature.

GCM	Institution	Stream Flow Model	Stream Temperature Model
ACCESS1.0	Commonwealth Scientific and Industrial Research Organisation (CSIRO), UK	Y	N
ACCESS1.3	Commonwealth Scientific and Industrial Research Organisation (CSIRO), UK	Y	N
BCC-CSM1.1	Beijing Climate Center, China	Y	N
CanESM2	Canadian Center for Climate Modeling and Analysis, Canada	Y	Y
CCSM4	National Center for Atmospheric Research (NCAR)	Y	Y
CNRM-CM5	National Center of Meteorological Research (NCMR), France	N	Y
CSIRO-Mk3-6-0	Commonwealth Scientific and Industrial Research Organisation (CSIRO), UK	Y	Y
FGOALS-g2	Chinese Academy of Sciences, China	Y	N
GDFL-ESM2M	NOAA Geophysical Fluid Dynamics Laboratory	N	Y
GFDL-CM3	NOAA Geophysical Fluid Dynamics Laboratory	Y	N
GISS-E2-H	NASA Goddard Institute for Space Studies	Y	N
HadGEM2-CC	Met Office Hadley Center, UK	N	Y
HadGEM2-ES	Met Office Hadley Center, UK	N	Y
INM-CM4	Institute for Numerical Mathematics (INM), Russia	N	Y
IPSL-CM5A-MR	Institute Pierre Simon Laplace, France	N	Y
MIROC5	National Institute for Environmental Studies, Japan	Y	Y
MRI-CGCM3	Meteorological Research Institute, Japan	Y	N
NoRESM1-M	Norwegian Climate Center, Norway	Y	N

Appendix C. Chinook Restoration Scenarios

Summary of the six multi-action restoration scenarios (Tables C-1 to C-6) modeled for three climate periods, current, 2050s and 2080s. Maps of the distribution of each action type are shown in Figures C-1 to C-3.

Table C-1. TAG 1 restoration scenario. Estuary restoration is 20%.

Subbasin Number	Subbasin Name	Fine Sediment	Wood	Shade	Bank Armor	Beaver Ponds	Floodplain
1	Mainstem Stillaguamish	0%	10%	10%	10%	10%	10%
2	Mainstem NF Stillaguamish 1	0%	25%	25%	25%	0%	25%
3	Mainstem NF Stillaguamish 2	0%	10%	10%	5%	10%	5%
4	Mainstem NF Stillaguamish 3	0%	10%	10%	5%	10%	5%
5	Mainstem NF Stillaguamish 4	0%	5%	0%	2%	0%	0%
6	Mainstem SF Stillaguamish 1	0%	5%	5%	5%	5%	5%
7	Mainstem SF Stillaguamish 2	0%	0%	0%	0%	0%	0%
8	Mainstem SF Stillaguamish 3	0%	5%	0%	2%	0%	0%
9	Mainstem SF Stillaguamish 4	0%	5%	0%	2%	0%	0%
10	Mainstem SF Stillaguamish 5	0%	5%	0%	2%	0%	0%
11	Squire Creek	0%	3%	3%	3%	0%	0%
12	Pilchuck Creek	0%	3%	5%	3%	0%	3%
13	Jim Creek	0%	3%	3%	3%	3%	3%
14	Canyon Creek	0%	2%	2%	2%	2%	2%
15	Deer Creek	10%	5%	2%	0%	0%	0%
16	Boulder River	5%	5%	5%	5%	0%	5%

Table C-2. TAG 2 restoration scenario. Estuary restoration is 80%.

Subbasin Number	Subbasin Name	Fine Sediment	Wood	Shade	Bank Armor	Beaver Ponds	Floodplain
1	Mainstem Stillaguamish*	0%	75%	50%	25%	25%	25%
2	Mainstem NF Stillaguamish 1	0%	50%	50%	50%	25%	50%
3	Mainstem NF Stillaguamish 2	0%	25%	25%	5%	25%	25%
4	Mainstem NF Stillaguamish 3	0%	50%	25%	5%	25%	25%
5	Mainstem NF Stillaguamish 4	0%	25%	0%	5%	0%	0%
6	Mainstem SF Stillaguamish 1	0%	25%	25%	5%	25%	20%
7	Mainstem SF Stillaguamish 2	0%	0%	0%	0%	0%	0%
8	Mainstem SF Stillaguamish 3	0%	25%	0%	5%	0%	0%
9	Mainstem SF Stillaguamish 4	0%	25%	0%	5%	0%	0%
10	Mainstem SF Stillaguamish 5	0%	25%	0%	5%	0%	0%
11	Squire Creek	0%	10%	10%	10%	5%	5%
12	Pilchuck Creek	0%	10%	10%	10%	10%	10%
13	Jim Creek	0%	10%	10%	10%	10%	10%
14	Canyon Creek	0%	5%	50%	5%	5%	5%
15	Deer Creek	20%	10%	5%	0%	0%	0%
16	Boulder River	50%	50%	50%	50%	0%	50%
19	Portage Creek	0%	5%	5%	0%	5%	5%

*In this restoration strategy, 100% of barriers are removed in the mainstem Stillaguamish subbasin.

Table C-3. Chinook 1a restoration scenario. Estuary restoration is 25%.

Subbasin Number	Subbasin Name	Fine Sediment	Wood	Shade	Bank Armor	Beaver Ponds	Floodplain
1	Mainstem Stillaguamish	0%	75%	0%	75%	0%	0%
2	Mainstem NF Stillaguamish 1	0%	0%	75%	0%	0%	75%
3	Mainstem NF Stillaguamish 2	0%	0%	25%	0%	0%	25%
4	Mainstem NF Stillaguamish 3	0%	0%	0%	0%	0%	25%
5	Mainstem NF Stillaguamish 4	0%	0%	0%	0%	0%	25%
6	Mainstem SF Stillaguamish 1	0%	0%	25%	0%	0%	75%
7	Mainstem SF Stillaguamish 2	0%	0%	0%	0%	0%	25%
8	Mainstem SF Stillaguamish 3	0%	0%	25%	0%	0%	25%
9	Mainstem SF Stillaguamish 4	0%	0%	0%	0%	0%	0%
10	Mainstem SF Stillaguamish 5	0%	0%	0%	25%	0%	0%
11	Squire Creek	25%	25%	0%	0%	0%	0%
12	Pilchuck Creek	0%	25%	75%	0%	0%	75%
13	Jim Creek	25%	25%	25%	0%	0%	25%
14	Canyon Creek	0%	25%	25%	25%	0%	25%
15	Deer Creek	0%	0%	25%	0%	0%	25%
16	Boulder River	0%	0%	0%	0%	0%	0%

Table C-4. Chinook 1b restoration scenario. Estuary restoration is 25%.

Subbasin Number	Subbasin Name	Fine Sediment	Wood	Shade	Bank Armor	Beaver Ponds	Floodplain
1	Mainstem Stillaguamish	0%	75%	0%	75%	0%	0%
2	Mainstem NF Stillaguamish 1	0%	0%	0%	0%	0%	0%
3	Mainstem NF Stillaguamish 2	0%	0%	25%	0%	0%	75%
4	Mainstem NF Stillaguamish 3	0%	0%	25%	0%	0%	75%
5	Mainstem NF Stillaguamish 4	0%	0%	25%	0%	0%	75%
6	Mainstem SF Stillaguamish 1	0%	0%	75%	0%	0%	75%
7	Mainstem SF Stillaguamish 2	0%	0%	0%	0%	0%	75%
8	Mainstem SF Stillaguamish 3	0%	0%	0%	0%	0%	0%
9	Mainstem SF Stillaguamish 4	0%	0%	25%	0%	0%	25%
10	Mainstem SF Stillaguamish 5	0%	0%	0%	25%	0%	25%
11	Squire Creek	25%	25%	0%	0%	0%	0%
12	Pilchuck Creek	0%	0%	0%	0%	0%	0%
13	Jim Creek	25%	25%	25%	0%	0%	75%
14	Canyon Creek	0%	75%	75%	25%	0%	75%
15	Deer Creek	0%	25%	75%	0%	0%	75%
16	Boulder River	0%	0%	0%	0%	0%	0%

Table C-5. Chinook 2a restoration scenario. Estuary restoration is 25%.

Subbasin Number	Subbasin Name	Fine Sediment	Wood	Shade	Bank Armor	Beaver Ponds	Floodplain
1	Mainstem Stillaguamish	0%	75%	0%	75%	0%	0%
2	Mainstem NF Stillaguamish 1	0%	0%	75%	0%	0%	75%
3	Mainstem NF Stillaguamish 2	0%	0%	75%	0%	0%	75%
4	Mainstem NF Stillaguamish 3	0%	0%	0%	0%	0%	75%
5	Mainstem NF Stillaguamish 4	0%	0%	0%	0%	0%	75%
6	Mainstem SF Stillaguamish 1	0%	0%	75%	0%	0%	75%
7	Mainstem SF Stillaguamish 2	0%	0%	0%	0%	0%	75%
8	Mainstem SF Stillaguamish 3	0%	0%	75%	0%	0%	75%
9	Mainstem SF Stillaguamish 4	0%	0%	0%	0%	0%	0%
10	Mainstem SF Stillaguamish 5	0%	0%	0%	75%	0%	0%
11	Squire Creek	0%	0%	0%	0%	0%	0%
12	Pilchuck Creek	0%	0%	0%	0%	0%	0%
13	Jim Creek	0%	0%	0%	0%	0%	0%
14	Canyon Creek	0%	0%	0%	0%	0%	0%
15	Deer Creek	0%	0%	0%	0%	0%	0%
16	Boulder River	0%	0%	0%	0%	0%	0%
23	Upland French-Segelsen	0%	0%	0%	0%	0%	0%

Table C-6. Chinook 2b restoration scenario. Estuary restoration is 25%.

Subbasin Number	Subbasin Name	Fine Sediment	Wood	Shade	Bank Armor	Beaver Ponds	Floodplain
1	Mainstem Stillaguamish	0%	75%	0%	75%	0%	0%
2	Mainstem NF Stillaguamish 1	0%	0%	0%	0%	0%	0%
3	Mainstem NF Stillaguamish 2	0%	0%	75%	0%	0%	75%
4	Mainstem NF Stillaguamish 3	0%	0%	75%	0%	0%	75%
5	Mainstem NF Stillaguamish 4	0%	0%	75%	0%	0%	75%
6	Mainstem SF Stillaguamish 1	0%	0%	75%	0%	0%	75%
7	Mainstem SF Stillaguamish 2	0%	0%	0%	0%	0%	75%
8	Mainstem SF Stillaguamish 3	0%	0%	0%	0%	0%	0%
9	Mainstem SF Stillaguamish 4	0%	0%	75%	0%	0%	75%
10	Mainstem SF Stillaguamish 5	0%	0%	0%	75%	0%	75%
11	Squire Creek	0%	0%	0%	0%	0%	0%
12	Pilchuck Creek	0%	0%	0%	0%	0%	0%
13	Jim Creek	0%	0%	0%	0%	0%	0%
14	Canyon Creek	0%	0%	0%	0%	0%	0%
15	Deer Creek	0%	0%	0%	0%	0%	0%
16	Boulder River	0%	0%	0%	0%	0%	0%
23	Upland French-Segelsen	0%	0%	0%	0%	0%	0%

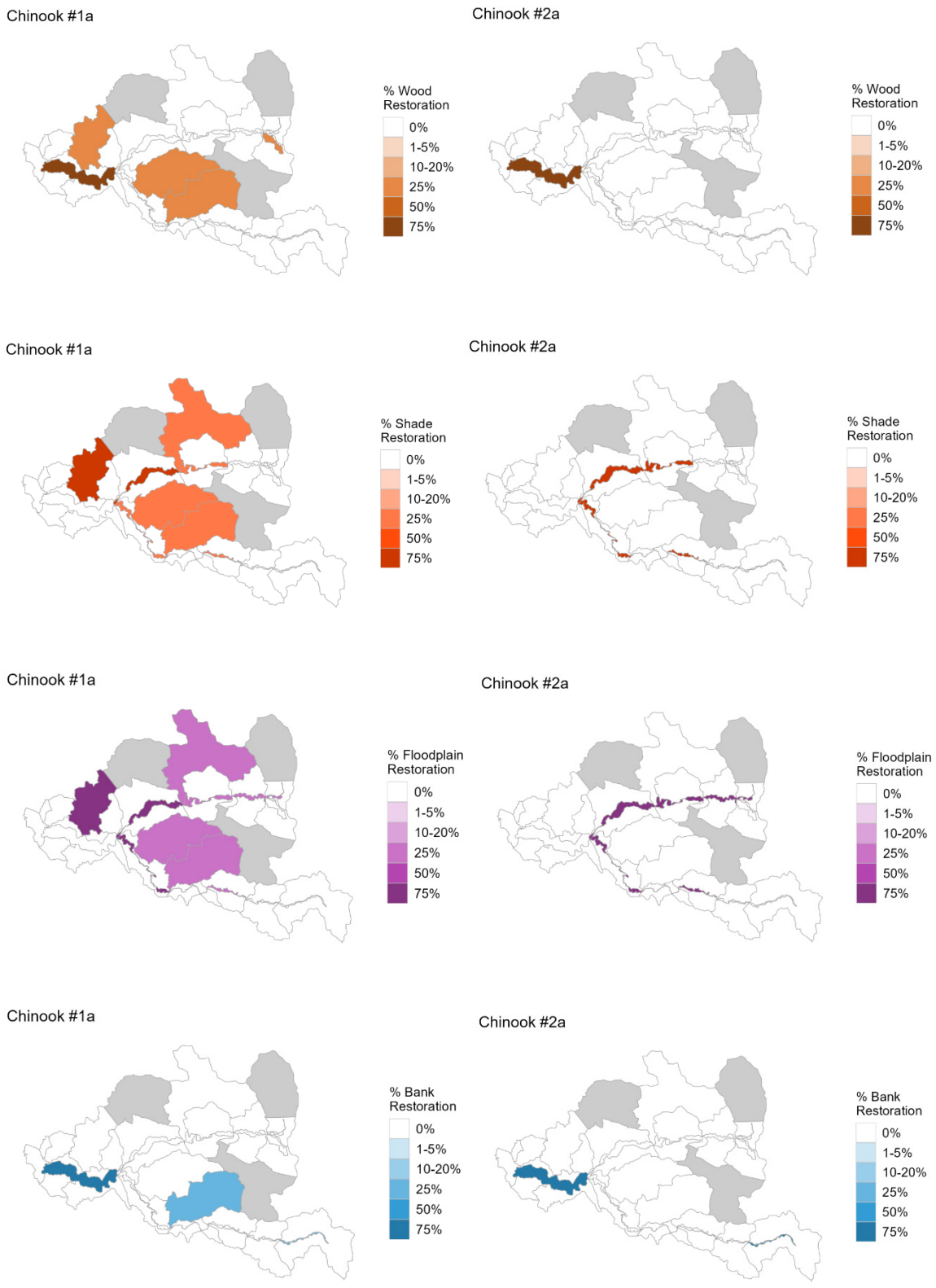

Figure C-1. Spatial distribution of restoration effort in the Chinook 1a and 2a scenarios.

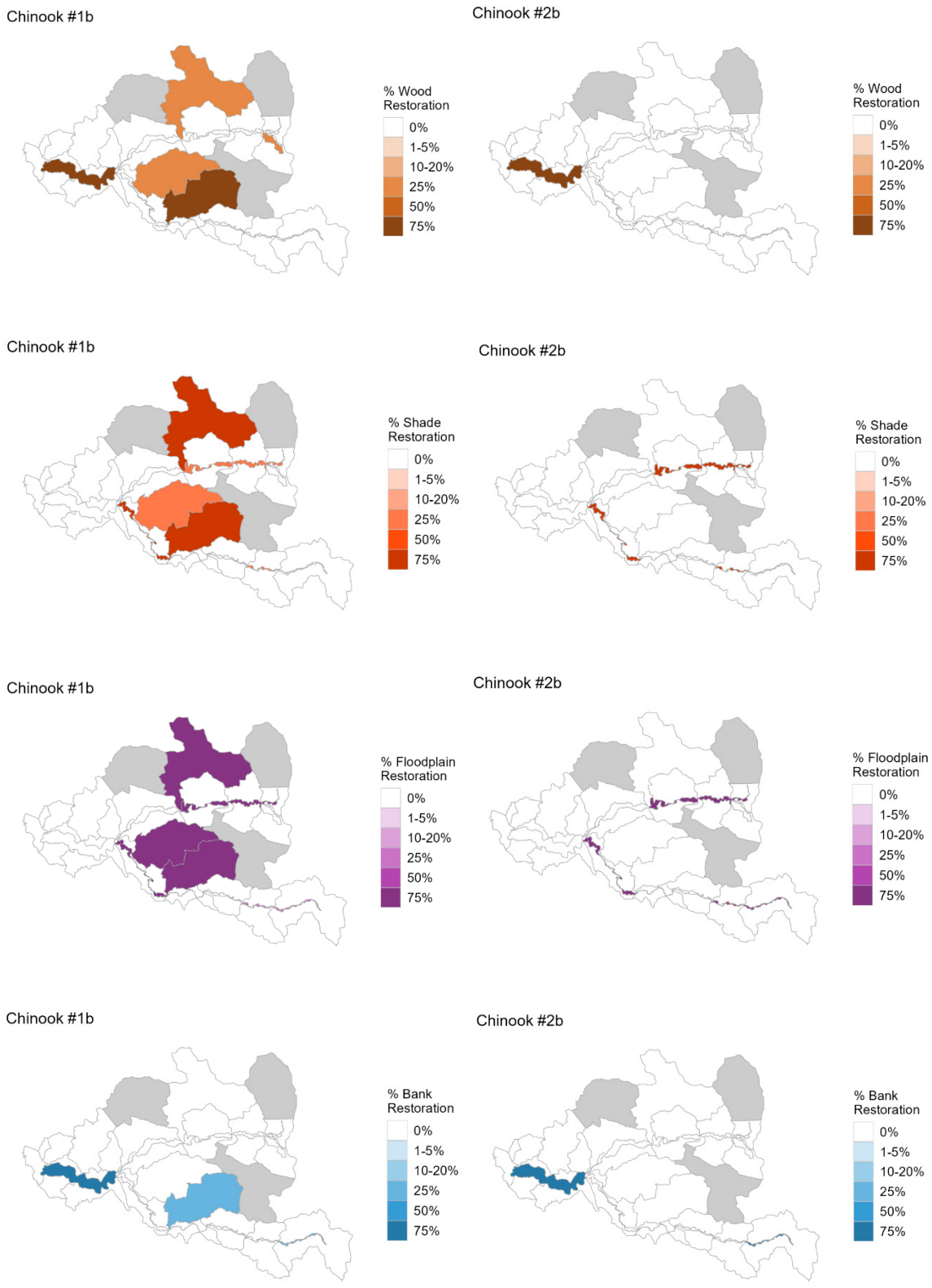

Figure C-2. Spatial distribution of restoration effort in the Chinook 1b and 2b scenarios.

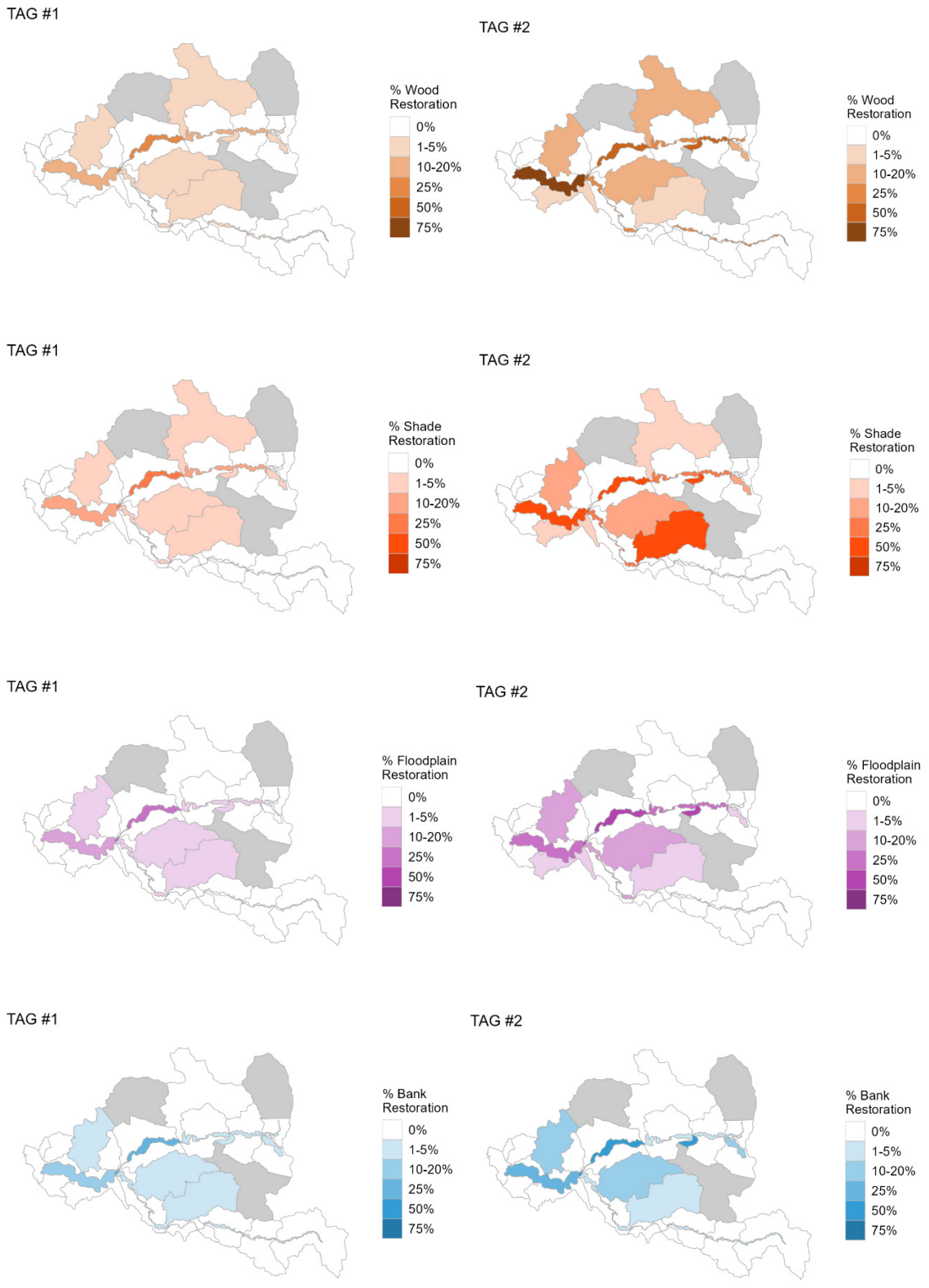

Figure C-3. Spatial distribution of restoration effort in the TAG 1 and Tag 2 scenarios.

Appendix D. Calibration Sensitivity

Several unknown parameters used in the HARP Model are calibrated based on observed ratios between different life stage abundances. However, these observations are subject to some level of uncertainty. We performed one-at-a-time diagnostic testing to determine how sensitive the model calibration process is to various model assumptions. Here we present diagnostic results for several different assumptions about the sizes of juvenile passing the smolt trap and about the proportion of non-Stillaguamish-origin fish rearing in the Stillaguamish estuary.

The model is very sensitive to current assumptions about the proportion of fry-sized fish passing the smolt trap (Table D-1). It produces a 7-fold difference in the equilibrium number of natural-origin returners if the model is calibrated to a 20% fry proportion and an 80% fry proportion. The current calibration target, 30.4%, based on smolt trap observations, produces a close-to-observed number of natural-origin spawners.

Table D-1. Sensitivity of calibrated model parameters to the size distribution of subyearling migrants passing the smolt trap under current conditions (2020s no-action scenario). The model was recalibrated under a range of values representing hypothetical proportions of fry currently passing the smolt trap to assess how responsive the calibration protocol is to varying current-conditions input data. All other calibration targets were held constant. The resulting number of spawners and calibrated model parameters are shown for each hypothetical fry percentage. The highlighted row indicates mean fry percentage for brood years 2011-2020 and the calibrated value (30.4%) used in the final model.

Calibration target: % fry in subyearling outmigrants	Median natural-origin spawners (2020s, no-action scenario)	Fry migration productivity	Percent out-migrating parr	Early marine survival plus harvest (subyearling)	Early marine survival plus harvest (yearling)
20%	637	8.8%	95%	1.5%	2.0%
30.4%	846	13%	94%	1.6%	2.0%
40%	1,258	16%	97%	1.9%	1.9%
60%	2,125	22%	85%	2.9%	1.9%
80%	4,476	28%	67%	5.8%	2.0%

The diagnostic targets presented in Table D-1 only represent alternate hypotheses about current conditions. They do not represent restoration scenarios. In a restoration scenario, the proportion of fry-sized fish passing the smolt trap might change, but other values, including smolt-to-adult return ratios, would change concurrently. In these one-at-a-time diagnostic calibrations, all other values except a single calibration target are held constant.

The model is minimally sensitive to current assumptions about the proportion of Stillaguamish-origin juveniles rearing in the Stillaguamish estuary (Table D-2). It produces a less than 3% difference in the equilibrium abundance of natural-origin returners under current conditions if the model is calibrated to a 20% natal basin proportion and a 100% natal basin proportion (used in Phase 1). Likewise, the equilibrium abundance under the estuary-only restoration scenario varies by less than 7%. Estuary restoration potential does vary between estuary occupancy hypotheses. The estuary restoration diagnostic scenario yields an 11% increase in spawners under 2020s climate conditions under the lowest estuary occupancy hypothesis and a 7% increase under the highest estuary occupancy hypothesis.

Table D-2. Sensitivity of calibrated model parameters to assumptions regarding the use of Stillaguamish estuary habitat by Stillaguamish-origin Chinook fry and non-natal fry under current conditions (2020s no-action scenario). The model was recalibrated under a range of values representing hypothetical proportions of natal-basin fry using the estuary to assess how responsive the calibration protocol is to varying estuary fry composition. The resulting number of spawners in both the 2020s no-action scenario and 2020s 100% estuary restoration scenario are shown along with the corresponding calibrated model parameters. The highlighted row indicates estimated natal fry percentage and calibrated values used in the final model.

Percent of estuary-rearing fry originating in Stillaguamish basin	Median natural-origin spawners (2020s, no-action scenario)	Median natural-origin spawners (2020s, estuary restoration scenario)	Fry migration productivity	Percent out-migrating parr	Early marine survival plus harvest (subyearling)	Early marine survival plus harvest (yearling)
20%	863	956	13%	94%	1.7%	2.0%
40%	853	936	13%	94%	1.7%	2.0%
60%	846	919	13%	94%	1.7%	2.0%
80%	843	905	13%	94%	1.6%	2.0%
100%	840	895	13%	94%	1.6%	2.0%

Appendix E. Calibration of Movement and Survival Parameters to Age Structure Data

The Chinook life-cycle model contains several parameters for which we do not have literature values and that cannot be derived from a system of linear equations. We used a nonlinear optimization method to estimate the value of these parameters so that the model would produce known (target) values for certain life stages or ratios between life stages. During model development, we recalibrated the model after any major change to the habitat model inputs, habitat model mechanics, or life-cycle model mechanics.

For the Chinook model, there were four unknown parameters and four target life-stage values (Table E-1). We created a custom objective function calculating the root mean square difference between the modeled target life-stage values and the observed target life stage values in the deterministic model under current habitat conditions. We then minimized each objective function for each basin using the locally biased dividing rectangles algorithm, “NLOPT_GN_DIRECT_L” (Gablonsky and Kelley 2001) followed by the constrained optimization by linear approximations "NLOPT_LN_COBYLA" algorithm (Powell 1994) via the “nloptr” package in R, an interface to Nlopt (Johnson 2022). We provided a best-guess starting value for each parameter and allowed them to range between 0 and 1. In the interest of time, we allowed each algorithm to run for 2,000 iterations. The outputs of the algorithm were the “best estimate” of values for the four unknown Chinook parameters.

Table E-1. Unknown parameters and known parameter target values for the Chinook salmon life-cycle model.

Parameter or Target Value	Description
Unknown Parameter	
Fry outmigrant survival	The in-river survival rate of fry migrants traveling between their natal basins and the estuary
Percent outmigrating parr	The percent of parr-sized fish that smolt after 12 weeks rather than remaining in freshwater to become yearlings
Parr survival in Puget Sound plus harvest	The survival rate of parr-sized fish in Puget Sound plus harvest (i.e., all components of SAR except the fixed annual ocean survivals)
Yearling survival in Puget Sound plus harvest	The survival rate of yearling-aged fish in Puget Sound plus harvest (i.e., all components of SAR except the fixed annual ocean survivals)
Known Parameter Target Value	
Ratio of fry to parr outmigrants	The ratio of fry-sized fish to parr-sized fish passing the smolt trap on the way to the estuary
Ratio of sub-yearling-origin spawners to yearling-origin spawners	The ratio of spawners that had outmigrated as subyearling-aged fish to spawners that had outmigrated as yearling-aged fish
Subyearling natural-origin Smolt-to-Adult-Return rate (SAR)	SAR calculated as the ratio of the total number of subyearling natural-origin spawners plus the number of natural-origin broodstock (following Lisi et al 2022), divided by the total number of natural-origin subyearling outmigrants at the trap
Smolt-to-Adult-Return rate (SAR)	SAR calculated as the ratio of the total number natural-origin spawners that outmigrated as yearlings plus, divided by the total number of natural-origin subyearling outmigrants at the trap

Appendix F. Comparison of Model 1 and Model 2 Results

Because of uncertainty in the sensitivity of returning adult spawners to elevated temperatures during the holding period, we ran two alternative HARP models: Model 1 with temperature-related prespawn mortality and Model 2 without temperature-related prespawn mortality. The following figures are side-by-side comparisons of the results of the two models.

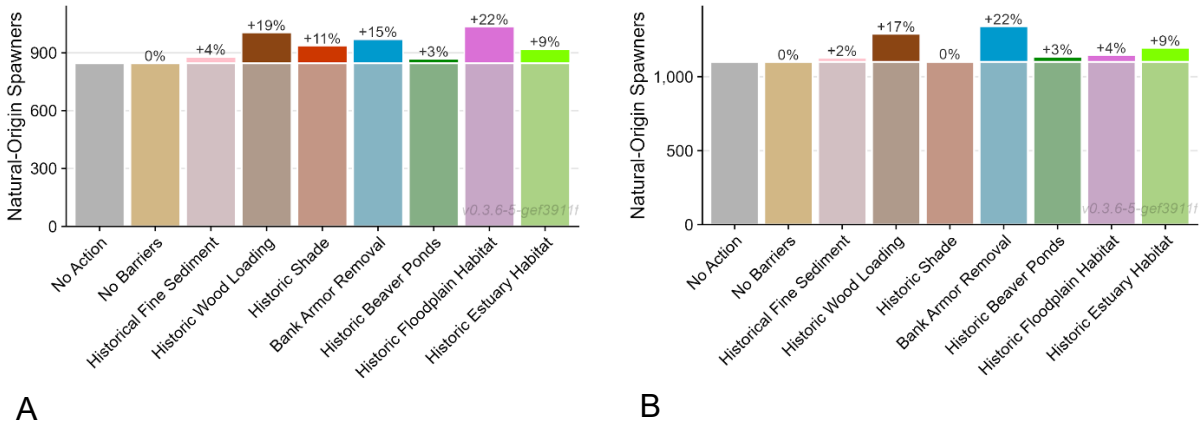

Figure F-1. Change in natural-origin Chinook salmon spawner abundance for each diagnostic scenario using (A) Model 1 with temperature-related prespawn mortality and (B) Model 2 without temperature-related prespawn mortality. Figure F-1(A) is a copy of Figure 4-1.

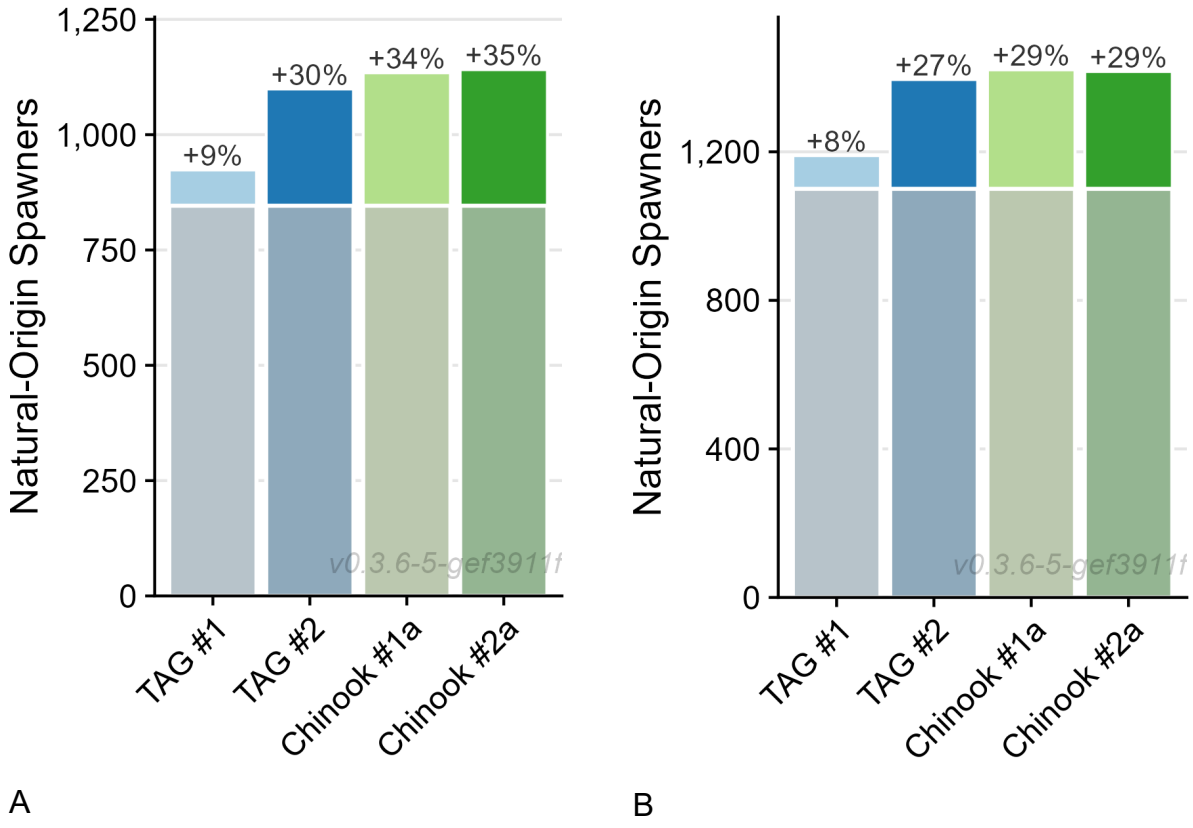

Figure F-2. Change in natural-origin Chinook salmon spawner abundance for the four restoration scenarios under current climate conditions using (A) Model 1 with temperature-related prespawn mortality and (B) Model 2 without temperature-related prespawn mortality. Figure F-2(A) is a copy of Figure 4-2.

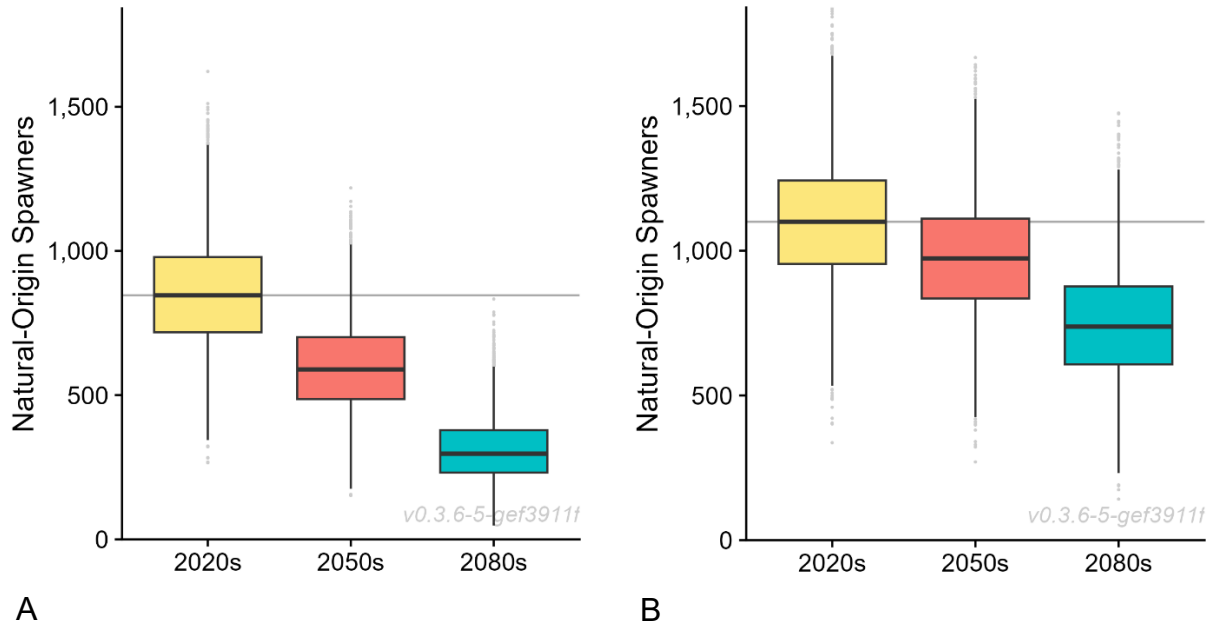

Figure F-3. Modeled change in natural-origin Chinook salmon spawner abundance for current climate, mid-century climate and late century climate using (A) Model 1 with temperature-related prespawn mortality and (B) Model 2 without temperature-related prespawn mortality. Figure F-3(A) is a copy of Figure 4-3.

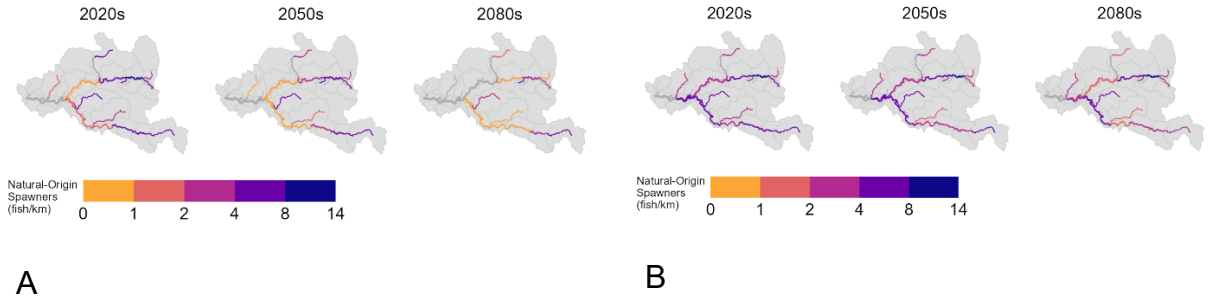

Figure F-4. Modeled change in natural-origin Chinook salmon spawner distribution for current climate, mid-century climate and late century climate using (A) Model 1 with temperature-related prespawn mortality and (B) Model 2 without temperature-related prespawn mortality. Figure F-4(A) is a copy of Figure 4-4.

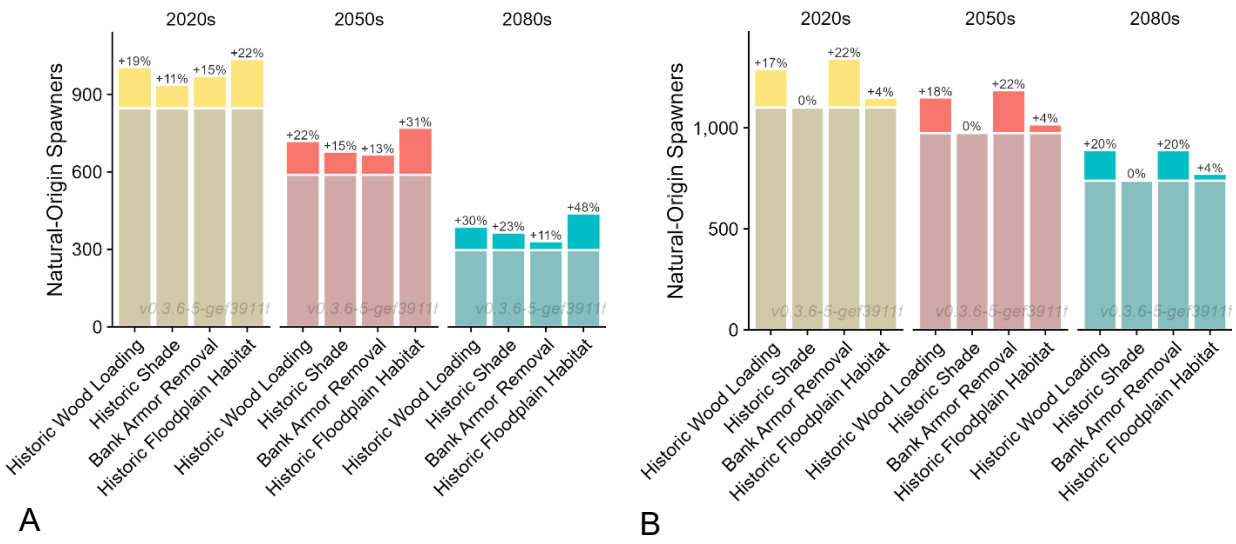

Figure F-5. Modeled change in natural-origin Chinook salmon spawner abundance for the four most responsive diagnostic scenarios under current climate, mid-century climate and late century climate using (A) Model 1 with temperature-related prespawn mortality and (B) Model 2 without temperature-related prespawn mortality. Figure F-5(A) is a copy of Figure 4-5.

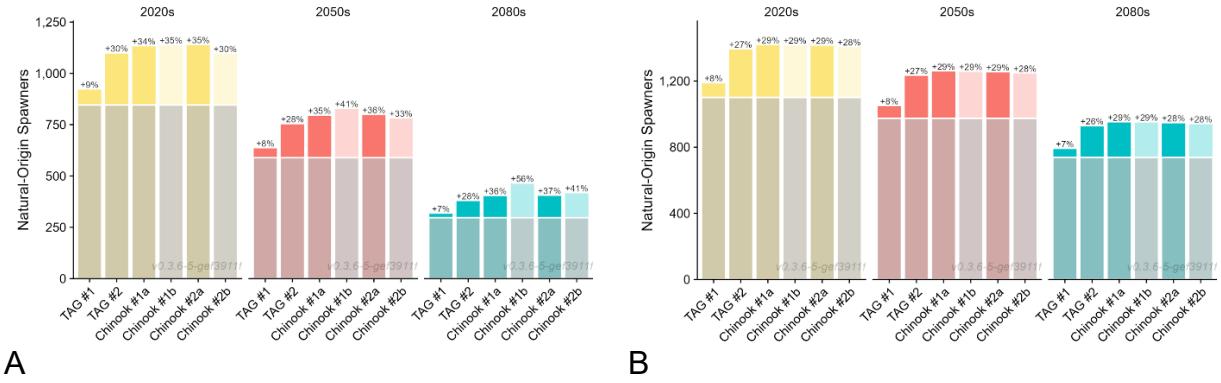

Figure F-6. Modeled change in natural-origin Chinook salmon spawner abundance for all six restoration scenarios under current climate, mid-century climate and late century climate using (A) Model 1 with temperature-related prespawn mortality and (B) Model 2 without temperature-related prespawn mortality. Figure F-6(A) is a copy of Figure 4-6.

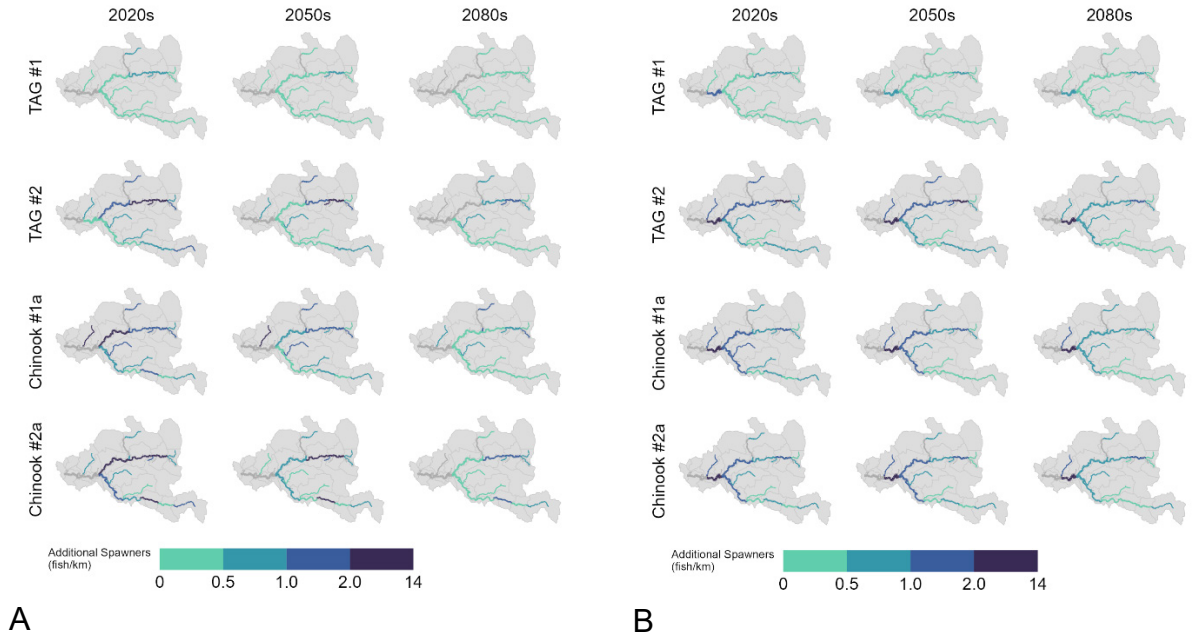

Figure F-7. Modeled spatial distributions of natural-origin Chinook salmon spawner abundance for four restoration scenarios under current climate, mid-century climate and late century climate using (A) Model 1 with temperature-related prespawn mortality and (B) Model 2 without temperature-related prespawn mortality. Figure F-7(A) is a copy of Figure 4-7.

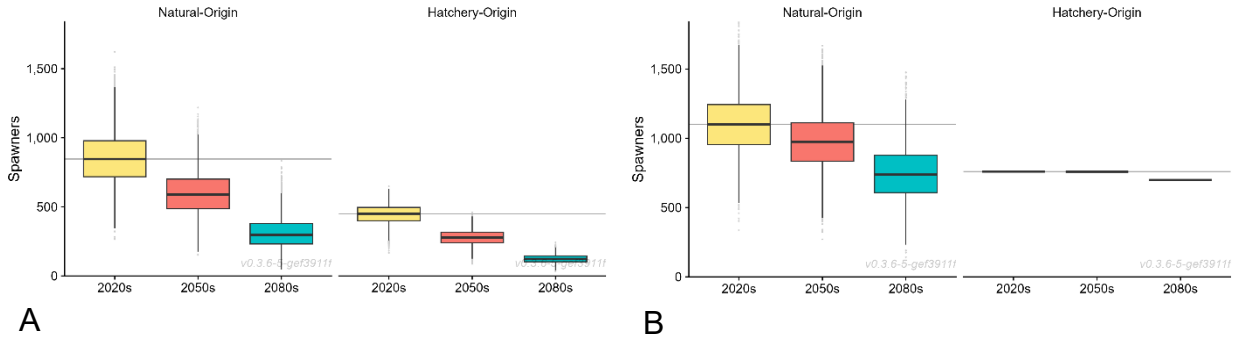

Figure F-8. Modeled natural-origin (left) and hatchery-origin (right) spawner abundances under current (2020s), mid-century (2050s), and late-century (2080s) climate conditions without habitat restoration. using (A) Model 1 with temperature-related prespawn mortality and (B) Model 2 without temperature-related prespawn mortality. Figure F-8(A) is a copy of Figure 4-8.

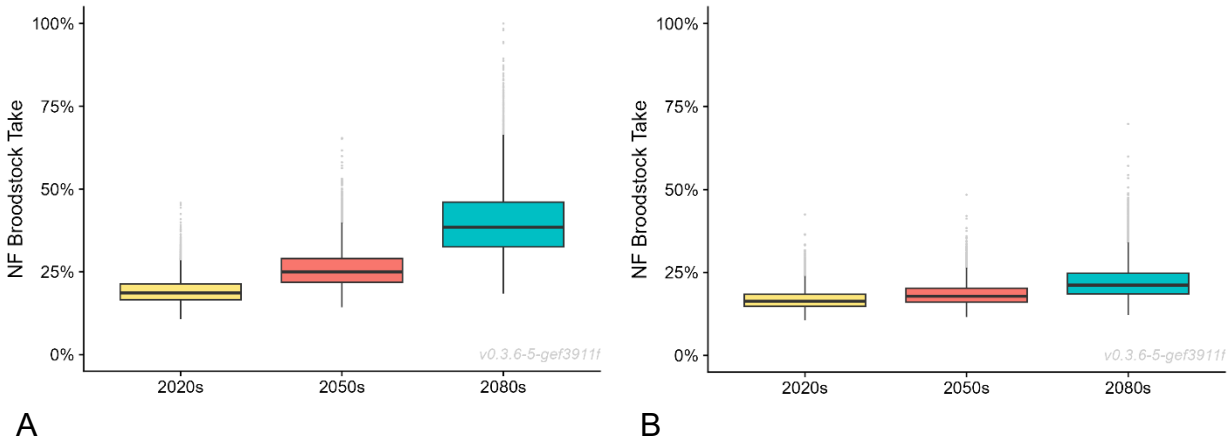

Figure F-9. Modeled percent of the North Fork Stillaguamish natural-origin run required to be taken as broodstock to maintain a pNOB of 0.5 and 140 total broodstock at the Harvey Creek Hatchery under current (2020s), mid-century (2050s), and late-century (2080s) climate conditions without habitat restoration using (A) Model 1 with temperature-related prespawn mortality and (B) Model 2 without temperature-related prespawn mortality. Figure F-9(A) is a copy of Figure 4-9.

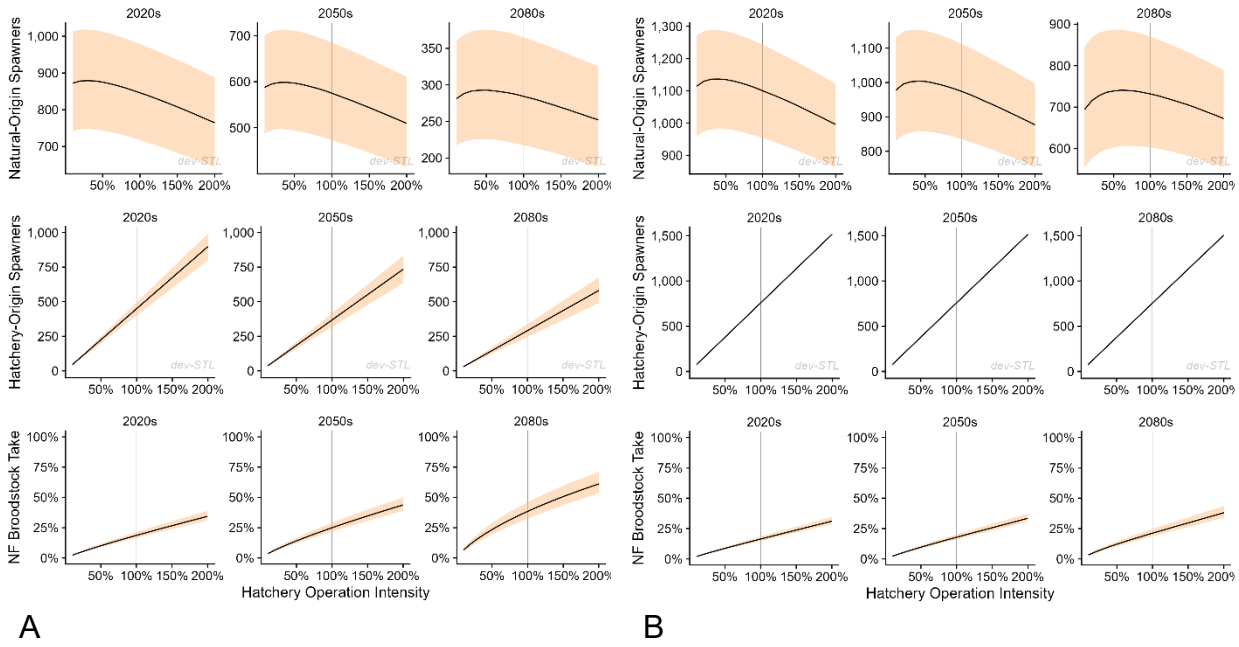

Figure F-10. Modeled response of natural-origin spawner abundance (top row), hatchery-origin spawner abundance (middle row), and percent broodstock take (bottom row) for lower hatchery operation intensity (10% of current broodstock take and juveniles released, x axis) to higher intensity (200% of current broodstock take and juveniles released, x axis) in the three climate periods (2020s, 2050s, and 2080s, columns) using (A) Model 1 with temperature-related prespawn mortality and (B) Model 2 without temperature-related prespawn mortality. Current intensity is 100% on the x-axis (gray vertical line). Black lines show median values and shaded regions show interquartile (25th-75th percentile) ranges. Figure F-10(A) is a copy of Figure 4-10.

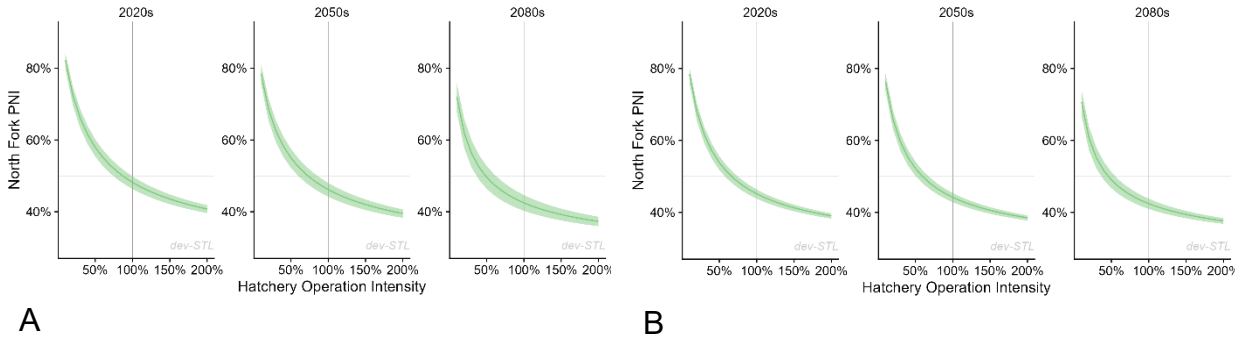

Figure F-11. Modeled PNI (y axis) as a function of modeled hatchery operation intensity (x axis) under three climate conditions (2020s, 2050s, and 2080s) using (A) Model 1 with temperature-related prespawn mortality and (B) Model 2 without temperature-related prespawn mortality. The x-axis is the percent of current smolt release numbers from both hatcheries and current broodstock removal for Harvey Creek operations, with 100% intensity (gray vertical line) representing current operations. Green lines show median values and shaded regions show interquartile (25th-75th percentile) ranges. PNI of 50% is shown by a horizontal gray line. Figure F-11(A) is a copy of Figure 4-11.

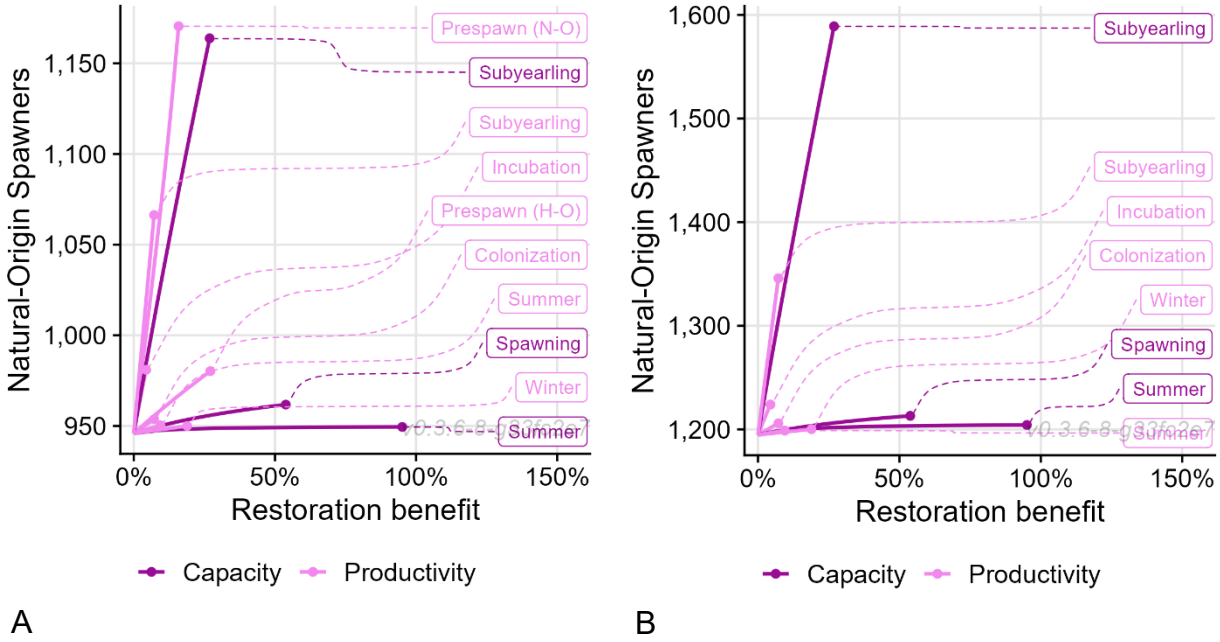

Figure F-12. One-at-a-time sensitivity analysis of life-stage parameters using (A) Model 1 with temperature-related prespawn mortality and (B) Model 2 without temperature-related prespawn mortality. The baseline (0% on the x-axis) is the modeled natural-origin spawner abundance with current habitat conditions. The x axis is percent increase in a capacity or productivity parameter from the current condition up to the maximum (historical) value of the parameter, and the y axis is modeled natural-origin spawner abundance. Figure F-12(A) is a copy of Figure 4-14.

U.S. Secretary of Commerce
Gina M. Raimondo

Under Secretary of Commerce for
Oceans and Atmosphere
Dr. Richard W. Spinrad

Assistant Administrator for Fisheries
Janet Coit

October 2023

fisheries.noaa.gov

OFFICIAL BUSINESS

National Marine
Fisheries Service
Northwest Fisheries Science Center
2725 Montlake Boulevard East
Seattle, Washington 98112